Thermo- and pH-Responsive Hydrogels and Their Controlled Release Properties

Hua Yu

B.S., China Textile University, China, 1984

M.S., China Textile University, China, 1987

A dissertation submitted to the faculty of the
Oregon Graduate Institute of Sciences & Technology
in partial fulfillment of the
requirements for the degree
Doctor of Philosophy
in
Chemistry

Feburary, 1994

The dissertation "Thermo- and pH-Responsive Hydrogels and Their Controlled Release Properties" by Hua Yu has been examined and approved by the following Examination Committee:

David W. Grainger, Thesis Advisor
Associate Professor

Ninian J. Blackburn
Professor

Allan S. Hoffman
Professor, University of Washington

Jeffrey Hollinger
Professor, Oregon Health Sciences University

To My Parents

Acknowledgments

I would like to thank my dissertation committee, Dr. David Grainger, Dr. Ninian Blackburn, Dr. Allan Hoffman, Dr. Jeffrey Hollinger, for reviewing my dissertation, special thanks to Dr. David Grainger, my thesis advisor. This research was made possible through funding from Merck Academic Predoctoral Fellowship. Discussions with Dr. Allan Hoffman, Dr. Teruo Okano, Dr. You Han Bae, and Dr. Sung-Wan Kim are gratefully appreciated. The help provided in the laboratory by Dr. Joan Sanders-Loher, Dr. Tom Loher, Dr. Jim Huntzicker and the help provided on the document by Nancy Christie, Terry Hadfield are gratefully appreciated. Also, I would like to give thanks to Jennifer Peterson and Tracey Fuller for spending their summer internship with me.

TABLE OF CONTENTS

Dedication i

Acknowledgments ii

Nomenclature vii

List of Figures viii

List of Tables xvi

Abstract xvii

Chapter 1 Introduction

1.1 Background 1

1.2 Advantages of Controlled Delivery 2

1.3 Conventional Controlled Delivery Systems 4

1.3.1 Oil-Suspension Systems 5

1.3.2 Encapsulation Systems 6

1.3.3 Diffusion-Controlled Systems 6

1.3.3.1 Monolithic Devices 6

1.3.3.2 Reservoir Devices 7

1.3.4 Biodegradable Systems 9

1.4 Pulsatile and Self-Regulated Delivery Systems 10

1.5 Hydrogel Controlled Delivery Systems 11

1.5.1 Structure and Physicochemical Properties of Hydrogels 12

1.5.1.1 Thermodynamics of Hydrogel Swelling Behavior 12

1.5.2 Methods of Hydrogel Preparation 12

1.5.2.1 Addition Polymerization 12

1.5.2.2 Condensation Polymerization 13

1.5.2.3 Preparation from Pre-Formed Water-Soluble Polymers 13

1.5.2.4 Purification 13

1.5.3 Diffusion in Hydrogels and Their Controlled Delivery Applications 14

1.5.3.1 Diffusion in the Swollen State 14

1.5.3.1.1 Diffusion and Release Kinetics 14

1.5.3.2 Diffusion in Initially Glassy Gels 15

1.5.3.2.1 Swelling Controlled Delivery Systems 15

1.5.3.2.2 Swelling and Diffusion Controlled Delivery Systems 16
1.5.4 Stimuli-Responsive Hydrogel Controlled Delivery Systems 17
1.6 Objectives of This Research 18

Topical References 20

Chapter 2 Thermo-Sensitive Swelling Behavior in Crosslinked N-isopropylacrylamide Networks: Cationic, Anionic and Ampholytic Hydrogels

2.1 Introduction 25
2.2 Experimental 28
2.2.1 Materials 28
2.2.2 Copolymer Gel Fabrication 29
2.2.3 Swelling Measurement 29
3.1 Results and Discussion 30
3.2 Swelling Effects Derived from Ionic Co-Monomer Incorporation 38

References 46

Chapter 3 Amphiphilic Thermosensitive N-Isopropylacrylamide Terpolymer Hydrogels Prepared by Micellar Polymerization in Aqueous Media

3.1 Introduction 49
3.2 Crosslinked PNiPAAm Gel Synthesis 50
3.2.1 Macroscopic Gels 50
3.2.2 Microgels and Latices 50
3.3 Synthesis of Crosslinked Amphiphilic Gel Networks 52
3.4 Theoretical Models for Critical Swelling Behavior of PNiPAAm Gels 54
3.4.1 Mixing Contributions to Gel Swelling 54
3.4.2 Elastic Contributions to Gel Swelling 56
3.4.3 Osmotic Contributions to Gel Swelling 58
3.5 Experimental 58
3.5.1 Materials 58
3.5.2 Synthesis of Hydrophobic Acrylamide Monomers Containing Alkyl Chains 59

3.5.3 Synthesis of N,N'-Bis-Acryloyl-Cystamine (BAC) Crosslinker 61
3.5.4 Synthesis of Terpolymer Poly (NiPAAm-co-SA -N-Alkylacrylamide) Networks 62
3.5.5 Swelling Measurements 63
3.5.6 Model Amphiphile SDS Loading and Release Measurement 63
4.1 Results and Discussion 64

References 75

Chapter 4 Controlled Release Studies of Model Bioactive Compounds from Novel PNiPAAm Hydrogels

4.1 Introduction 81
4.2 Theoretical Framework for Mass Transfer in Hydrogels 83
4.2.1 Fick's First and Second Laws 83
4.2.1.1 Description of Diffusion 83
4.2.1.2 Molecule Size and Diffusivity 86
4.2.1.3 Solute Binding and Its Diffusivity 87
4.2.2 Modeling Studies of Drug Release and Diffusion from Polymers 88
4.2.2.1 Reservoir Systems 88
4.2.2.2 Monolithic Systems 89
4.2.2.2.1 Drug Dissolved in the Device 89
4.2.2.2.2 Drug Dispersed in the Device 90
4.2.3 Diffusion in Heterogeneous Systems 91
4.2.4 Modeling Studies for Hydrogel Swelling-Controlled Release Systems 92
4.2.4.1 One-Phase Models 92
4.2.4.2 Two-Phase Models 93
4.3 Experimental 96
4.3.1 Materials 96
4.3.2 Copolymer (PNiPAAm-co-SA) Gel Synthesis 97
4.3.3 Terpolymer (PNiPAAm-co-SA-co-RAAm) Gel Synthesis 97
4.3.4 FITC Fluorescent Modification of Peptides 98
4.3.5 Drug Loading 98

4.3.5.1 Solvent Sorption Methods 98
4.3.5.2 *In situ* Polymerization Methods 98
4.3.6 Drug Release Measurements 99
4.4 Results and Discussion 100
4.4.1 Controlled Release of Hydrophilic Vitamin B_{12} 100
4.4.2 Controlled Release of Amphiphilic Peptides: Insulin and Interferon 105
4.4.3 Controlled Release of Hydrophobic Steroid Progeterone 112
4.4.4 Further Discussions 114
4.4.4.1 Multicomponent Controlled Diffusion--- A Different View 115

References 119

Chapter 5 Summary 125

Appendix

Biographical Sketch

NOMENCLATURE

c_j	= ion concentration	
F	= network constraint constant (Chapter 3)	
ΔG_{elas}	= Gibbs free energy of elasticity	
ΔG_{mix}	= Gibbs free energy of mixing	
ΔG_{ion}	= Gibbs free energy of osmotic contributions	
k	= Boltzmann constant	
n	= the number of the solvent molecules inthe gel	
R	= ideal gas constant	
S.W.	= swelling ratio	
T	= absolute temperature	[°K]
W_0	= fully hydrated weight of gel	[g]
W_d	= gel dry weight	[g]
W_t	= gel weight at temperature, t	[g]
x_c	= the average number of segments per network chain	

Greek Symbols

α	= the linear swelling ratio
φ	= the volume fraction of the polymer network
ϕ_2	= the volume fraction of the gels
ϕ_2^0	= the volume fraction of the gels in the reference state
κ	= a measure of constraints on junction fluctuations
λ	= (ϕ_2^0/ϕ_2)
χ	= the polymer-solvent iteraction parameter
ν	= the total number of chains in the gels

List of Figures

Fig. 1-1 Schematic diagram of drug level vs. time for (a) single bolus administration (oral dose or intraveneous injection) and (b) ideal controlledhe delivery. 2

Fig. 1-2 Schematic diagram of pulsatile delivery of drug by external trigger. 4

Fig. 1-3 Schematic diagram of encapsulation device. 5

Fig. 1-4 Schematic diagram of a monolithic device. 6

Fig. 1-5 Schematic diagram of release profile for a simple monolithic device. 6

Fig. 1-6 Schematic diagram of a simple resorvoir device. 7

Fig. 1-7 Schematic diagram of release profile for a simple resorvoir device. 7

Fig. 1-8 Schematic diagram of complex microencapsulation systems. 8

Fig. 1-9 Schematic diagram of surface and bulk erosion for biodegradable systems. 9

Fig. 1-10 Schematic diagram of open-loop and closed-loop controlled delivery. 10

Fig. 1-11 Schematic diagram of hydrogel controlled delivery system. 14

Fig. 1-12 Model release profiles in hydrogels (1) diffusion controlled; (2) swelling and diffusion controlled; and (3) swelling controlled. 16

Fig. 1-13 Schematic diagram of gel phase transition. 17

Fig. 2-1 Contrasting collapse kinetics between 100% NiPAAm and NiPAAm /SA (97:3) hydrogels at pH 7 (0.1M PBS buffer) undergoing thermal transition from 20 to 40 °C. 31

Fig. 2-2 Swelling behavior of poly (NiPAAm-co-SA, 97/5) hydrogels undergoing thermal transition from 25 to 40 °C in different pH media. 32

Fig. 2-3 Swelling behavior of anionic NiPAAm copolymer hydrogels containing various amounts of sodium acrylate comonomer at pH 8 as a function of temperature. Buffer: Tris, 50 mM. 32

Fig. 2-4 Swelling behavior of anionic NiPAAm copolymer hydrogels containing various amounts of sodium acrylate comonomer at pH 3 as a function of temperature. Buffer: potassium phthalate, 50 mM. 34

Fig. 2-5 Swelling behavior of anionic NiPAAm copolymer hydrogels containing various amounts of sodium acrylate comonomer at pH 9 as a function of temperature. Buffer: Tris, 50 mM. 35

Fig. 2-6 Influence of pH on the swelling behavior of anionic NiPAAm/SA copolymer (95:5) hydrogels a s a function of temperature. Buffer concentration: 50 mM. 36

Fig. 2-7 Swelling behavior of ampholytic NiPAAm copolymer hydrogels containing various amounts of cationic MAT and anionic SA comonomers at pH 3 as a function of temperature. Buffer: potassium phthalate, 50 mM. 37

Fig. 2-8 Influence of pH on the swelling behavior of ampholytic NiPAAm copolymer gels as a function of temperature at constant buffer concentration (50mM). 38

Fig. 2-9 Effect of buffer chemistry on swelling ratios of a NiPAAm/SA copolymer hydrogel (96:4) as a function of temperature at pH 9, constant buffer concentration (50 mM). 42

Fig. 2-10 Effect of ionic strength (NaCl addition) on NiPAAm/SA copolymer gel swelling (97:3 copolymer) as a function of temperature at pH 7 in phosphate buffer. 43

Fig. 2-11 Effect of crosslinker concentration on copolymer gel swelling as a function of temperature in 0.1 M PBS, pH 7, for NiPAAm/SA gels (97:3) at 10 mol% monomer feed concentration during polymerization. 44

Fig. 2-12 Aqueous solvent content of NiPAAm/SA copolymer gels (97:3) as a function of temperature for gel preparations containing increasing MBAAm crosslinker concentrations in the feed. Buffer: 0.1M PBS, pH 7. 44

Fig. 2-13 Effect of total monomer feed concentration in the aqueous polymerization medium on the resulting NiPAAm/SA (97:3) copolymer gel swelling as a function of temperature. Buffer type: Tris buffer (pH 8, 50 mM). 45

Fig. 2-14 Swelling kinetics for PNiPAAm hydrogels of different thickness es undergoing thermo-transitions from 25 to 40 °C at pH 7. 46

Fig. 3-1 Schematic diagram of micellar copolymerization of poly (NiPAAm -co-SA-co-n-N-Alkylacrylamide) networks in aqueous media, with MBAAm or BAC as crosslinker, SDS or Brij 30 as surfactant stabilizers, and AP/TEMED as initiators. 55

Fig. 3-2 Thermo-sensitive swelling behavior of terpolymer (NiPAAm/SA/Cn, 95/3/2, 0.8 mol% MBAAm) gels in 0.05 M PBS buffer (pH 7.3). 66

Fig. 3-3 Thermo-sensitive swelling behavior of terpolymer (NiPAAm/SA/Cn, 95/3/2, 1.5 mol% BAC) gels in 0.05M PBS buffer (pH 7.3). 67

Fig. 3-4 Thermo-sensitive swelling behavior of terpolymer (NiPAAm/SA/C4, 0.8 mol% MBAAm) gels in 0.05M PBS buffer (pH 7.3). 67

Fig. 3-5 Thermo-sensitive swelling behavior of terpolymer (NiPAAm/SA/C12, 0.8 mol% MBAAm) gels in 0.05M PBS buffer (pH 7.3). 68

Fig. 3-6 Thermo-sensitive swelling behavior of terpolymer (NiPAAm/SA/C4, 0.8 mol% MBAAm) gels in 0.05M PBS buffer (pH 7.3). 69

Fig. 3-7 Thermo-sensitive swelling behavior of terpolymer (NiPAAm/SA/C14, 0.8 mol% MBAAm) gels in 0.05M PBS buffer (pH 7.3). 70

Fig. 3-8 Swelling kinetics of terpolymer (NiPAAm/SA/C4, 95/3/2, 0.8 mol% MBAAm) gels undergoing thermo-transition from 25 to 40 °C in different pH media. 70

Fig. 3-9 Effect of crosslinker concentration on thermo-sensitive swelling behavior of terpolymer (NiPAAm/SA/C4, 95/3/2) gels in 0.05M PBS buffer. (*mol% to monomer). 71

Fig. 3-10 Temperature-dependent swelling equilibraof amphiphilic networks, crosslinked poly (NiPAAm-co-SA-n-N-butylacrylamide), vs. hydrophilic SA and hydrophobic RMAAm comonomer ratio in 0.05M PBS buffer (pH 7). 72

Fig. 3-11 SDS release from terpolymer (PNiPAAm/SA/Cn, 95/2.5/2.5, 0.8 mol% MBAAm) in water under "normal" conditions (no release media changing) at 25 °C measured by HPLC. 73

Fig. 3-12 SDS release from terpolymer (PNiPAAm/SA/Cn, 95/2.5/2.5, 0.8 mol% MBAAm) in water under "sink" conditions at 25 °C measured by swelling ratio monitoring. 74

Fig. 3-13 SDS release from terpolymer (PNiPAAm/SA/C10, 0.8 mol% MBAAm) in water under "normal" conditions (no release media changing) at 25 °C measured by HPLC. 75

Fig. 3-14 SDS release vs. square root of time from terpolymer (PNiPAAm/SA/Cn, 95/2.5/2.5, 0.8 mol% MBAAm) during the first 16-hrs in water under "normal" conditions at 25 °C measured by HPLC. 76

Fig. 3-15 Schematic diagram of the hydrophobic chain-chain interaction between terpolymer networks and SDS. 76

Fig. 4-1 Mass flow through a rectangular box (dx is a length and A is a cross sectional area), J_{in} is the influx and J_{out} is outflux. 87

Fig. 4-2 Schematic diagram of the concentration profile in reservoir system. 91

Fig. 4-3 Schematic diagram of concentration profile of drug loading C_0 and solubility C_s within a monolithic device. 93

Fig. 4-4 Schematic diagram of the simulation results of two-phase models for a semi-infinite gel slab without considering volume change. 97

Fig. 4-5 Vitamin B12 release from PNiPAAm-co-SA (97/3, 4 mol% of MBAAm) gels in different pH media (0.05M buffer concentration) at 37 °C. Loading: solvent sorption (2.5% solution). 103

Fig. 4-6 Vitamin B12 release from PNiPAAm-co-SA (97/3, 4 mol% of MBAAm) gels in different pH media (0.05M buffer concentration) at 37 °C. Loading: solvent sorption (2.5% solution). 104

Fig. 4-7 Vitamin B12 release from PNiPAAm-co-SA (97/3, 4 mol% of MBAAm) gels in 0.05M PBS (pH 7.3, 37 °C). Loading: solvent sorption (1.5% solution). 105

Fig. 4-8 Vitamin B12 release from PNiPAAm-co-SA (97/3) gels at 37 °C in 0.05M PBS (pH 7.3). Loading: solvent sorption (1.5% solution). 105

Fig. 4-9 VB12 thermo-stimulated release profiles from PNiPAAm/SA (97/3, 2 mol% MBA) gels in PBS (pH 7.3). Loading: solvent sorption (4% solution). 106

Fig. 4-10 Vitamin B12 pulsatile release profiles from PNiPAAm/SA (97/3, 2 mol% MBA) gels at various temperatures (2 min heating) in PBS (pH 7.3). Loading: solvent sorption (4% solution). 107

Fig. 4-11 Schematic diagram of thermo-stimulated release of drug from ionized and non-ionized PNiPAAm gels. 108

Fig. 4-12 Effect of vitamin B12 loading on its release profiles from NiPAAm/SA (97:3) hydrogels at 25 °C in 0.05M PBS buffer (pH 7.3). 109

Fig. 4-13 Insulin release from terpolymer (PNiPAAm/SA/Cn, 95/3/2, 1.0 mol% BAC) gels in 0.05M PBS (pH 7.3) at 25 °C, loading: solvent sorption (0.7% solution). 110

Fig. 4-14 Insulin release from terpolymer (PNiPAAm/SA/Cn, 3% fixed with BAC) gels in 0.05M PBS (pH 7.3) at 25 °C, loading: solvent sorption (0.7% solution). 111

Fig. 4-15 The effect of the amount of hydrophobic comonomer incorporation on insulin release from terpolymer (PNiPAAm/SA/C4, 3 mol% SA fixed with 1% mol BAC) gels in 0.05M PBS (pH 7.3) at 25 °C, loading: solvent sorption (0.7% solution). 112

Fig. 4-16 Insulin release from terpolymer (PNiPAAm/SA/Cn, 95/3/2 with 1.5 mol% BAC) gels in 0.05M PBS (pH 7.3) at 25 °C, loading: *in situ* polymerization (0.5% solution). 113

Fig. 4-17 The effect on pendent alkyl chain length of the gels on the release of insulin from terpolymer gels, PNiPAAm-co-SA-RMAAm (95/3/2, with 1.5 mol% BAC) in 0.05M PBS (pH7.3, 25 °C). Loading: *in situ* polymerization. 114

Fig. 4-18 Insulin pulsatile release from terpolymer gels (PNiAAm/SA/C12, 95/3/2, 1.5 mol% BAC) by temperaturestimuli in 0.05M PBS (pH 7.3). Loading: *in situ* polymerization (0.5% solution). 115

Fig. 4-19 Effect of crosslinking density on interferon release from terpolymer gels (PNiAAm/SA/C12, 95/3/2, 1.5 mol% BAC) by temperaturestimuli in 0.05M PBS (pH 7.3). Loading: *in situ* polymerization (0.24% solution). 116

Fig. 4-20 Progesterone release from terpolymer (PNiAAm/SA/C14, 3% SA fixed, 1.0 mol% MBAAm) in 0.05M PBS (pH 7.3, 25°C). Loading: solvent sorption (3% solution). 117

Fig. 4-21 Effect of crosslinking density on progesteron release from terpolymer gels (PNiAAm/SA/C14, 95/3/2) in 0.05M PBS (pH 7.3, 25 °C). Loading: solvent sorption (3% solution). 118

Fig. 4-22 Scheme of the friction equation for diffusion (subscripts, d refers to drug; w, to water; p, to polymer). 119

List of Tables

Table 3.1 Synthesis of microgels and latexes 53

Table 3.2 Characterization of n-N-alkylacrylamide 62

Table 4.1 Diffusion coefficient of some molecules 89

Table 4.2 Values of n and the corresponding release mechanisms 98

Abstract

Crosslinked polymer networks of N-isopropylacrylamide (NiPAAm) containing small amounts of either anionic or cationic co-monomers, or mixtures of both were fabricated and characterized in terms of their aqueous swelling and critical behavior. These gels demonstrate critical transition temperatures in aqueous media between a highly solvated, swollen gel state and a collapsed, dehydrated network over temperature ranges comparable to that of pure NiPAAm, with modifications of gel critical points and respective temperature ranges dependent upon co-monomer type and content. Copolymer gel swelling ratios are significantly larger than those reported for pure homopolymer NiPAAm gels, even when only 0.5 mol% of co-monomer is incorporated. At temperatures exceeding the collapse transition point, all copolymer gels collapse to a state of nearly complete dehydration, demonstrating short-time collapsed-state swelling ratios far lower than those of pure NiPAAm networks. Collapse kinetics for the ionomeric gels are much more rapid than those of pure NiPAAm, achieving collapse state equilibrium on time scales of seconds. Swelling behavior as a function of pH, buffer type, ionic strength, crosslinking and temperature is detailed over a range of copolymer compositions.

New amphiphilic terpolymer hydrogels containing a thermosensitive N-isopropylacrylamide component, a hydrophilic comonomer (sodium acrylate), and hydrophobic alkylated comonomers (n-N-alkylacrylamides) of various lengths were fabricated using a micellar polymerization technique in aqueous media. These gels exhibit compositionally dependent swelling as a function of both pH and temperature, demonstrating large, rapid discontinuous collapse in aqueous media between 30 and 40 °C. Surfactant release from these gels can be modulated by gel composition, demonstrating extended release over several weeks in some cases. The influence of

hydrophobic chains in these networks is manifested in their robust mechanical properties, significant alteration of swelling, and influence on release of entrapped moieties.

Controlled release of hydrophilic and hydrophobic small molecules (vitamin B12 and progesterone) as well as insulin and interferon was investigated for a terpolymer hydrogel network containing the thermosensitive monomer, N-isopropylacrylamide. Drugs and proteins were entrapped directly from aqueous dispersions containing all of the network components stabilized in micelles. Hydrophobic alkyl chain incorporation in these networks influenced NiPAAm swelling, gel critical behavior with temperature and drug release kinetics. Chain-length dependent drug release is observed to be modified over that for gels containing no alkyl co-monomer. Release of insulin and interferon is shown to be prolonged over weeks, displaying a zero-order release profile when entrapped (loaded) by *in situ* network polymerization. Hydrophobic micro-depots resulting from micellar stabilized n-alkyl acrylamide monomer microstructures in the swelling gels are implicated in creating this release profile.

Chapter 1 Introduction

1.1 Background

The human body has devised elaborate mechanisms to control the production, protection, and target delivery of endogenous "bioactive agents" such as hormones, enzymes, antibodies, and mediators of the immune system. Conversely, unwanted pathogens have also devised ways to evade immunological surveillance and cause human diseases. Only with recent advances in cellular and molecular biology are the intricacies of these mechanisms becoming more fully appreciated. Although the emergence of a great many novel pharmacologically and biologically active compounds have provided significant benefits to the quality of human life, it has become clear that major improvements in their efficacy and performance in the living organism can be made by optimizing their delivery, generally, by manipulating the site and timing of action of the agent. This effort to improve drug efficacy and pharmacology is the primary motivation behind modern concepts of so-called controlled drug delivery.

In recent years, scientific advances regarding pharmaceutical technologies have been discovered and developed at an astounding rate. Two investigative approaches have been pursued: (1) discovery and development of natural and synthetic bioactive agents, and (2) development of strategies to deliver drugs more effectively by enhancing drug activity or specificity, reducing cost or toxicity.

In this regard, significant advances in synthetic chemistry of polypeptides and recombinant DNA technology for production of proteins have created a vast potential for novel types of drug therapy. However, major problems associated with their administration are: (1) short biological half-life of polypeptides, and (2) strong systemic side-effects often correlated with highly active and effective new polypeptide drugs. These problems could be solved by controlled delivery approaches that protect these drugs against in vivo degradation and prolong their biological half-life. Furthermore, controlled delivery target

the drug to the desired tissue, thereby minimizing delivered doses and avoiding systemic side effects. Drug targeting and release in a controlled profile will play a major role in the development of future drug formulations involving both existing and new drug agents.

The multidisciplinary nature of the controlled delivery field has relied heavily on the design and use of polymers for controlled delivery of therapeutic agents. Fortunately, polymer science has advanced to the point where it is possible to design materials for high performance and favorable interaction in their intended environment, for example, within living biological systems. While medical research in the past tended to adopt materials which were available commercially, more and more polymer scientists are teaming with life scientists to custom-design polymeric biomaterials for specific controlled delivery applications.

1.2 Advantages of Controlled Delivery

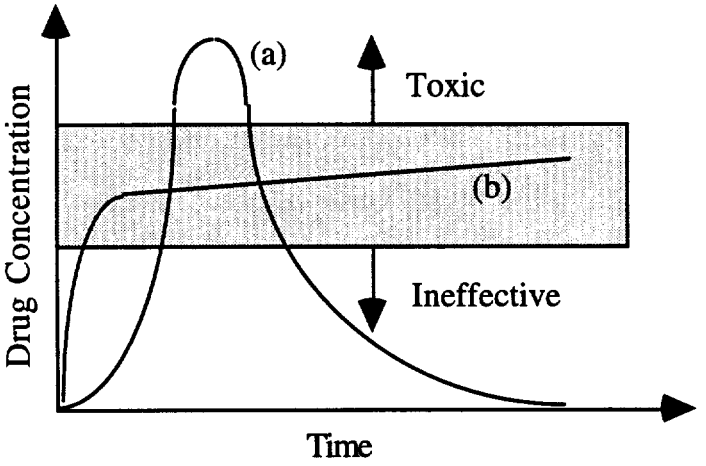

Fig. 1-1 Schematic diagram of drug level vs. time for (a) single bolus administation (oral dose or intraveneous injection) and (b) ideal controlled delivery.

Controlled delivery systems offer several principal advantages over conventional formulations that deliver all of the active agent over a short period of time. This difference can be appreciated by examining Fig. 1-1.

In this figure, drug concentration in a local environment is shown as a function of time after delivery in both conventional (a) and controlled (b) strategies. Typically, after the agent is administrated in the conventional way (oral or intraveneous), the systemic concentration first rises rapidly. It may approach toxic levels as the maximum concentration is achieved. Once bodily absorption (metabolization, excretion, degradation) has countered this threat, drug activity is steadily reduced to a level which is ineffective in treating the patient. Therapeutic levels are only briefly and transiently encountered between maximum and minimum dosages. A controlled delivery formulation, by contrast, releases a quantity of the drug which has been determined to achieve the optimal concentration (effective, but not toxic). It supplements the initial burst at a preprogrammed rate, i.e., equal to that of bodily absorption, degradation, and excretion (e.g., zero-order or first-order kinetics). Devices take on many forms and their performance can be highly reproducible. The advantages of controlled delivery to provide a prolonged period of therapeutically effective drug activity are significant. Other advantages also include enhanced bioavailability, enhanced therapeutic index, reduced side-effects, improved patient compliance and acceptance.

In addition, therapy could be improved enormously if a drug could be equipped with target-selective moieties. Target selectivity in drug administration has traditionally been achieved by either differential sensitivity or differential accessibility. The property of differential sensitivity is ascribed to a drug which spreads throughout the body but acts only on the intended afflicted area. That of differential accessibility is ascribed to a drug which may act on the entire system, but is applied solely to the afflicted area. It is now theoretically possible to use differential accessibility as a tool in combating previously

indistinguishable cells, for example, those of viruses and cancers. Controlled delivery devices successfully adapted to these approaches would render conventional drug administration methods both inefficient and wasteful.

Controlled delivery systems also may be actively triggered by local environmental conditions (pH, temperature) to achieve either complex release patterns (i.e., pulsatile or intermitted delivery) or self-regulating feedback sequences to mimic physiological control cycles. Devices can be designed to be externally triggered to liberate their preloaded drug in a series of discrete bursts (depicted in Fig. 1-2) and their burst peak heights are controllable.

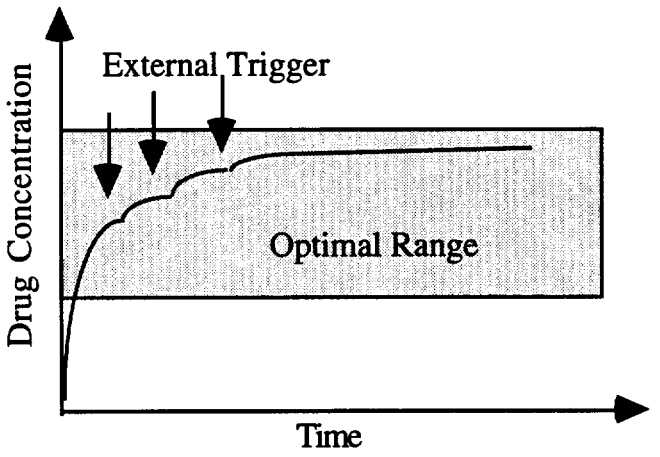

Fig. 1-2 Schematic diagram of pulsatile delivery of drug by external trigger.

1.3 Conventional Controlled Delivery Systems

The technologies designed to "control release" bioactive agents fall into a relatively small number of principal categories. These technologies will be discussed and distinguishing lectural noted. It should be emphasized that the performance of a device

operating in vivo or in situ may be influenced by a number of environmental and other factors that are not accounted for in the idealized (and rather simplistic) descriptions provided here.

1.3.1 Oil-Suspension Systems

One of the simplest formulations for controlled delivery relies on the partitioning of bioactive agent between oily and aqueous phases. If the agent is present as a particulate suspension within the oil droplets (e.g., as a parenteral formulation), its rate of release will depend on its own solubility in the oily phase, as well as on the oil/water partition coefficient. Developments in microemulsion technology are able to make this approach applicable to oral, parental, transdermal and aerosol delivery.

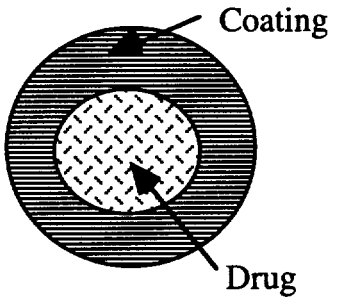

Fig. 1-3 Schematic diagram of encapsulation device.

1.3.2 Encapsulation Systems

The most extensively used controlled release technology currently is the encapsulation coating where a drug is entrapped within an excipient core surrounded by a coating designed to dissolve under the appropriate conditions, or form pores of certain size permitting drug to be released at desired rate (Fig. 1-3). Such formulations provide the possibility to mask unpleasant-tasting agents and protect acid-labile drugs from degradation in the stomach media of low pH.

1.3.3 Diffusion-Controlled Systems

1.3.3.1 Monolithic Devices

A variety of traditional implants and some of the simplest microparticulate formulations fall into the category of monolithic diffusion controlled systems.

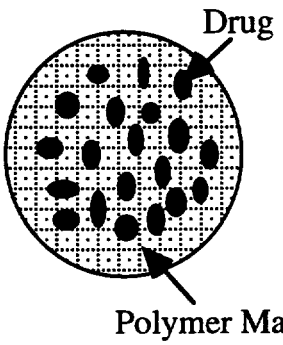

Fig. 1-4 Schematic diagram of of a monolithic device.

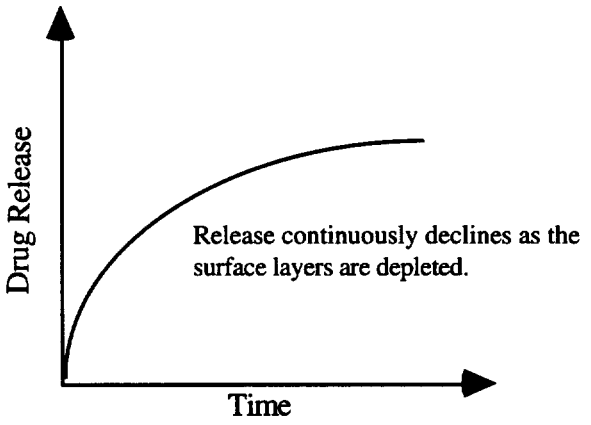

Fig. 1-5 Schematic diagram of release profile for a simple monolithic device.

Usually the agent is homogeneously dissolved or dispersed throughout a hydrophilic or hydrophobic polymer matrix (Fig. 1-4). Most models agree that the release rate of drug will fall in proportion to the inverse of the square root of time (Fig. 1-5).

Monolithic devices have found many applications not only in traditional implant delivery but also in the oral delivery, despite the fact that device diffusion geometry changes cause variation in drug release rates. Their application in transdermal delivery have been successful.

1.3.3.2 Reservoir Devices

Similar to encapsulation systems, the agent is totally contained within a rate-controlling membrane in reservoir devices (Fig. 1-6). With such a system, the release rate can be constant as long as a constant thermodynamic activity of the diffusant is maintained within the device. This allows for zero-order release kinetics. However, device fabrication is usually more expensive and difficult than for a monolithic system. The release character is where the release rate is dependent on the thickness, surface area and permeability of the membrane barrier (Fig. 1-7).

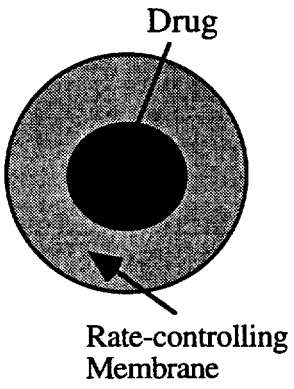

Fig. 1-6 Schematic diagram of a simple reservoir device.

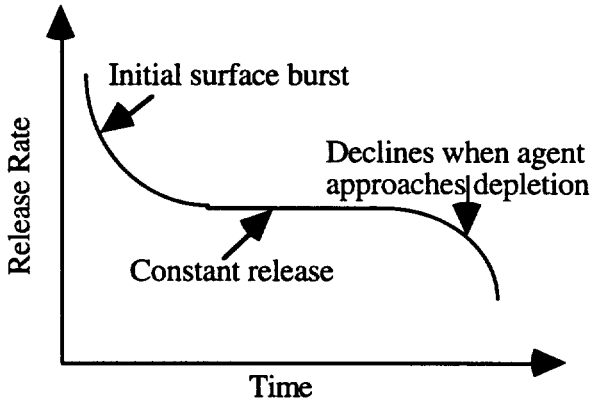

Fig. 1-7 Schematic diagram of release profile for a simple reservoir device.

Membrane diffusion-controlled devices are a more sophisticated development of simple barrier coatings. Parenteral devices of this type can be divided into solid implant and microcapsules.

Microencapsulation involves enclosure of the bioactive agent in solid, liquid, or gaseous form, within a non-porous or semi-permeable membrane that can be made from a variety of natural or synthetic polymers. Some type of multicomponent micro-encapsulates are relatively sophisticated, (Fig. 1-8).

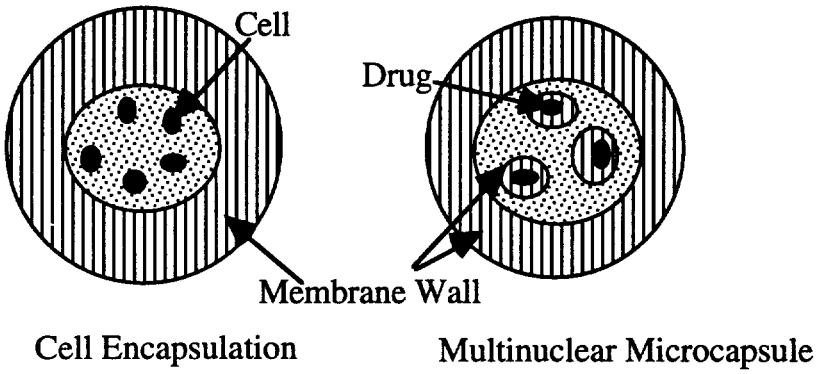

Fig. 1-8 Schematic diagram of complex microencapsulation systems.

Among the most interesting for these systems have been those developed for micro-encapsulation of cells for release of cell products (e.g., insulin, dopamine). These technologies facilitate in vitro scale-up production of cell products, and also allow cells to survive within a foreign organism within a protective barrier, permitting them to produce bioactive molecules which escape the capsule and exert a therapeutic effect, with controlled release of product.

Microcapsulation has been applied successfully for both oral and transdermal drug delivery. Nevertheless, it can be difficult to fabricate uniform and reproducible coatings to maintain desired release rates and avoid premature dumping of the entrapped drugs.

1.3.4 Biodegradable Systems

Some natural and synthetic polymer systems are biodegrade when they are exposed to water or to enzymes in the body. Using these polymers, it is possible to program the release of entrapped agents by controlling the erosion of materials comprising the device. One class of biodegradable polymers is termed "surface eroding". These polymers degrade from their outer, exposed surface inward, providing a decreasing surface area with time which determines their release properties. Another and more common class of biodegradable polymers is termed "bulk eroding". Devices made from these polymers initially have a period of slow erosion, and subsequently increase the degradation rate rapidly throughout the entire matrix until the bulk is eroded. This type of polymer is usually used to make reservoir or monolithic diffusion-controlled systems that degrade after their delivery role is over. Some devices can deliver an agent by a combination of both diffusion and degradation as shown in Fig. 1-9.

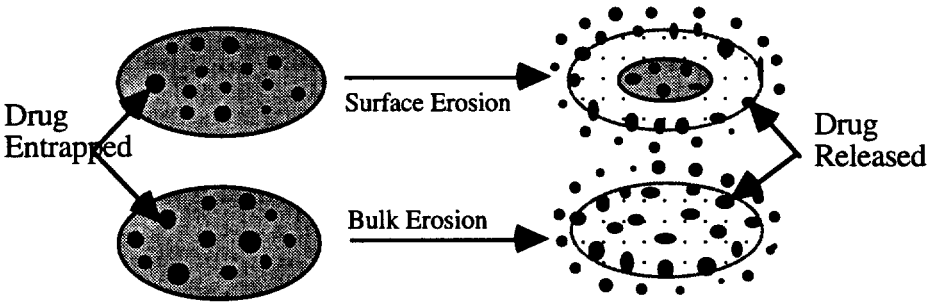

Fig. 1-9 Schematic diagram of surface and bulk erosion for biodegradable systems.

Other controlled delivery systems include liposomes (lipid vesicles) and microparticle devices, soluble macromolecule devices (i.e., polymer-drug, protein-drug, antibody-drug conjugates), bioadhesive devices, and cleavable prodrugs. Detailed descriptions of these systems can be found in the literature listed at the end of this chapter.

1.4. Pulsatile and Self-Regulated Delivery Systems

Recent studies in the field of chronopharmacology have shown that the onset of certain diseases exhibits strong circadian temporal dependency. Thus, conventional controlled delivery approaches for delivery of agents such as insulin for patients with diabetes mellitus, antiarrhythmics for heart rhythm disorders, hormones for birth control, general hormone replacement, immunization, and cancer chemotherapy would be inappropriate or insufficient. These drug delivery patterns could be achieved using pulsatile or self-regulated delivery systems which can minic the control and feedback of natural physiological rhythms.

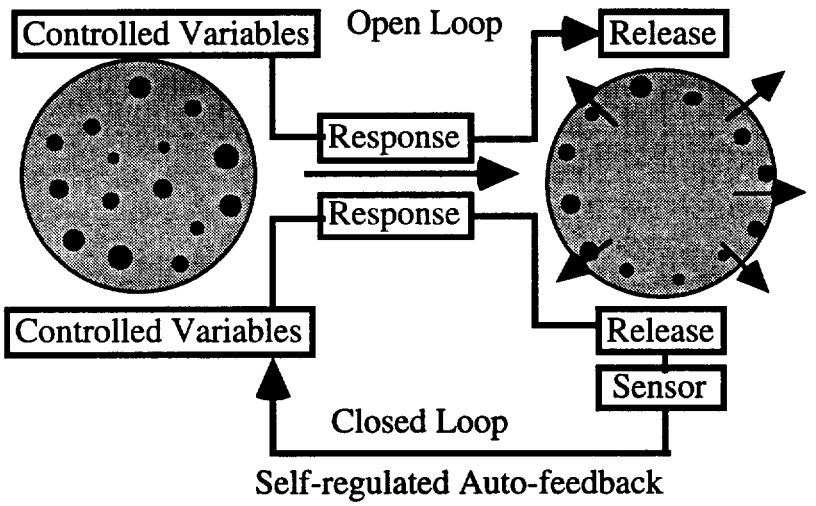

Fig. 1-10 Schematic diagram of open-loop and closed-loop controlled delivery.

Pulsatile and self-regulated controlled delivery systems can be classified as open or closed-loop systems (Fig. 1-10). Open-loop control systems, known as external stimuli-responsive devices, are those in which information about the control variable is not automatically used to adjust the system inputs to compensate for the change in the process variable but instead are controlled externally. Closed-loop control systems, known as self-regulated or auto-feedback devices, detect the controlled variables and, as a result, the

system output is adjusted accordingly. External stimuli which have been studied include thermal, pH, ionic strength, light, magnetic, electric, and ultrasonic. Self-regulated controlled delivery systems utilize several environmentally reponsive polymers, chemical and biochemical reaction sequences such as enzyme-substrate reactions, pH-sensitive polymer/drug characters, competitive binding, and metal concentration-dependent hydrolysis, to accomplish delivery rate control.

1.5 Hydrogel Controlled Delivery Systems

Hydrogels are crosslinked hydrophilic polymer networks able to retain high amounts of water, forming a swollen gel phase which cannot dissolve. The combination of high water content with water insolubility makes these materials well-suited to a number of applications in biomedical and pharmaceutical areas. When used as implants, the rubbery nature of the hydrated hydrogels has been found to minimize mechanical irritation to surrounding tissue. The low interfacial tension between the hydrogel surface and aqueous media has been found to decrease protein adsorption and cell adhesion problems. More specifically, there have been considerable interests in exploiting the properties of hydrogel for applications in the field of controlled delivery,

The fundamental building blocks of hydrogels are monomers which may range from hydrophilic to mildly hydrophobic. The monomer composition of copolymer networks as well as their crosslinking density can be manipulated to alter many physicochemical properties of hydrogels important to controlled delivery applications including loading, diffusivity, swelling equilibrium, and mechanical strength.

1.5.1 Structure and Physicochemical Properties of Hydrogels

1.5.1.1 Thermodynamics of Hydrogel Swelling Behavior

Theoretical treatments of polymer network swelling are based on thermodynamic descriptions of the two counterbalancing forces: swelling forces from polymer-solvent interactions and retractive mechanical forces of the network. According to classical Flory and co-workers' treatments, the free energy change due to swelling may be described as the sum of the change due to mixing of the polymer with the solvent, plus the change in elastic free energy due to deformation of the network, both of which can be calculated, respectively. Although the original Flory theory has been widely adopted, both polymer solution thermodynamics and network theory are still the areas of active research interest now and very few current theories are successful. Copolymers represent a step of even further complexity and approaches used to model these networks will be reviewed in Chapter 3.

1.5.2 Methods of Hydrogel Preparation

1.5.2.1 Addition Polymerization

Addition polymerization is a familiar mechanism used for vinyl and related monomer polymerization. Common hydrophilic monomers used to prepare hydrogels by this mechanism include N-substituted methacrylate, acrylamide, acrylate, and crosslinkers. Addition polymerization is usually initiated by free radical initiators in solution or as bulk systems.

1.5.2.2 Condensation Polymerization

Condensation polymerization techniques are used to form hydrophilic polyurethane, polyester, and polyamide networks. Some types of these networks have varying susceptibility to hydrolysis which can also be utilized for biodegradable controlled delivery.

Other polymerization methods such as bulk polymerization are not frequently utilized for hydrogel preparation due to the difficulty of controlling network crosslinking.

1.5.2.3 Preparation from Pre-formed Water-Soluble Polymers

One convenient way to prepare hydrogels is to crosslink water-soluble polymers. Polymers with pendent -OH groups can be crosslinked with a variety of bifunctional agents such as glutaraldehyde or adipic acid. Ionizing radiation, such as $^{60}C_O$-γ or electron beams also can be used to crosslink water-soluble polymers.

1.5.2.4 Purification

Hydrogels must undergo a purification procedure to remove unreacted monomers, traces of initiator, and side products for biomedical and pharmaceutical applications. Solvent extraction or dialysis by water is commonly the method of choice. However, hydrophobic co-monomers can be extracted by other solvents.

1.5.3 Diffusion in Hydrogels and their Controlled Delivery Applications

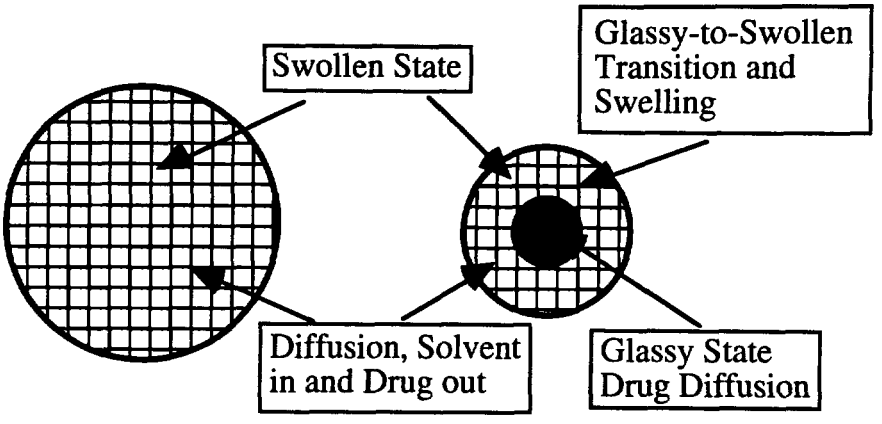

Fig. 1-11 Schematic diagram of hydrogel controlled delivery system.

The most common drug release mechanism for hydrogels is passive diffusion driven by the concentration gradient of the drug between the device and external medium. A distinction has been made between completely swollen state and glassy-to-swollen state-mediated diffusion mechanisms, and essentially, their diffusivities are different (Fig. 1-1).

1.5.3.1 Diffusion in the Swollen State

1.5.3.1.1 Diffusion and Release Kinetics

Historically, Fick's Law, $J = D_{i,eff}(\partial C_i / \partial X_i)$ is considered to govern diffusive transport in swollen gels. The most important parameter is the drug diffusion coefficient which is determined by many factors, such as network structure and properties, water content, and drug properties. Diffusion of small molecules in hydrogels is most often treated by the free volume approach. In the free-volume model, the volume of the polymer is assumed to be apportioned between the occupied volume of the polymer molecules themselves and the free volume left unoccupied. The latter consists of interstitial free volume between chains, inherent in the closest packing arrangement of the molecules, and

the free hole volume. The theories assume that the free hole volume can be redistributed (e.g., chain swelling and relaxation) as needed for transport. For a swollen polymer, the solvent also contributes occupied and free volume to the system. The general expression for diffusion coefficients by this theory is

$$D = (\text{preexponential term}) \exp\{-(\text{penetrant volume})/(\text{free volume})\}$$

The free-volume approach can have considerable predictive power. However, for dealing with large molecules (solutes) and heterogeneous systems, more modifications and refinements are needed.

Release of a drug from a swollen hydrogel can be described by the solution to the diffusion equations with the appropriate geometry and boundary conditions:

$$\partial C/\partial t = D\,(\partial^2 C/\partial X^2).$$

The solution to the diffusion equation gives concentration as a function of position and time. Normally, a scaling relationship between time, physical dimensions, and amount released exists.

1.5.3.2 Diffusion in Initially Glassy Gels

1.5.3.2.1 Swelling Controlled Delivery Systems

During gel swelling processes, drug release is primarily governed by the swelling kinetics rather than drug diffusion: drug diffusivity increases many orders of magnitude by polymer network swelling. A further complication is that the behavior of glassy polymers placed in a swelling solvent is not well describled by Fick's law. Instead, Case-II transport which is dependent on molecular relaxation of the polymer chains is widely used. In a

swelling-controlled delivery system, the polymer swells relatively slowly, preferably by a Case-II mechanism. The slow swelling process results in growth of a highly permeable gel layer on the outside of the polymer device, while the interior of the polymer remain glassy (unsolvated). Diffusion of the drug in the gel layer is relatively rapid; thus, swelling is the rate-determining process. In this case, constant rate of release (zero-order kinetics) is possible.

1.5.3.2.2 Swelling and Diffusion Controlled Delivery Systems

Three basic release profiles in hydrogels have been predicted and are schematically shown in Fig. 1-12. In reality, most hydrogel swelling behavior is anomalous (type 2) where both diffusion (type1) and polymer molecular relaxation (type 3) exist together but neither completely predominates.

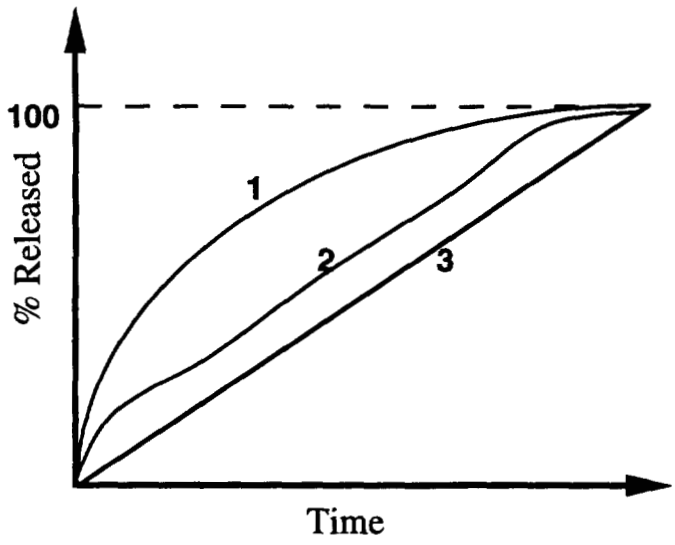

Fig. 1-12 Model release profiles in hydrogels
(1) diffusion controlled; (2) swelling and diffusion controlled; and (3) swelling controlled.

1.5.4 Stimuli-Responsive Hydrogel Controlled Delivery Systems

Some hydrogels undergo phase transitions and demonstrate large swelling-deswelling changes in response to external stimuli such as light, temperature, pH, ionic strength, solvent, and electric field. The phase transition of a hydrogel is manifested by a reversible, discontinuous collapse and expansion of the polymer network as depicted in Fig. 1-13.

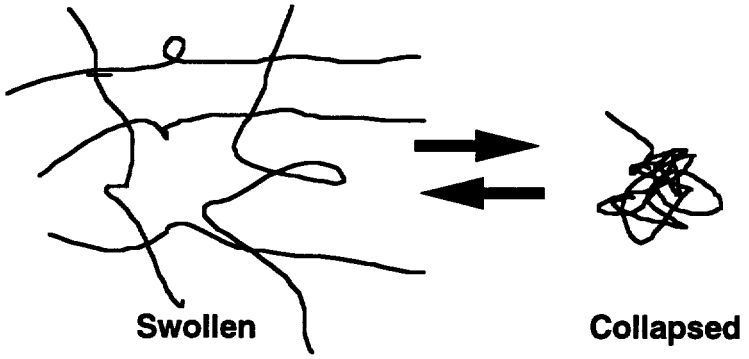

Fig. 1-13 Schematic diagram of gel phase transition.

Four fundamental inter- or intra-molecular interactions are responsible for hydrogel phase transitions:.van der Waals interactions, hydrophobic interactions, hydrogen bonding, and electrostatic attraction Both repulsive and attractive interactions and their balance of competing interactions influenced by the externally applied stimuli are essential driving forces for a gel to undergo a phase transition.

Recently, pulsatile and self-regulated controlled drug delivery have been attempted using stimuli-responsive hydrogels. Temperature- and pH-responsive hydrogels based on crosslinked poly(N-isopropylacrylamide) (PNiPAAm) systems have receieved great attention both scientifically and technologically. Temperature-induced collapse of PNiPAAm gels is analogous to the lower critical solution temperature observed for PNiPAAm near 33°C in aqueous polymer solutions, and to the coil-globule transition of a single polymer chain in solution. For a hydrogel with ionizable groups, gel swelling

changes drastically when ionization state of groups in the gels changes. This alters the gel's specific solute interaction and swelling equilibrium, changing gel water content and swelling. The potential application of these systems for controlled delivery is being actively investigated.

1.6 Objectives of This Research

New scientific developments in many fields related to biomedical and pharmaceutical science now allow exploration of more advanced and complex strategies for controlled drug delivery. Two distinct general research approaches are commonly chosen: one is a basic research approach to validate the concepts underlying controlled delivery for various active species, while another one is a research and development approach, pursuring a single technology with the sole goal of developing a specific delivery system for commercial use with a chosen bioactive agent.

The main impetus for this research is to utilize novel thermal swelling behavior of poly(N-isopropylacrylamide) (PNiPAAm) gels in aqueous media with application to controlled delivery (pulsatile and sustained delivery) of macromolecular drugs, such as polypeptides and protein drugs. Techniques and principle from polymer and biomaterial sciences as well as pharmaceutical science were used to accomplish the following research goals:

(1) Synthesis and physicochemical characterization of new ionizable poly(N-isopropylacrylamide) hydrogels.

(2) Synthesis and characterization of novel thermo- and pH-responsive amphiphlic networks based on poly(N-isopropylacrylamide) systems.

(3) Controlled delivery (pulsatile and sustained) studies using model small and large molecular weight bioactive species with new polymers developed in this research.

(4) Theoretical modeling studies of release kinetics based on multicomponent controlled diffusion treatments.

Topical References

1. Drug Delivery Strategies

Borchardt, R. T., Repta, A. J. and Stella, V. J., *Drug Delivery: A Multi-disciplinary Problem*, Humana Press, Clifton (1985).

Chien, T. Y., *Novel Drug Delivery Systems,* Marcel Dekker, New York (1982).

Christel, P., Meunier, A. and Lee, A. J. C. (Eds), *Biological and Biomechemical Performance of Biomaterials*, Elsevier, Amsterdam (1987).

Davis, S. S., Illum, L., and Tomlinson, E., (Eds), *Delivery Systems for Peptide Drugs, Plenum*, New York (1987).

Ferruti, P. and Tanzi, M. C., *New Polymeric and Oligomeric Matrices as Drug Carriers.*, CRC Crit. Rev. Ther. Drug Carri. Syst., 2, 175 (1986).

Freeman, A. I. and Mayhew, E., *Targeted Drug Delivery.*, Cancer, 58, 573 (1986).

Heller, J., *Self-regulated Drug Delivery Systems*, Med. Devi. and Diagn. Ind., 7, 33 (1985).

Illum, L. and Davis, S. S. (Eds), *Polymers in Controlled Drug Delivery*, IOP Publishing Ltd., Bristol (1987).

Johnson, P. and Lloyd-Jones, J. G., *Drug Delivery Systems*, Ellis Horwood Ltd., Bristol (1987).

Koettig, S., Hahn, H. J., Famr, F. and Fluether, F. V., *Controlled Release Dosage Forms: Evaluation of Their Efficacy with Special Regard to Therapeutic Aspects*, Pharmazie, 43, 58 (1988).

Kost, J. (Ed.), *Pulsed and Self-Regulated Drug Delivery*, CRC Press, Boca Raton (1990).

Langer, R. S. and Wise, D. L. (Eds), *Medical Applications of Controlled Release*, Vol.1 and 2, CRC Press, Boca Raton (1984).

Levy, G., *Targeted Drug Delivery - Some Pharmacokinetic Considerations*, Pharm. Res., 4, 3 (1987).

Lee, V. H. L., *Peptide and Protein Drug Delivery Systems*, Biopharm, March, 24 (1988).

Pouton, C. W., *Drug-Targeting- Current Aspects and Future Prospects,* J. Clin. Hosp. Pharm., 10, 45 (1985).

Reilly, R. and Sheldon, K., *Monoclonal Antibody in Cancer Diagnosis and Therapy,* Can. J. Hosp. Pharm., 40, 209 (1987).

Robinson, J. R. and Lee, V. H. L. (Eds), *Controlled Drug Delivery, Fundamentals and Applications*, 2nd Edition, Marcel Dekker Inc., New York (1987).

Roche, E. B. (Ed), *Bioreversable Carrier in Drug Design Theory and Application*, Pergamon, New York (1987).

Rubinstein, M. H. (Ed), *Pharmaceutical Technology: Controlled Drug Release* Vol.1, Ellis Horwood Ltd., Chichester (1987).

Tomlinson, E., *Theory and Practice of Site-Specific Delivery*, Adv. Drug Delivery Rev. 1, 87 1987).

Tyle, P. (Ed), *Drug Delivery Devices*, Marcel Dekker Inc., New York (1988).

Vanbrunt, J., *Novel Drug Delivery Systems*, Biotechnol., 7, 127 (1989).

2. Drug Delivery Systems as Biomaterials

DeRossi, D., Kajiwara, K., Osada, Y. and Yamauchi, A. (Eds), *Polymer Gels*, Plenum, New York (1991).

Gebelein, C. G., (Ed), *Advances in Biomedical Polymers*, Plenum, New York (1985).

Gebelein, C. G. and Carraher, C. E., *Bioactive Polymeric Systems: An Overview, Plenum*, New York (1985).

Hoffman, A. S., in *Polymer Gels*, DeRossi, D, Kajiwara, K., Osada, Y. and Yamauchi, A. (Eds), Plenum, New York, 289 (1991)

Hoffman, A. S., Afrassiabi, A. and Dong, L. C., *Thermally Reversable Hydrogels: Delivery and Selective Removal of Substances from Aqueous Solutions*, J. Contr. Rel., 4, 213 (1986).

Kim, S. W., Bae, Y. H., and Okano, T., *Hydrogels: Swelling, Drug Loading, and Release*. Pharm. Res., 9, 283, (1992).

Kramer, O. (Ed.), *Biological and Synthetic Polymer Networks*, Elsevier, New York (1988).

Molyneux, P., *Water Soluble Synthetic Polymers: Properties and Behavior,* Vol. 1 and 2, CRC Press, Boca Raton (1984).

Pizzoferato, A., Marchetti, P. G., Ravaglioli, A., and Lee, A. J. C., *Biomaterials and Clinical Applications*, Elsevier and Science Publishers B. V., Amsterdam (1987).

Peppas, N. A. (Ed.), *Hydrogels in Medicine and Pharmacy*, Vol. 1 and 2, CRC Press, Boca Raton (1986).

Ratner, B. D., *Surface Characterization of Biomaterials, Progress in Biomedical Engineering*, Vol. 6, Elsevier, Amsterdam (1989).

Seymour, R. B. and Mark, H. F. (Eds), *Application of Polymers.*, Plenum, New York (1987).

3. Theoretical Discussions

Crank, J. M., *The Mathematics of Diffusion*, Clarendon Press, Oxford (1975)

Cussler, E. L., Diffusion, *Mass Transfer in Fluid Systems*, Cambridge University Press, New York (1984)

Flory, P. J., *Principle of Polymer Chemistry*, Cornell University Press, Ithaca, NY (1953)

Tanaka, T., Gels, in *Encyclopedia of Polymer Science*, Vol. 2, 2nd Ed., Wiley Interscience, New York, 515 (1987).

Yasuda, H. and Lamaze, C. E., *Permselectivity of Solutes in Homogeneous Water-Swollen Polymer Membranes*, J. Macromol. Sci. Phys. B5, 111 (1971).

Chapter 2 Thermo-Sensitive Swelling Behavior in Crosslinked N-isopropylacrylamide Networks: Cationic, Anionic and Ampholytic Hydrogels

2.1 Introduction

A number of water-soluble polymer systems--poly(methyl methacrylic acid) (1), poly(vinyl alcohol-co-ethylacetate) (2), poly(ethylene oxide) (3), and N-isopropylacrylamide (4,5)--demonstrate critical behavior leading to phase separation from solution at elevated temperatures. The temperature characteristic of this event for each system is termed the Lower Critical Solution Temperature (LCST) and has been analyzed in terms of a large negative entropy change in the water-swollen polymer network at this critical point. Phase separation is usually manifested as a large, discontinuous volume change of polymer coils (collapse) and precipitation from solution.

N-isopropylacrylamide (NiPAAm) hydrogels demonstrate a nearly continuous (diffuse first order or second order) volume transition and associated phase transition from a low temperature, highly swollen gel network to a collapsed, higher temperature phase near its critical point between 31-35°C (4-6). The phase transition in gels is analogous to, though fundamentally distinct from, the LCST of its linear, soluble form and has been identified with the increase in entropy of the solvent--water--in the polymer network with increasing temperature, compensating for the decrease in entropy of the relatively hydrophobic polymer network as it collapses near the critical point (7). The overall contribution to the free energy of the gel system is negative, leading to this spontaneous and reversible behavior at this critical temperature.

Recently, efforts to incorporate hydrophilic (8,9), hydrophobic (10), and amphiphilic co-monomers (11), as well as build interpenetrating networks (IPNs) (12,13) into NiPAAm systems have been reported for various applications as well as fundamental studies on its critical behavior. This has been followed by recent efforts to characterize the LCST of water-soluble linear NiPAAm solutions in the presence of various co-dissolved solutes, including salts and ionic polymers (14,15).

Gel phase transitions, by contrast, are critically dependent on gel composition: all efforts have shown that increasing the amount of co-monomer in the system, whether by IPN incorporation or by direct copolymerization, increases the critical point of each system and broadens the temperature range of the transition. At sufficiently high contents of co-monomers or other network additives, critical behavior is no longer observed. Moreover, addition of salts to soluble NiPAAm depresses its LCST.

NiPAAm gels containing sodium acrylate (SA) in pure water have been studied previously by Tanaka and coworkers (5,16-18). Their results have indicated that incorporation of small amounts of anionic SA (0-2 mM) into NiPAAm networks produces continuous swelling transitions in macroscopic gels at critical temperatures, while higher SA contents elicit a discontinuous swelling transition. Moreover, the gel transition temperature increases monotonically as a function of SA content. Volume changes associated with gel transitions dramatically increase as a function of increasing SA content, indicating the effect of ionized groups within the hydrogel network. NiPAAm gels containing cationic co-monomers have also been reported (19,20). Swelling behaviors for these systems generally reflect the influence of the basic co-monomer in broadening the NiPAAm swelling transition over all pH ranges, although some large pH-induced increases in swelling ratio are observed with pH-sensitive cationic co-monomers (19). Most recently, acrylamide ampholyte hydrogels containing both sodium styrene sulfonate and methacrylamidopropyl trimethylammonium chloride (MAT) as oppositely charged ionic co-monomers have also been recently reported (21). These gels show asymmetric swelling behavior in aqueous salt solutions, demonstrating higher swelling ratios in ampholyte gels of high cationic monomer content than for similarly prepared gels containing anionic monomer. The hydrophobicity of anionic styrene sulfonate was rationalized to inhibit swelling in the net anionic ampholyte gels and produce swelling asymmetry through a number of mechanisms. As co-monomer ratios approach unity, ampholyte gels were

observed to approach a single swelling ratio at higher ionic strengths, indicating that charge screening becomes a dominant effect governing gel swelling.

Okano and coworkers have published extensively about the behavior and properties of various NiPAAm gels in aqueous media (6,10,12,13,22-26). One significant feature reported regards formation of a collapsed NiPAAm skin layer on the hydrogel surface above the critical temperature for these gels (18,22-27). This skin thickens with time above the critical temperature to become rate-limiting to water permeation or flux out of the gel as it attempts to collapse at temperatures above the critical temperature. A hydrostatic pressure gradient develops in these collapsing gels, resulting in a dynamic surface rupture, or alternatively, a slow outward *water permeation through the skin which can last for months* until collapsed state equilibrium is reached (28). Surface skin formation in NiPAAm copolymers have shown to be influenced by co-monomer content. Hydrophobic co-monomers, including N-alkyl methacrylates, show a chain length dependence on NiPAAm skin properties (23-27). Novel solute release properties of these copolymer gels, including reversible on-off switching and pulsatile release kinetics (10,22-27) are relevant to a number of pharmaceutical and materials engineering interests.

The present work has been motivated by the interest in **effecting rapid discontinuous transitions in hydrogels with increased volume changes** over those observed for pure NiPAAm. The efforts have been directed at modulating the NiPAAm skin layer which forms on the gel surface as the network starts to collapse with increasing temperature. Incorporation of co-monomers into NiPAAm networks influences the structure of the collapsed network and its permeability and barrier properties. Additionally, the effects of different charged species in NiPAAm networks--anionic, cationic, and ampholytic gel networks--on gel swelling and collapse have been compared. The aqueous swelling behavior of crosslinked NiPAAm copolymer networks containing small amounts of either anionic sodium acrylate (SA) or cationic methacrylamidopropyl

trimethylamine (MAT), or both species as co-monomers have been reported in this chapter. The effects of charged co-monomers on thermal, ionic strength, pH, and compositionally dependent NiPAAm gel properties have been investigated. Addition of minute amounts of ionic co-monomers to NiPAAm networks produces hydrogel systems with greatly enhanced swelling ratios while retaining critical behavior. Incorporation of only 0.5 to 5 mol% of the anionic SA or cationic MAT produces marked influences on both swelling and collapse equilibrium states and kinetics of these processes over homopolymer NiPAAm gel systems. Ampholyte NiPAAm gels containing ratios of each co-monomer produce gels with charge compensated swelling behavior.

2.2 Experimental

2.2.1 Materials

All solvents used were reagent grade. NiPAAm monomer (Eastman-Kodak) was recrystallized twice from hexane/benzene (4:6 ratio). Sodium acrylate (SA, Pfaltz & Bauer) was used as received. Methylene-bis-acrylamide (MBAAm, Aldrich) was recrystallized from ethanol. Tetramethylethylenediamine (TEMED) and ammonium persulfate were both obtained from Aldrich and used as received. Methacrylamidopropyl trimethylammonium chloride (MAT) was purchased from Polysciences as a 50 wt% aqueous solution and used as received. All buffer salts and solutes were reagent grade compounds. Water for buffers and gel swelling was first reverse-osmosis filtered (deionized) and then Millipore filtered to yield purified water having 18 MΩ/cm resistivity.

2.2.2 Copolymer Gel Fabrication

NiPAAm-co-SA, NiPAAM-co-MAT, and NiPAAM-co-SA-co-MAT hydrogels were synthesized using MBAAm as a crosslinking agent. For aqueous redox polymerizations, ammonium persulfate and TEMED were used as initiators in a procedure adapted from that used by Hoffman and coworkers (29). Aqueous solutions of mixed monomers of NiPAAm and SA, MAT, or SA/MAT were made in nitrogen-bubbled Millipore water in a series of compositions (NiPAAm/SA, NiPAAm/MAT, and NiPAAm/SA/MAT mole ratios: 100:0, 99.5:0.5, 99:1, 98:2, 97:3, 96:4, 95:5, 90:10) and concentrations (5.0, 7.5, 10.0, 12.5, 15 mol% total monomer content in water). A range of MBAAm concentrations (0.5, 0.7, 1.0, 1.2, 1.5, and 2 mol%) were used with the monomer solutions. Before the addition of ammonium persulfate, TEMED was mixed into the aqueous solutions and bubbled with nitrogen for 15 minutes. The complete mixtures were injected between clean glass plates separated by 2 mm thick gaskets (2 mm OD crosslinked silicone rubber O-ring material) with care taken to avoid the introduction of air bubbles into the gel after adding AP. The plates were clamped securely and suspended in a water bath at 20°C for one hour. The resulting hydrogel films were then separated from the plates and allowed to swell in deionized water/ethanol (30% alcohol) for 3 days, followed by swelling in pure deionized water for one week. Swollen copolymer hydrogel membranes were subsequently cut into disks of 1 cm diameter using a cork borer, dried ambiently for one day, and under vacuum for three days at room temperature.

2.2.3 Swelling Measurements

For measurements across a range of pH conditions, a series of buffers with maximum buffering capacities at various pH values were made. Potassium phthalate (pH 3), sodium acetate (pH 5), phosphate (pH 7-9), Tris (pH 8-10), and borate (pH 10) buffers

were made in a series of ionic strengths as stocks in stoppered, acid-cleaned flasks. Small amounts of 0.1 N NaOH or HCl were added to adjust final buffer pH. Dried hydrogel disks were initially immersed and equilibrated in buffer solutions in glass vials at 20°C for two days. These vials were in turn immersed in a shaking water bath (American Scientific Model YB-521) at a series of temperatures from 20 to 70°C for 2 hours. Each sample was then removed from the water bath and from its respective vial, tapped with a dampened Kim-wipe towel to remove excess surface water, and weighed directly using an electrobalance (Ohaus GA200D). The dry weights were measured on the same balance after desiccating the same gels for 3 days under vacuum at room temperature until constant dry weights were maintained. Swelling ratios (S.R.) were calculated from the following formula:

$$\text{S.R.} = \text{(wet weight - dry weight)/(dry weight) or } (W_t - W_d)/W_d \qquad [2\text{-}1]$$

Water content in gels as a function of temperature was calculated as:

$$\% \text{ water} = (W_t - W_d)/(W_0 - W_d) \qquad [2\text{-}2]$$

where W_t = gel weight at temperature, t, W_d = gel dry weight, and W_0 = fully hydrated weight of gel.

Swelling measurements were determined as a function of SA, MAT, or SA/MAT content, MBAAm crosslink content, pH, ionic strength, monomer concentration during polymerization, and temperature.

3.1 Results and Discussion

It should be noted here that experimental techniques used in this work contrast work by others in observing critical behavior in NiPAAm gels. Most other work reported for

this gel has examined temperature dependent behavior by approaching the critical point from higher temperatures--that is, observing the collapsed-to-swollen state transition by cooling. We report temperature-dependent swelling by warming gels from fully swollen states below the critical point and incubating at elevated temperatures for 2 hours before measuring swelling changes. These two methods will produce different results for gel swelling/deswelling kinetics (18).

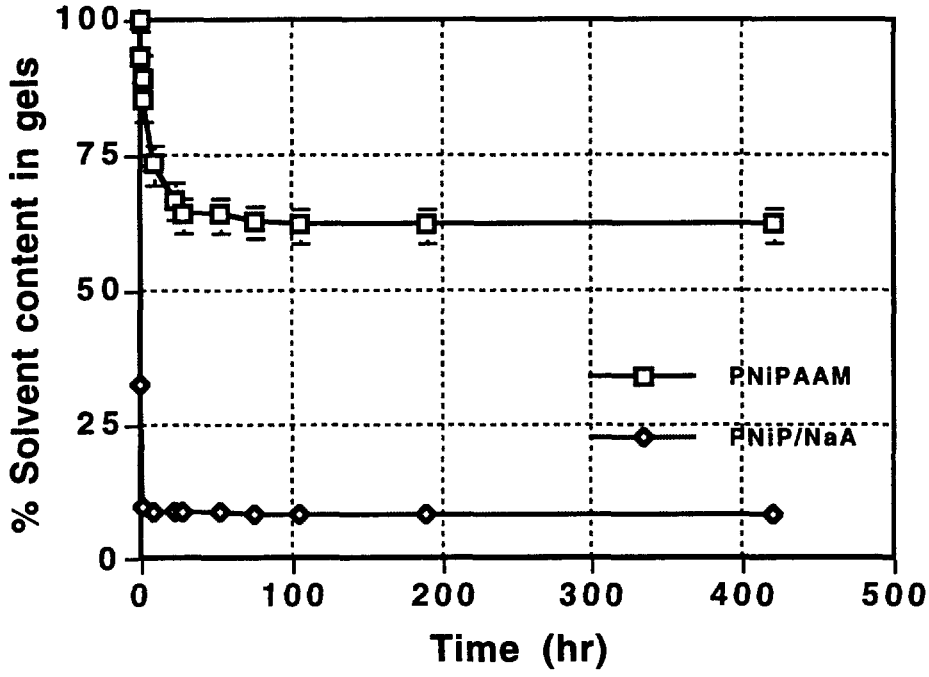

Fig. 2-1 Contrasting collapse kinetics between 100% NiPAAm and NiPAAm/SA (97:3) hydrogels at pH 7 (0.1M PBS buffer) undergoing thermal transition from 20 to 40 °C.

Figure 2-1 shows the differences between pure NiPAAm gel collapse and that for NiPAAM/SA 97:3 after a temperature jump from swollen (20°C) to deswollen (40°C) states as a function of time. The anionic NiPAAm gel shows a very rapid collapse directly to equilibrium within a few minutes, while the kinetics for pure NiPAAm are orders of magnitude slower (18) and equilibrium is achieved only after long times. For ionic gels, swelling-collapse equilibria are achieved well within the 2 hour incubation times for these

measurements. *Formation of the collapsed NiPAAm skin on the gel surfaces directly influences these kinetics and will be addressed later in detail.*

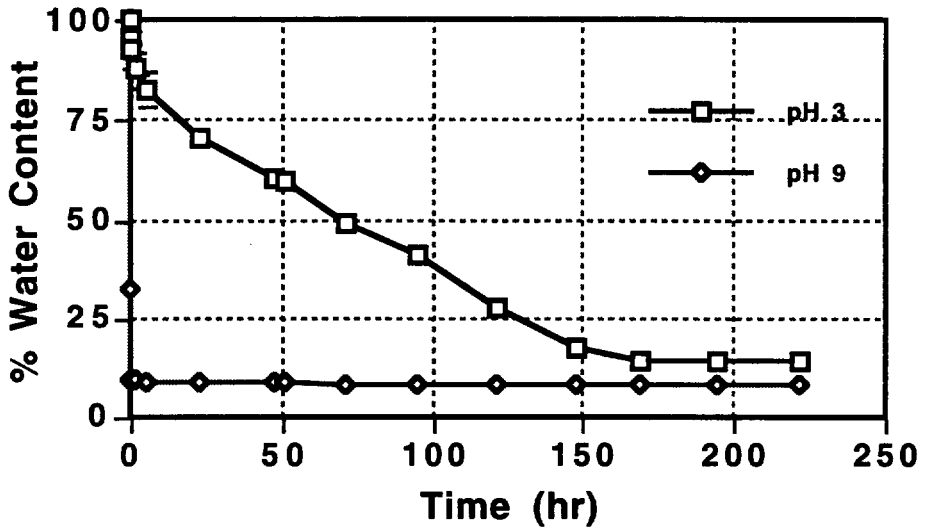

Fig. 2-2 Swelling behavior of poly (NiPAAm-co-SA, 97/5) hydrogels undergoing thermo-transition from 25 to 40°C in different pH media.

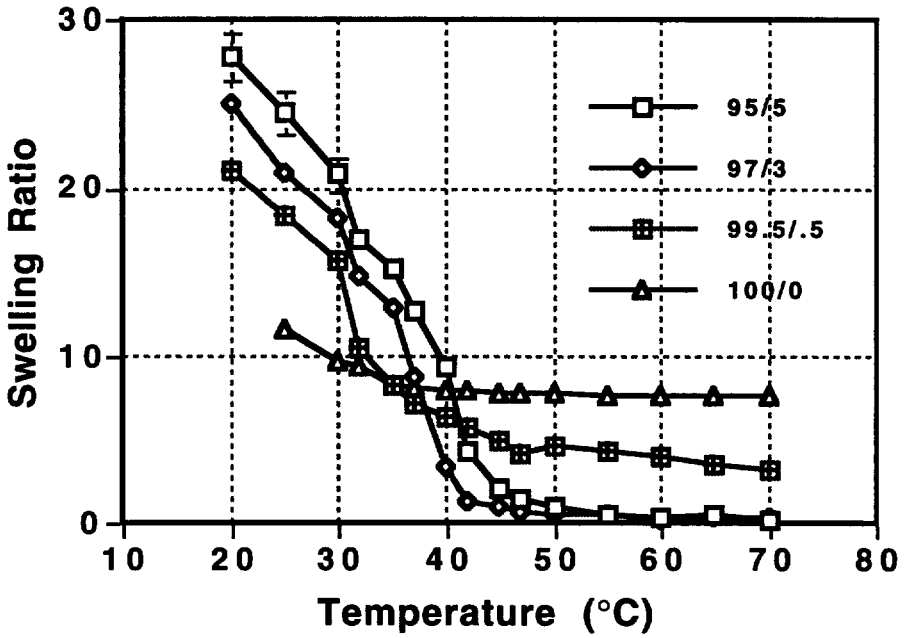

Fig. 2-3 Swelling behavior of anionic NiPAAm copolymer hydrogels containing various amounts of sodium acrylate comonomer at pH 8 as a function of temperature. Buffer: Tris, 50 mM.

Changing pH with constant osmolarity should influence the protonation of only SA groups in the NiPAAm gels. Changes in gel swelling, therefore, should reflect SA ionization and both SA and MAT content in the NiPAAm gel networks. As shown in Figure 2-2, anionic NiPAAm gels undergo temperature-induced transition from 25 to 40 °C at both pH 3 and pH 9. The deswelling kinetics of protonated NiPAAm/SA gels (at pH 3) are very slow but still approach the same dehydrated final state as the ionized NiPAAm/SA gels (at pH 9). These data show the ability of ionized SA in accelerating NiPAAm copolymer gel swelling: low pH protonates the SA, neutralizing the network and promoting behavior close to pure NiPAAm. In Figure 2-3, pure NiPAAm, as a reference, shows very limited collapse behavior upon heating at pH 7 in contrast to that already reported for cooling (9). The pure NiPAAm gel shows an initial swelling ratio of nearly 12 at 20°C which decreases to approximately 8.5 above 35°C (350% decrease in swelling). Qualitatively, the gel goes from a transparent disc at low temperature to a smaller, condensed white, opaque disc above the critical point. Both of these swelling results for pure NiPAAm gels are independent of buffer or pH--that is, roughly equivalent NiPAAm swelling behavior is observed in all buffer systems presented herein.

Incorporation of the anionic co-monomer, SA, produces swelling ratios which increase drastically at all pH values over that seen for pure NiPAAm. At pH 8 (Figure 2-3), relatively high levels of SA incorporation (95:5 mole ratio) demonstrate maximum swelling capability (S.R.=28) at low temperature as well as the maximum transition to a collapsed state above the transition (S.R.~1). Also notable is the fact that the addition of only minute amounts of SA co-monomer (0.5 mol%) radically changes the swelling behavior of the gels over pure NiPAAm without changing the critical point. The hierarchy of swelling at this and all pH values is directly related to SA content, with the gel of lowest SA ratio (99.5:0.5) showing lowest swelling ratios at low temperature and lowest degree of collapse at higher temperatures. Nevertheless, all anionic gel swelling behaviors are substantially greater than those observed for pure NiPAAm gels over these time courses.

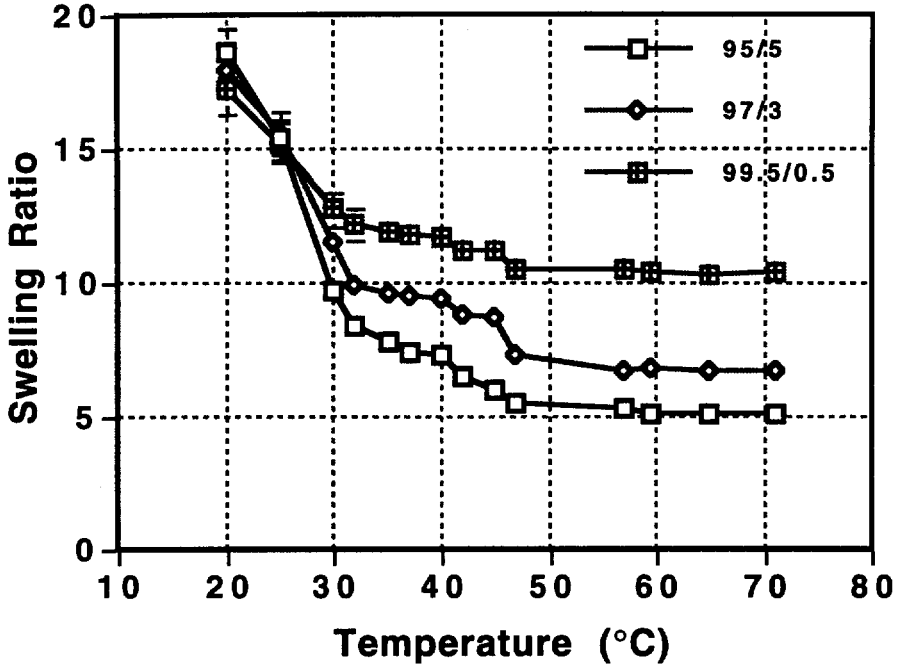

Fig. 2-4 Swelling behavior of anionic NiPAAm copolymer hydrogels containing various amounts of sodium acrylate comonomer at pH 3 as a function of temperature. Buffer: potassium phthalate, 50 mM.

At pH 3, swelling trends remain generally the same as at pH 8 (Figure 2-4). However, magnitudes for low-temperature swelling ratios for the 95:5 NiPAAm/SA gel system are significantly reduced over that seen at pH 8. Moreover, swelling ratios of the collapsed states decrease for all compositions. The contrast with hydrogel behavior at pH 8 is a direct effect of protonation of the co-monomer carboxylate groups at this lower pH (bulk carboxylate $pK_a \approx 5.6$). Hydrophilic, ionized SA at high pH produces electrostatic repulsion, yielding highly expanded gel networks (greater S.R.) at lower temperatures. Additionally, the ionized groups disrupt NiPAAm skin formation at high temperatures, allowing both water to rapidly escape outward with gel collapse and gels to collapse further without hydrostatic pressure opposition.

Data taken from higher pH buffers (pH 9) continues the swelling/deswelling trends seen at pH 8, that is, swelling ratios for all compositions increase drastically over those at

low pH and over pure NiPAAm. Figure 2-5 shows data for copolymer gel swelling at pH 9. Maximum swelling ratios for 95:5 gels are over double (S.R.>30) the swelling observed for pure NiPAAm. Only swelling ratios for gels of higher SA content are significantly increased over those at pH 8, indicating that SA-containing gels further ionize between pH 8 and pH 9. This reflects the differing activity of counterions and charged SA groups within the gel compared to free solution ionized states. Moreover, copolymer gel collapsed states above the transition temperature show swelling ratios which approach a value of 1.

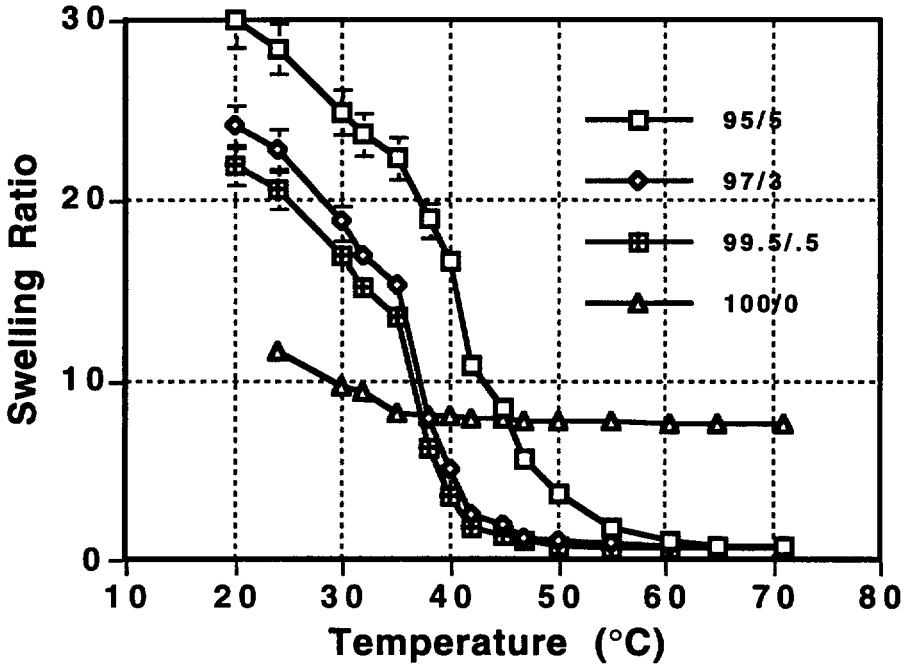

Fig. 2-5 Swelling behavior of anionic NiPAAm copolymer hydrogels containing various amounts of sodium acrylate comonomer at pH 9 as a function of temperature. Buffer: Tris, 50 mM.

Recalling that the pure NiPAAm gel collapses to a shrunken state above the critical transition region, yielding a swelling ratio of 8.5 under these conditions, a swelling ratio near unity is a remarkable condition reflecting the dramatic phase transition these systems undergo which is completely dependent upon SA addition to the gel. Qualitatively, this is observed as a shrunken gel state that is many times smaller and condensed than the starting

gel. In these cases, where the swelling ratio approaches unity, the collapsed copolymer gel is nearly completely dehydrated, even though it is immersed in water. This situation is very different from that observed for pure NiPAAm gels, where equilibrium collapse produces a swelling ratio nearly an order of magnitude higher. Small bubbles of gel, similar to those reported by others (18,22), are observed to emerge from the edges of the copolymer discs under these completely collapsed conditions, due to the formation of a NiPAAm skin on the disc surface (18,22-27). In addition, the gel physically completely deforms to a small, clear polymer bead with a bubbled surface, qualitatively much different than the white, opaque appearance of the collapsed, pure NiPAAm gel. This condition indicates nearly complete expulsion of water from the copolymer network, due to the incorporation of the ionic co-monomer.

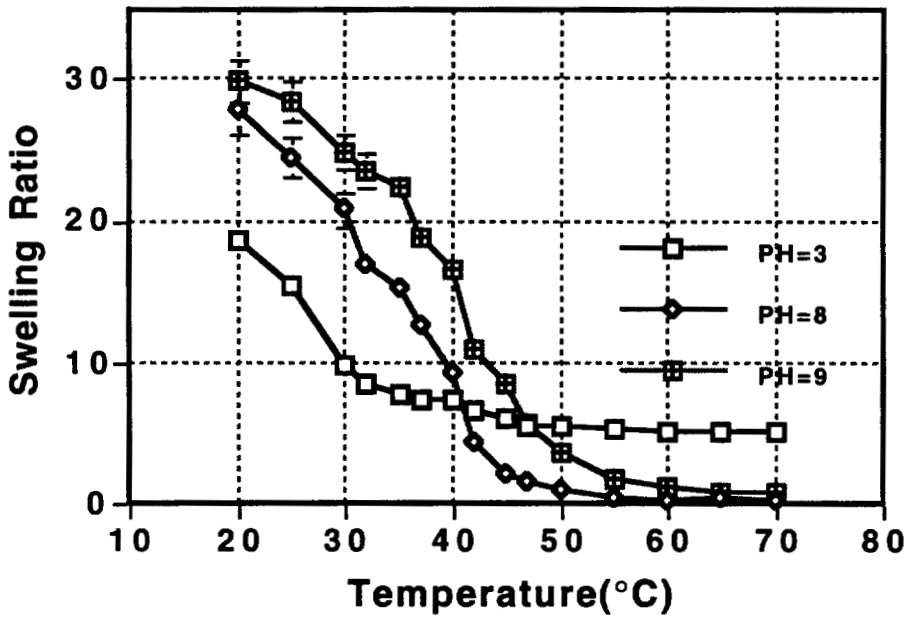

Fig. 2-6 Influence of pH on the swelling behavior of anionic NiPAAm/SA copolymer (95:5) hydrogels as a function of temperature. Buffer concentration : 50 mM.

The pH-dependent data for 95:5 gels at different pH values analyzed are collected in Figure 2-6 for comparison. Swollen gel weights at various temperatures were compared to

completely desiccated gel weights to yield data on water contents within gels at various states. The data (not shown) indicate that only 30% of the water in pure NiPAAm gels is expelled by the collapse transition at pH 7 before the overlying collapsed NiPAAm skin layer blocks efflux. Addition of 1 mol% SA to these gels allows 80% water content reduction, while 3-5 mol% SA incorporation produces collapsed gels above the critical transition having only 5% water content or less. These data demonstrate the remarkable result of this collapse transition to mechanically expel hydrogel water and produce networks of varying hydration after collapse.

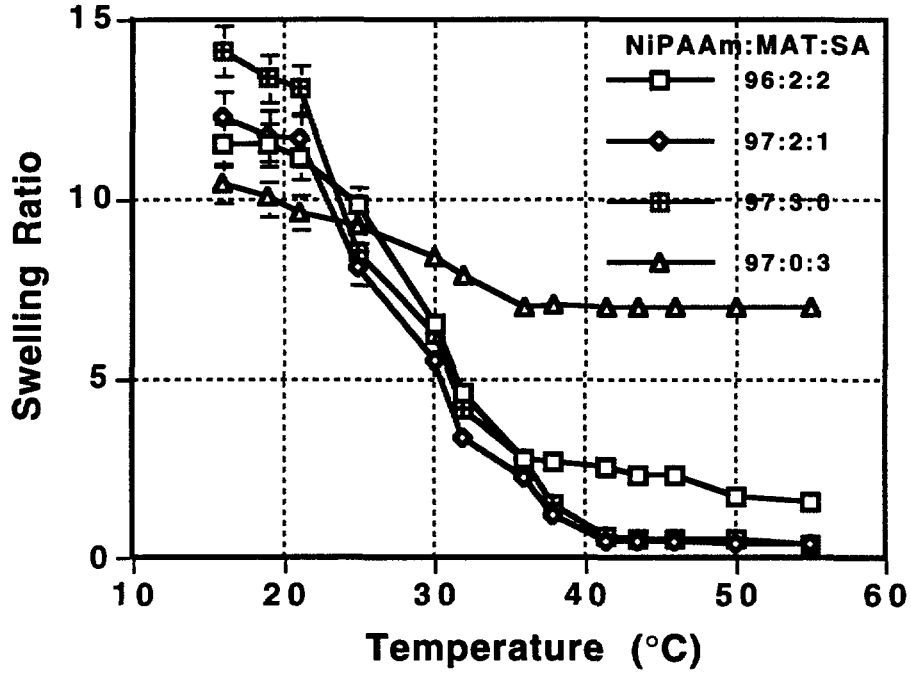

Fig. 2-7 Swelling behavior of ampholytic NiPAAm copolymer hydrogels containing various amounts of cationic MAT and anionic SA comonomers at pH 3 as a function of temperature. Buffer: potassium phthalate, 50 mM.

Swelling curves for NiPAAm gels containing either MAT alone (97:3) or both SA and MAT are shown in Figure 2-7 at pH 3. Under these conditions, the SA group is fully protonated and swelling of the gel sample containing NiPAAm/SA 97:3 (no MAT) is reduced due to the lack of charge at this pH. MAT is cationically charged at all pH values

studied and its incorporation into NiPAAm gels produces similar pH-independent swelling effects as observed for ionized SA at basic pH (data not shown). In ampholytic NiPAAm gels containing both SA and MAT in various stoichiometries at pH 3, all swelling ratios are significantly increased at lower temperatures and decreased at temperatures above the transition, resulting in greatly enhanced collapse volumes over that shown for NiPAAm/SA gels containing no MAT (NiPAAm:MAT:SA 97:0:3). Increasing the MAT ratio over SA in these gels results in systematic increases in swollen phase (low temperature) swelling ratios. Collapsed swelling ratios increase with MAT content only up to 2:1 MAT/SA ratios then remain constant with increasing cationic content.

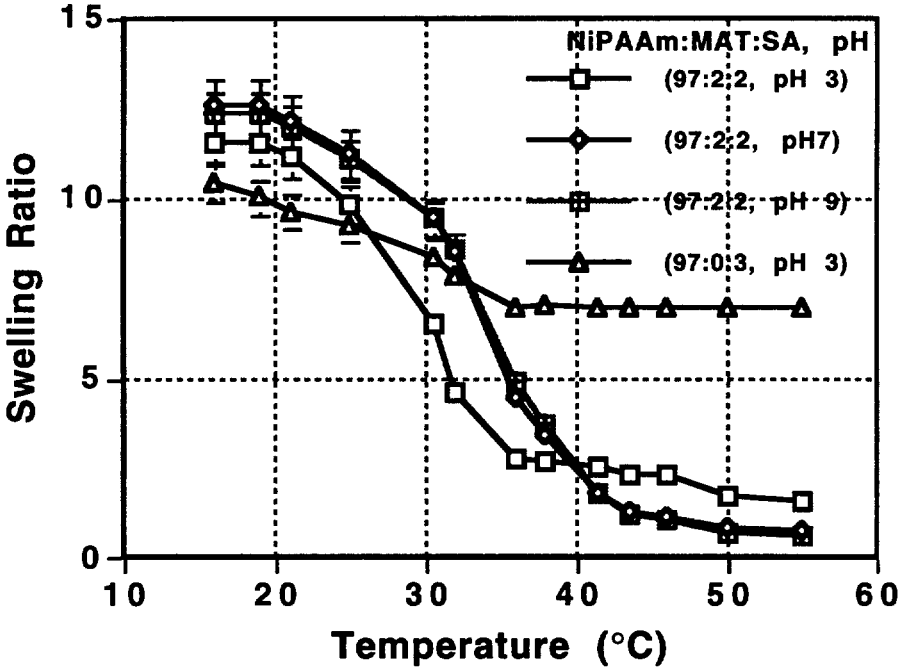

Fig. 2-8 Influence of pH on the swelling behavior of ampholytic NiPAAm copolymer gels as a function of temperature at constant buffer concentration (50 mM).

Combination of MAT and SA in NiPAAm gels enhances swelling and collapse even at 1:1 molar ratios. Figure 2-8 shows the influence of pH on NiPAAm gels containing 1:1 molar ratios of MAT/SA. The presence of MAT's cationic residue enhances swelling at

low pH. At basic pH (pH 7 and 9), SA becomes ionized. The net competitive effects of MAT-SA electrostatic attraction and SA-SA and MAT-MAT charge-charge repulsive interactions are demonstrated as enhanced swelling at low temperatures and very low collapse ratios approaching unity at elevated temperatures.

3.2 Swelling Effects Derived from Ionic Co-monomer Incorporation:

Incorporation of negatively charged SA components into the gel networks provides a number of important interactions. Initially, the acrylate salt dissociates easily, presenting mutually repulsive negative carboxylate residues which prompt network expansion and swelling. These polar groups also add a significant hydrophilic component to a largely hydrophobic (or at least critically balanced amphipathic) NiPAAm network. These two effects support the significant enhancement in aqueous swelling behavior below the critical point seen in these systems over NiPAAm. At and above the critical point, the ionized acrylate groups still attract water. However, being such a small minority component, the acrylate's contribution to swelling above the thermally induced transition is overwhelmed by the entropic drive for NiPAAm dehydration and collapse. This influence can also be analogously attributed to cationic MAT with notable exception of its pH independence.

The magnitude of gel collapse above the critical point is observed to increase with increasing pH in all gels, demonstrating modest levels of collapse at acid pH, although still significantly greater than those seen for pure NiPAAm. Swelling ratios below the critical temperature regime continue to increase with increasing pH (as pH moves above the pK_a for SA and more ionized groups are created in the network). Final collapse states appear to be independent of gel composition at neutral and basic pHs, indicating the dominant collapse effect of NiPAAm in the networks at all contents tested. Nevertheless, despite

minute levels of incorporation, anionic SA and cationic MAT remain essential to augmenting collapse, allowing the copolymer gel to expel water through hydrophilic charged domains as it collapses during thermal transition. This is the critical difference between partial collapse states observed in a pure NiPAAm gel and complete collapse seen in those which incorporate just a small amount of ionic co-monomers.

Incorporation of small amounts of charged species are proposed to provide the NiPAAm gel matrix with hydrophilic channels which facilitate water movement during thermally induced transitions. Pure NiPAAm and NiPAAm copolymer gels with hydrophobic co-monomers are reported to shrink above the transition point only to a degree limited by how much water is allowed to escape from the gel before a collapsed "polymeric skin" of NiPAAm covers the gel surface to block water (and solute) release. Because such polymer skin formation is reversible with temperature, this has been called the "on-off switching effect" for various controlled release strategies (22-27). In the NiPAAm copolymer gels, collapse can therefore be more complete (approach a swelling ratio close to 1) because the NiPAAm polymeric skin layer which controls and limits water release is, in the charged copolymer gels, perforated with hydrophilic channels which allow water movement out of the gel even above the collapse transition. More importantly, this effect can be created with small amounts of charged constituents that do not significantly alter the position of the critical point. Additionally, the phenomenon is completely reversible; after such a radical collapse above the collapse point, the gel is able to fully recover both its original dimensions and swelling ratio upon cooling.

Physically, the critical behavior exhibited by pure NiPAAm networks during the volumetric change represents a two-phase, nonequilibrium phenomenon, at least over the kinetic regime typically studied (hours to days). The transition itself is diffusion-controlled (30), mediated via thermal convection as the aqueous medium surrounding the gel is heated. Water of higher temperature is transported from bulk media through the boundary

layer to the gel surface, causing the surface-exposed polymer chains to react first to the increased temperature and to collapse as their hydration shells are broken. The resulting collapsed polymeric skin formed upon contact with water heated above the critical point slows further convection and diffusion of higher temperature water into the network. At least in pure NiPAAm systems, the network collapse from the outside eventually produces a situation where diffusion and transport in both directions is inhibited and, over shorter experimental time scales, likely prevented. Gel collapse from its exterior inward traps a pool of hydration water associated with collapsing polymer in the gel interior. Because thermal transport is much more rapid than mass transport in these systems (30), the gel's dehydrated interior then coexists with the collapsed polymer shell around it, and a gradient of hydrostatic pressure of entrapped water exists across these regions (23-26). This pressure gradient resulting from entrapped water distinguishes experimentally those pure NiPAAm networks which cannot collapse completely because of water trapped in their swollen interiors from NiPAAm copolymer gels which preserve their critical behavior, yet permit complete collapse of the polymer network at the transition point. Differences are due solely to the introduction of small amounts of hydrophilic components which act to channel water through a collapsed polymer network during the critical phenomena. Water channeling is bidirectional--that is, both into and out of the gel during transition - in order to promote both inward diffusion of higher temperature water producing network collapse, and outward flow of once-bound water necessary in producing the initial swollen state.

Figure 2-9 shows the effect of buffer chemistry on swelling ratios of a NiPAAm-SA copolymer hydrogel (96:4) as a function of temperature at pH 9 at constant ionic strength (50 mM buffer). These data indicate that while inorganic buffers show consistent influences on swelling ratios, the organic Tris buffer enhances swelling at pH 9 by nearly 30%. This effect is proposed to arise from the different activity of tri(hydroxyethyl) ammonium counterions in their association with negatively charged acrylate sites within the gel network compared to bulk ions, leading to unusual osmotic effects which promote more

extensive network hydration in the case of the organic buffer, Tris. Coworkers have observed similar effects of buffers (specifically organic buffers) on shifting phase transition temperatures in lipid dispersions (31), but no data are currently available to explain these phenomena.

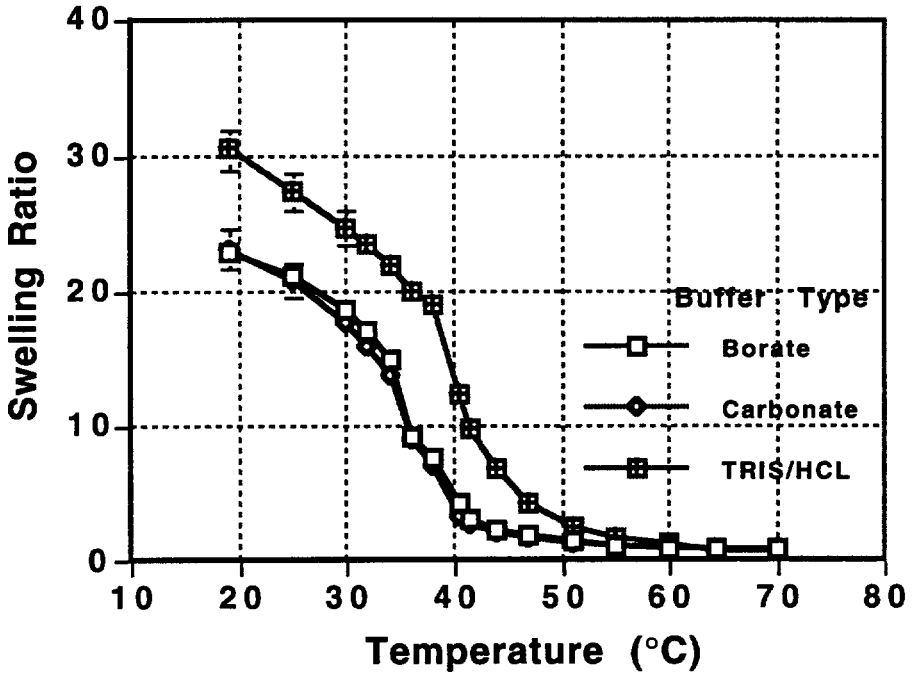

Fig. 2-9 Effect of buffer chemistry on swelling ratios of a NiPAAm/SA copolymer hydrogel (96:4) as a function of temperature at pH 9, constant buffer concentration (50 mM).

Increasing ionic strength serves to electrostatically screen the anionic carboxylate residues and cationic ammonium groups in the copolymer gel matrix, decreasing the effective distance of their mutually attractive or repulsive interactions and reducing the swelling propensity. Figure 2-10 shows the effect of ionic strength on gel swelling (96:4 copolymer) as a function of temperature in the NiPAAm/SA 97:3 copolymer system pH of 7 (phosphate buffer). The apparent trend here is that increasing ionic strength of the aqueous media decreases the swelling ratio when below the collapse transition (swollen condition), but does not affect the final collapsed state above the critical region. Moreover,

increasing ionic strength leads to decreasing critical temperature values. Extremely high ionic strength values (0.5 M) completely erase the swelling behavior of the copolymer gel as well as any observable transition. These results can be rationalized in terms chain salting-out properties resulting from removal of hydrating water molecules from the polymer chains to solvate excessive salt present at high ionic strength.

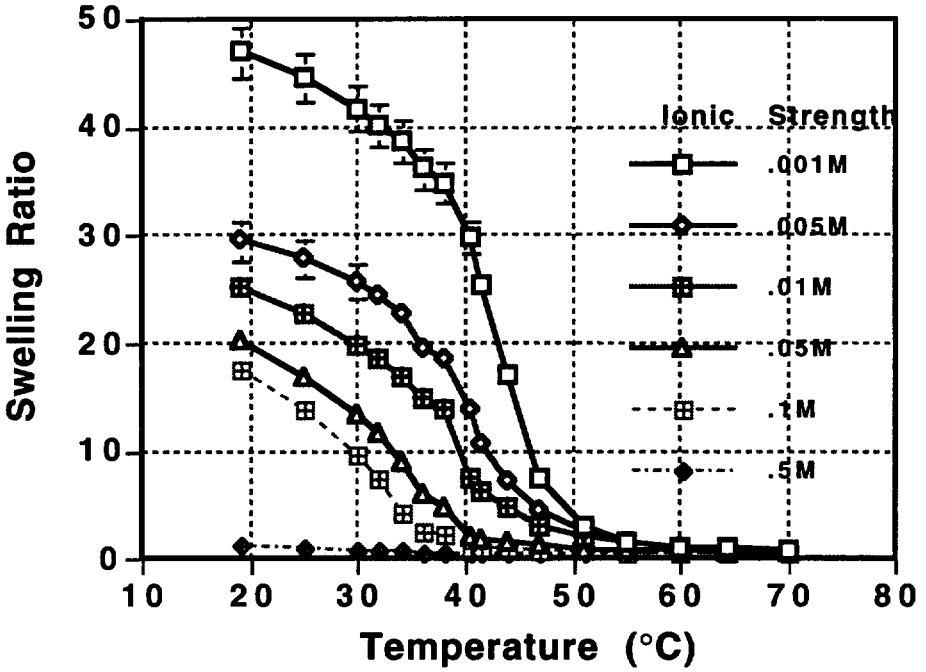

Fig. 2-10 Effect of ionic strength (NaCl addition) on NiPAAm/SA copolymer gel swelling (97:3 copolymer) as a function of temperature at pH 7 in phosphate buffer.

Figure 2-11 shows the effect of increasing crosslinker concentration on copolymer gel swelling as a function of temperature in phosphate buffer at pH 7 (0.1 M) for NiPAAm-SA gel (97:3 mole ratio) at 10 mol% monomer concentration. The trend is that increasing crosslinking leads to predictably decreased swelling ratios in the swollen state when below the critical temperature regime. Collapsed swelling ratios above this point are not affected. However, crosslink density has little apparent effect on critical behavior outside of changing its magnitude. When these data are normalized to reflect the amount of

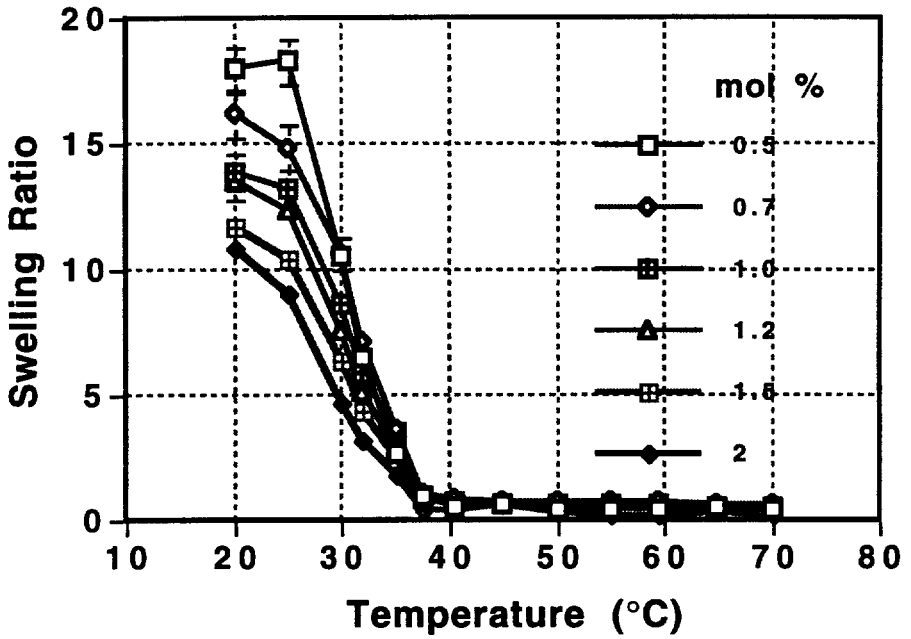

Fig. 2-11 Effect of crosslinker concentration on copolymer gel swelling as a function of temperature in 0.1M PBS, pH 7, for NiPAAm/SA gels (97:3) at 10 mol % monomer feed concentration

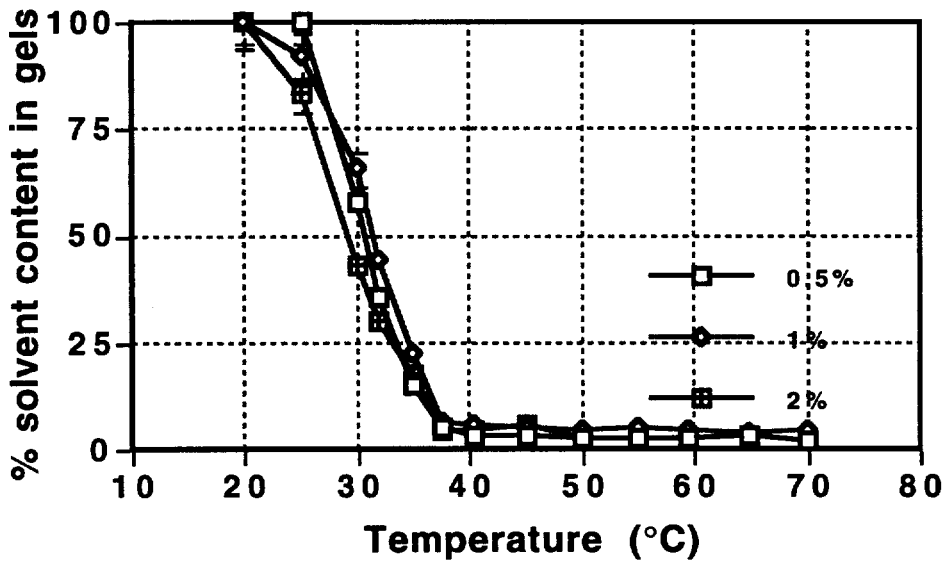

Fig. 2-12 Aqueous solvent content of NiPAAm/SA copolymer gels (97:3) as a function of temperature for gel preparations containing increasing MBAAm crosslinker concentrations in the feed. Buffer: 0.1M PBS, pH 7.

solvent in each gel as a function of temperature compared to their completely desiccated states (Figure 2-12), no significant differences in the different samples are seen. This indicates that all copolymer gels, regardless of crosslink density, undergo collapse to the fullest extent to nearly complete dehydration.

Further data on effect of crosslinker chemistry (data not shown) demonstrates that swelling and collapse in NiPAAm copolymer gels are both independent of crosslinking architecture, although mechanical properties are significantly altered. Crosslinkers based on triallylamine, piperazine bisacrylamide, and cysteine bisacrylamide all show identical swelling ratios and critical transitions.

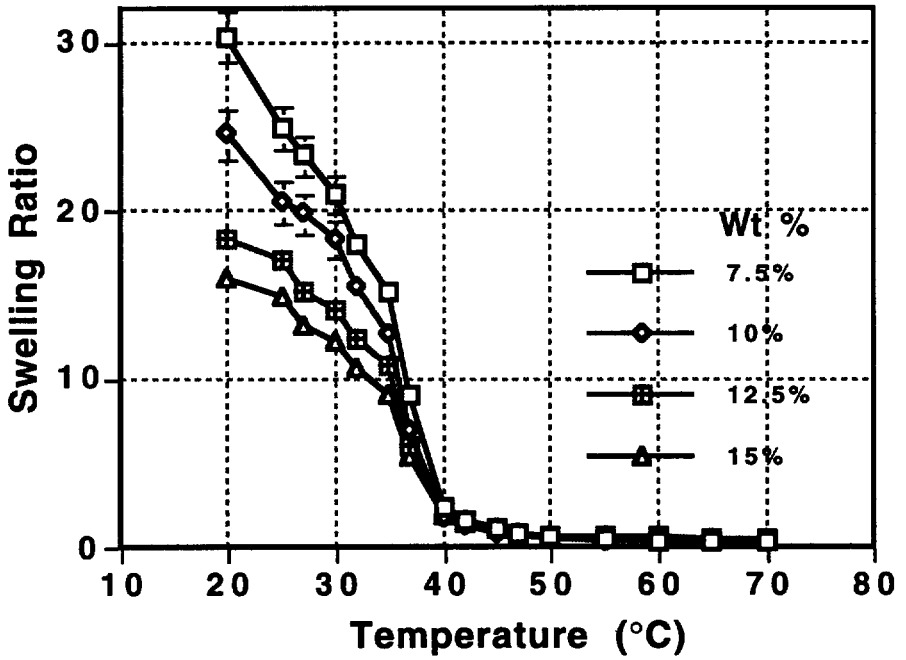

Fig. 2-13 Effect of total monomer feed concentration in the aqueous polymerization medium on the resulting NiPAAm/SA (97:3) copolymer gel swelling as a function of temperature. Buffer type: Tris buffer (pH 8, 50 mM).

Figure 2-13 demonstrates the effect of total monomer concentration in the polymerization medium on the copolymer gel swelling as a function of temperature at pH 8

in Tris buffer (50 mM). The rationale for this experiment was to study whether the copolymer network structure and swelling behavior was affected by the concentration of the monomer solution during polymerization. Again, while swelling ratios in the swollen gel state below the critical temperature regime with changing monomer ratios, the collapsed behavior above this regime remains constant, independent of monomer concentration. In addition, the collapse transition remains unchanged by total monomer concentration in the polymerization medium. This effect is analogous to that produced by changing the crosslinking concentration, resulting in polymer networks with different network architecture induced by monomer feed concentration.

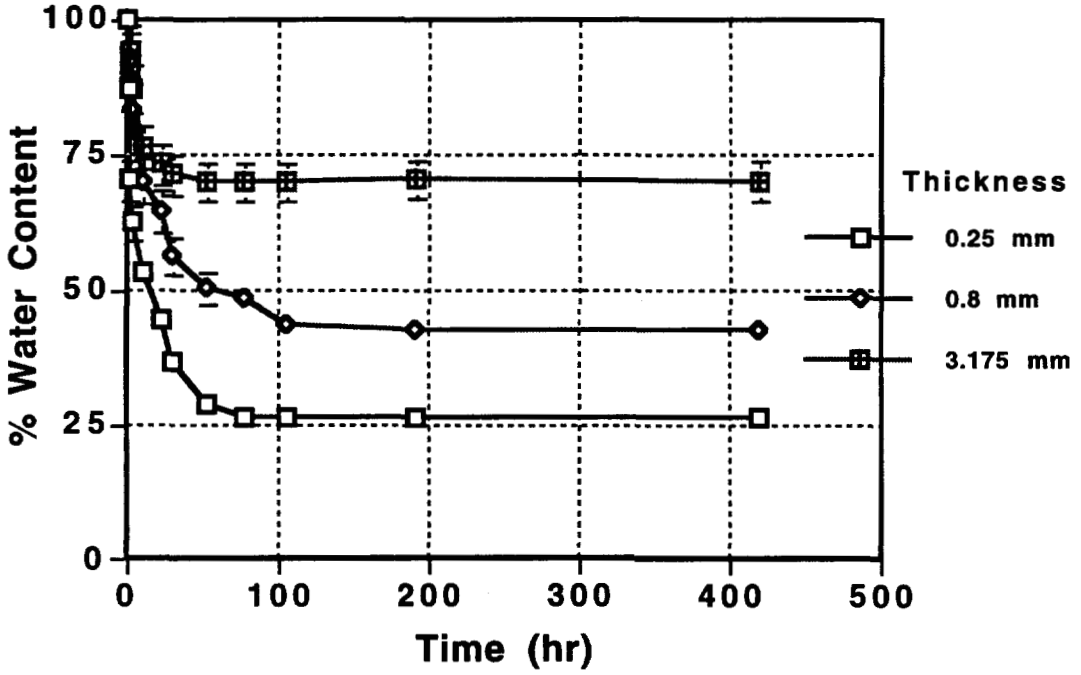

Fig. 2-14 Swelling kinetics for PNiPAAm hydrogels of different thickneses undergoing thermo-transitions from 25 to 40 °C at pH 7.

Fig. 2-14 shows swelling kinetics for PNiPAAm gels having three different thicknesses undergoing thermo-transitions from 25 to 40 °C at pH 7. The thermo-sensitive

deswelling of PNiPAAm gels is dependent on the gel physical dimension, especially on the gel thickness. Larger gel deswelling ratio can result from thinner gel thickness. This is a result of mass transport-limited deswelling kinetics where diffusion lengths for water within gels of varying dimension is altered.

References

1 J. Eliassaf, J. Polym. Sci. B 3, 767 (1965).

2. F. F. Nord, M. Bier, and S. N. Timasheff, J. Am. Chem. Soc. 73, 289 (1951).

3. F. E. Bailey and R. W. Callard, *J.* Appl. Polymer Sci. 1, 56 (1959); ibid., 373.

4. M. Heskins and J. E. Guillet, J. Macromol. Sci.-Chem. A2, 1441 (1968).

5. S. Hirotsu, Y. Hirokawa, and T. Tanaka, J. Chem. Phys. 87, 1392 (1987).

6. Y. H. Bae, T. Okano, and S. W. Kim, J. Polym. Sci. B 28, 923 (1990).

7. T. Tokuhiro, T. Amiya, and T. Tanaka, Macromolecules, 24, 2936 (1990).

8. E. L. Cussler, M. R. Stoker, and J. E. Varberg, AICHE J. 30, 578 (1984).

9. L. C. Dong and A. S. Hoffman, in *Reversible Polymeric Gels and Related Systems*, ACS Symposium Series 350, ACS Press, 1987, p. 236.

10. Y. H. Bae, T. Okano, R. Hsu, and S. W. Kim, Makromol. Chem. Rapid Commun. 9, 481 (1987).

11. F. M. Winnik, A. R. Davidson, G. K. Hamer, and H. Kitano, Macromolecules 25, 1876 (1992).

12. K. Mukae, Y. H. Bae, T. Okano, and S. W. Kim, Polym. J. 22, 206 (1990).

13. K. Mukae, Y. H. Bae, T. Okano, and S. W. Kim, Polym. J. 22, 250 (1990).

14. H. G. Schild and D. A. Tirrell, J. Phys. Chem. 94, 4352 (1990).

15. K. Otake, H. Inomata, M. Konno, and S. Saito, Macromolecules 23, 283 (1990).

16. Y. Hirose, T. Amiya, Y. Hirokawa, and T. Tanaka, Macromolecules 20, 1342 (1987).

17. Y. Hirokawa and T. Tanaka, J. Chem. Phys. 81, 6379 (1984).

18. E. S. Matsuo and T. Tanaka, J. Chem. Phys. 89, 1695 (1988).

19. S. Beltran, J. P. Baker, H. H. Hooper, H. W. Blanch, and J. M. Prausnitz, Macromolecules 24, 549 (1991).

20. S. Beltran, H. H. Hooper, H. W. Blanch, and J. M. Prausnitz, J. Chem. Phys. 92, 2061 (1990).

21. J. P. Baker, D. R. Stephens, H. W. Blanch, and J. M. Prausnitz, Macromolecules 25, 1955 (1992).

22. T. Okano, Y. H. Bae, H. Jacobs, and S. W. Kim, J. Contr. Rel. 11, 255 (1990).

23. Y. H. Bae, T. Okano, and S. W. Kim, Pharm. Res. 8, 531 (1991).

24. R. Yoshida, K. Sakai, T. Okano, and Y. Sakurai, J. Biomater. Sci., Polym. Ed. 3, 155 (1991).

25. R. Yoshida, K. Sakai, T. Okano, and Y. Sakurai, J. Biomater. Sci., Polym. Ed. 3, 243 (1992).

26. R. Yoshida, K. Sakai, T. Okano, and Y. Sakurai, Polym. J., 23, 1111 (1991).

27. T. Okano, Y. H. Bae, and S. W. Kim, in *Modulated Controlled Release Systems* (J. Kost, Ed.) CRC Press, Boca Raton, FL, 1990, p. 17.

28. R. Yoshida, K. Sakai, and T. Okano, in *Advanced Drug Delivery Reviews* (A. B. Scranton and N. A. Peppas, Eds.) Academic Press, New York, 1992, in press.

29. C. Cole, S. M. Schreiner, J. H. Priest, N. Monji, and A. S. Hoffman, in *Reversible Polymeric Gels and Related Systems,* ACS Symposium Series 350, ACS Press, 1987, p. 245.

30. S. H. Gehrke, L.-H. Lyu, and M.-C. Yang, Am. Chem. Soc. Polym. Preprints 482 (1987).

31. R. Humphrey-Baker, Y. Lei, D. H. Thompson, and J. K. Hurst, Langmuir, 7, 2592 (1991).

Chapter 3 Amphiphilic Thermosensitive N-Isopropylacrylamide Terpolymer Hydrogels Prepared by Micellar Polymerization in Aqueous Media

3.1 Introduction

Perhaps the most significant advance in water-soluble polymers during the past two decades has been their modification with hydrophobic moieties. Numerous achievements in polymeric surfactants, or water-soluble polymers with a moderate percentage of a hydrophobic groups that significantly lower the surface tension of water have been widely reported. These polymers play a very important role in biological systems and are of considerable interest in current biomedical and pharmaceutical applications.

Unfortunately, very few polymer gel systems studied to this point describe crosslinked networks that contain surfactant-type hydrophobes. Covalent and ionically crosslinked networks of water-soluble polymers, commonly referred as hydrogels in their swollen state, have been well-known for their successful biomedical applications, such as soft contact lenses, wound management, and controlled drug delivery. Recently, hydrophobically modified hydrogels or so-called amphiphilic networks which exhibit hydrophilic/hydrophobic microscopic domain structure have received attention on account of their many important and interesting properties (1-2). They might exhibit unique morphological features which can greatly influence their properties; they might have versatile controlled delivery features for hydrophilic, hydrophobic, as well as amphiphilic agents; they might have enhanced biocompatibility due to their hydrophobic/hydrophilic balance; they might also show improved mechnical strength.

The object of this chapter is to describe new amphiphilic networks based on poly (N-isopropylacrylamide)-co-sodium acrylate (PNiPAAm-co-SA) hydrogel systems discussed in Chapter 2 but incorporating a third hydrophobic species. The delicate balance of hydrophilic and hydrophobic properties of PNiPAAm hydrogels provides novel thermo-sensitive swelling behavior in aqueous solution. The incorporation of the hydrophilic ionic species, sodium acrylate, into the PNiPAAm hydrogels can radically change gel swelling

behavior in water. The effects of incorporating hydrophobic n-N-alkylacrylamide into "neutral" PNiPAAm networks together with hydrophilic comonomer SA on gel swelling behavior as well as other physicochemical properties such as solute diffusivity are extremely interesting.

3.2 Crosslinked PNiPAAm Gel Synthesis

3.2.1 Macroscopic Gels

The same polymerization methods used for linear PNiPAAm synthesis but with crosslinkers can be adopted to produce PNiPAAm gels. These methods include free radical initiation in organic solution (3-9), redox initiation in aqueous media (10-15), ionic polymerization (16-18), and radiation initiation (19-20). N,N'-methylene-bis-acrylamide (MBAAm) is the overwhelming choice for crosslinker. Polymerization is usually performed in "molds" such as micropipettes or glass plates with spacers. Different shaped DSC endotherms are observed for single chains prepared by redox-initiated polymerizations as opposed to those observed when using thermal free-radical initiation (21). Free radical polymerization in organic media (22) results in gels that exhibit a smaller change in dimensions when they deswell above the LCST compared to the results with corresponding redox systems. Both comonomer and additives have substantial effects on the properties of PNiPAAm gels.

3.2.2 Microgels and Latices

PNiPAAm gel beads or particles can be manufactured by a wide variety of techniques for many alternative applications such as quasi-elastic light scattering for theoretical studies of volume transitions (23). Most synthetic techniques employ aqueous

redox methods described in Table 3.1. Instead of homogeneous reaction media such as in bulk or solution, a heterogeneous medium is created by polymerizing NiPAAm monomer within the surfactant micelles of an emulsion. More highly organic emulsion-type systems with ethyl acetate as a second solvent have also been reported using PVA to suspend monomer while stirring (28). Also inverse suspension (water-in-oil) polymerizations have been performed by injecting aqueous polymerization mixtures into paraffin oil (24-25). In such a case, stirring is more important in determining product physical dimensions than with surfactants in which the size is controlled by the micelles. Stable, surfactant-free PNiPAAm latices have also been fabricated by thermal initiation of low solids (2.5%) aqueous solutions (29-30).

Table 3.1 Synthesis of Microgels and Latexes

Initiators[a]	Crosslinker[b]	Polymerization Media[c]	Swollen Size (μm)	Reference
AP/TEMED	MBAAm	SML/water	0.4	23
AP/TEMED	MBAAm	Paraffin/water	100-1000	24-25
KP/SM	MBAAm	Triton 770	0.2-0.5	26-27
Oleophilic Peroxide	various	ethyl acetate	ca. 100	28
KP	MBAAm	water	1	29-30

a. AP=ammonium peroxydisulfate; TEMED=N,N,N'N'-tetramethylethylenediamine; KP=potassium peroxydisulfate; SM=sodium metabisulfate.

b. MBAAm=N,N'-methylenebisacrylamide.

c. SML=sorbitan monolaurate.

3.3 Synthesis of Crosslinked Amphiphilic Gel Networks

A thorough search of the literature indicates that very little data is available regarding amphiphilic network synthesis, due mainly to synthetic difficulties of linking incompatible hydrophilic and hydrophobic polymers together in a gel. One such system based on poly(N,N-dimethylacrylamide)-1-polyisobutylene networks has been synthesized for its potential biomedical and pharmaceutical application (2). The networks were prepared by radical copolymerization of methacrylate-telechelic PIB macromonomers (MA-PAB-MA, also serves as crosslinker) with DMAAm in THF. THF is a common solvent for both PIB and DMAAm thereby allowing for a homogeneous reaction mixture.

For synthesizing amphiphilic poly(NiPAAm-co-SA-co-n-N-alkylacrylamide) networks no common solvent system has been found to prepare a homogeneous reaction mixture . Moreover, research results (as discussed in Section 3.2.1 of this chapter) have shown that PNiPAAm gels with distinct thermo-sensitive swelling characters are usually prepared in aqueous media with redox initiation. Thus, the synthesis of the amphiphilic terpolymer networks under such conditions remains extremely difficult and challenging.

In this chapter a novel micellar (or microemulsion) copolymerization technique, adopted from the similar technique developed for linear poly(acrylamide-co-n-N-alkylacrylamide) synthesis (31), has been used to synthesize terpolymer networks using low temperature redox initiation in aqueous media. In this system hydrophobic comonomer, n-N-alkylacrylamide (RAAm), was stabilized by surfactants such as sodium dodecylsulfate (SDS) or 4 lauryl ether (Brij 30) to form micelles, and MBAAm or N,N'-bis(acryloyl)-cystamine (BAC) were used as crosslinkers. The reaction scheme is illustrated in Fig. 3-1. AP/TEMED can be used to initiate the reaction at low temperaure in aqueous media. The comonomer properties, such as stability in the reaction system, are

significantly dependent on the type and amount of the amphiphile used as well as the mixing conditions (i.e. temperature, pH, and stirring.).

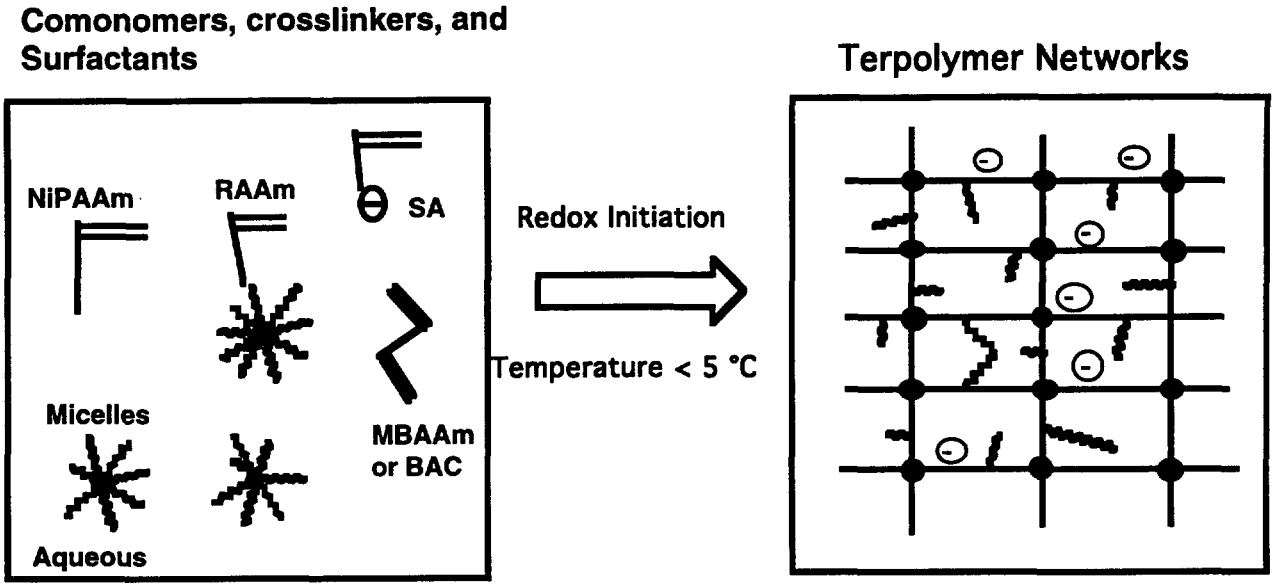

Fig. 3-1 Schematic diagram of micellar copolymerization of poly (NiPAAm-co-SA-co-n-N-Alkylacrylamide) networks in aqueous media, with MBAAm or BAC as crosslinker, SDS or Brij 30 as surfactant stabilizers, and AP/TEMED as initiators.

There are many advantages for using the micellar copolymerization technique to prepare amphiphilic polymeric networks for drug delivery applications:

(1). More efficient incorporation of hydrophobic components into a mainly hydrophilic framework when compared to the conventional approaches.

(2). Aqueous phase polymerization can be performed in presence of protein and polypeptide drugs at low temperature.

(3). Stability and bioactivity of entrapped proteins or peptides can be enhanced by this mild, encapsulating approach.

3.4 Theoretical Models for Critical Swelling Behavior of PNiPAAm Gels

In the explanation of thermo-sensitive critical swelling behavior observed for PNiPAAm gels discussed in Chapter 2, overwhelming efforts qualitatively surmised that both so-called hydrogen bonding and hydrophobic effects play major roles in determining swelling and deswelling states. Modern gel theories basically contain four terms reflecting the changes in the free energies of mixing, specific interactions, elasticity, and osmotic effects for a gel in aqueous media (32-39). These theories assume that the various contributions to the free energies of swelling are additive, for example, that the partition function for swelling can be factored into independent contributions. While this assumption has been questioned (40), there is (as yet) no tractable alternative for describing gel swelling equilibria.

3.4.1 Mixing Contributions to Gel Swelling

The extensively used model to describe the gel swelling behavior is Flory-Huggins mean field theory. (41) According to the theory, the Gibbs free energy of mixing can be expressed as

$$\Delta G_{mix} = kT\left[n\ln(1-\varphi)+\chi n\varphi\right] \qquad (3\text{-}1)$$

Where ΔG_{mix} is the sum of free energies of a pure solvent and a polymer network, n the number of the solvent molecules in the gel, φ the volume fraction of the polymer network, χ the polymer-solvent interaction parameter, k the Boltzmann constant, and T the absolute temperature.

However, Flory-Huggins theory is based on a random mixing lattice model which assumes that interaction potentials for solvent and polymer segments are homogeneous

over the segment surfaces. This theory does not account for orientation-dependent interactions (i.e., hydrogen bonds and hydrophobic interaction) which dramatically influence the behavior of PNiPAAm gels in aqueous systems.

Although the application of the Flory-Huggins model to such nonrandom mixtures is invalid, the general requirement of a negative excess entropy of mixing for an LCST (lower critical solution temperature) has been derived mathematically from thermodynamic principles (42). Much debate has been focused on whether "hydrophobic effects" or "hydrogen bonding effects" are dominant in general in aqueous solutions (43-45) and in the particular case of PNiPAAm gels. None of these effects can be independent. While Walker and Vause models can adequately describe LCST phenomena in general as resulting only from changes in preferences for hydrogen bonding (46), hydrogen bonding cannot be the sole cause of the LCST as no collapse of polyacrylamide gels happens is observed over all temperatures in water. In contrast, Fujishige (47-48) and Saito (11, 36, 49) proposed that the driving force is entirely "hydrophobic interaction". Fujisige models are applications of "blob theory" (50) used for UCST predictions of single chain collapse rather than the entire system.

Prausnitz et al. developed a quasichemical partition function to extend conventional lattice theory. (37) Each molecule/polymer segment is permitted to posses three energetically distinct types of contact sites: hydrogen bond donor, hydrogen bond acceptor, and dispersion force. The four resultant exchange energies are hydrogen bonding between like molecules, hydrogen bonding between unlike molecules, weak attractions between hydrogen bonding between unlike species, and attractions between nonhydrogen bonding units. This model still cannot fit its three adjustable parameters experimentally at all temperatures due to some simplified assumptions, such as Gaussian chains, nonclassical fluctuations, and temperature-independent exchange energies.

Instead of using a lattice model, an equation of state approach that also permits compressibility has been reported. (34-35, 39) The model derived an interaction energy from the various cohesive energy densities in the system which fit the experimental results. In addition, pressure-dependent gel swelling behaviors have been predicted. The authors suggested that they can compensate for these results by introducing specific hydrogen bonding interactions into their system (35).

In conclusion, a theoretical explanation of the mixing term of PNiPAAm gels in water is far from complete. More work detailing hydrogen bonding/hydrophobic interactions as well as network structural charcterization is needed.

3.4.2 Elastic Contributions to Gel Swelling

The formation of crosslinking points in networks increases the number of elastically active chains, leading to an increase in the elastic free energy. The well-known Flory theory of rubber elasticity has been used extensively to calculate the elastic free energy of gels (41). The general expression for the resulting chemical potential is

$$\Delta G_{elas} = \frac{3\nu kT}{2}(\alpha^2 - 1 - \ln\alpha) \qquad (3\text{-}2)$$

where ν is the total number of chains in the gels, α the linear swelling ratio, k the Boltzmann constant, and T the absolute temperature. Modern network theories can successfully deal with the two ideal networks affine (41) and phantom (51) types. In the affine network, junction point (crosslink) fluctuations are totally suppressed and components of each chain vector transform linearly with macroscopic deformation. The resulting chemical potential expression (for a perfect tetrafunctional network) is (41, 52)

$$\Delta\mu_{elas}^{affine} = \frac{1}{2}RT(\phi_2^0 / x_c)\lambda^{-1}(2 - \lambda^{-2}) \qquad (3\text{-}3)$$

where x_C is the average number of segments per network chain (where a segment is defined as having the same volume as that of a solvent molecule), ϕ_2^0 the volume fraction of the gels in the reference state (i.e., at preparation), and $\lambda = (\phi_2^0/\phi_2)^{1/3}$. In the phantom network, junction fluctuation is free and unaffected by the presence of neighboring chains or by the state of deformation. The resulting chemical potential change (for isotropic swelling) is (51-52)

$$\Delta\mu_{elas}^{phantom} = \frac{1}{2}RT(\phi_2^0 / x_c)\lambda^{-1} \tag{3-4}$$

Real networks conform to neither of these limiting cases. A modified model (known as constrained junction theory) can be written (53-54)

$$\Delta\mu_{elas} = \Delta\mu_{elas}^{phantom}(1-F) + \Delta\mu_{elas}^{affine}F \tag{3-5}$$

where F varies between 0 (no constraints on junctions) and 1 (complete constraints on junctions) and can be expressed as

$$F = K(\lambda,\kappa)/(1-\lambda^{-2}) \tag{3-6}$$

where is given by the Flory-Erman theory (53). Parameter κ is a measure of constraints on junction fluctuations and related to the degree of network interpenetration through (54)

$$\kappa = \frac{1}{4}P\phi_2^0 x_c^{1/2} \tag{3-7}$$

where dimensionless number P is determined by the type of polymer and the molar volume of the solvent. For a specific polymer/solvent (gel) system, P remains constant and κ depends only on network composition (crosslink density and monomer concentration at preparation).

3.4.3 Osmotic Contributions to Gel Swelling

Fixed charges on a network are confined (along with an equal number of counterions) to the gel phase, resulting in an unequal distribution of unbound ions between the gel and surrounding solution and an osmotic pressure difference between the two phases (41). The osmotic difference introduces an additional mixing contribution (of ions with solvent) to the swelling free energy and therefore to the solvent chemical potential. Although semiquantitative Donnan equilibria for describing this contribution can explain some basic features of polyelectrolyte gel swelling, (56) a complete description for the effect of ions on gel swelling would require expressions for ion-ion, ion-solvent, and ion-polymer interaction.

In the ideal Donnan equilibria theory

$$\Delta G_{ion} = \Delta G_{ion}^{gel} - \Delta G_{ion}^{ext} = -\bar{v}RT\sum_{j}(c_j^{gel} - c_j^{ext}) \qquad (3\text{-}8)$$

where $\bar{v}$ is the solvent partial molar volume, c_j^{gel} and c_j^{ext} respectively, ion concentrations within the gel and in the surrounding solution. The summation over j includes all mobile (unbound) ions. It can be seen that the Donnan theory ignores specific ion effects such as ion pairing of counterions to the fixed charge groups (57-58), polymer complexation phenomena (59).

3.5 Experimental

3.5.1 Materials

All solvents used were reagent grade. N-isopropylacrylamide (NiPAAm, Eastman Kodak) was recrystallized twice from benzene/hexane (4:6). Sodium acrylate (SA, Pfaltz & Bauer) was used as received. Methylene-bis-acrylamide (MBAAm, Aldrich) was

recrystallized from ethanol. Acryloyl chloride (Aldrich) was distilled under N_2 before use. Cystamine dihydrochloride (Sigma), n-alkylamine (n-octyl-, n-decyl, n-dodecyl, n-tetradecyl, and n-octadecylamine) (Aldrich) were used without further purification., n-N-butylacrylamide (Polysciences), tetramethylethylenediamine (TEMED, Aldrich), ammonium persulfate (AP, Aldrich), sodium dodecyl sulfate (SDS, Sigma), 4 lauryl ether (Brij 30, Sigma) were used as received without further purification. All buffer salts and solutes were reagent grade compounds. Water for buffers, gel swelling and release measurements was first reverse-osmosis filtered (deionized) and then Millipore filtered to yield purified water having 18 MΩ/cm resistivity.

3.5.2 Synthesis of Hydrophobic Acrylamide Monomers Containing Alkyl Chains

The classical way to prepare N-substituted acrylamide family is from the reaction of acryloyl chride with its respective amine at low temperature. The reaction equation is

$$CH_2 = CR^1COCl + R^2R^3NH \Rightarrow CH_2 = CR^1CONR^2R^3$$

(R^1 = H or Me, R^2 and R^3 = H, alkyl, aryl, aralkyl.)

Detail description of the chemistry and procedures of the reaction can be found in the original literature (60-62).

In this research, n-N-octyl-, n-N-decyl-, n-N-dodecyl-, n-N-tetradecyl-, n-N-octadecylacrylamide were prepared by the same reaction scheme above according to the following procedure:

n-Alkylamine (20mmol) and triethylamine (21mmol) were dissolved in 50 ml of tetrahydrofuran (THF). This solution was cooled in an acetone/ice bath and 20 ml of a

THF solution containing acryloyl chloride (20 mmol) was slowly added with constant stirring over 30 min. The reaction temperature was monitored and not permitted to exceed 0 °C. The reaction vessel was removed from the acetone/ice bath after addition of the acryloyl chloride and permitted to equilibrate to room temperature for 30 min. An inhibitor, hydroquinone (5mg) was added to the reaction mixture prior to filtration through a medium pore sintered glass filter. Tetraethylamine hydrochloride by-product was discarded and the

Table 3.2 Characterization of n-N-alkylacrylamide

Compound	mp (°C)	IR (cm^{-1})	^{1}H-NMR (ppm) (in $CDCl_3$)
Octyl-	-	3300, 3057, 2956, 2926, 1656, 1625, 1543, 1476, 1408, 1375, 1313, 1239, 990, 952	6.0-6.2, 6.2-6.4, 5.5-5.7, 3.3, 1.7-2.0, 1.4-1.6.,
Decyl-	44-45 45-46 [1]	3280, 3071, 2957, 2927, 1659, 1626, 1550, 1467, 1408, 1362, 1220	6.0-6.4, 5.6-5.65, 3.3-3.4, 2.2, 1.2-1.6, 0.9.
Dodecyl	54-55 55.5 [2]	3271, 3072, 2957, 2922, 1653, 1622, 1550, 1469, 1406, 1378, 1309, 1244, 989, 952.	6.0-6.4, 5.5-5.7, 3.7-3.8, 3.3, 2.2.
Tetradecyl-	63.5-64 61.5-62 [3]	3273, 3072, 2955, 2919, 1653, 1622, 1549, 1471, 1407, 1379, 1310, 1240, 993, 963.	6.0-6.4, 5.6-5.65, 3.3, 2.2.
Octadecyl-	68.5-69 69 [4]	3303, 2957, 2918, 1654, 1624, 1542, 1408, 1377, 1311, 1238, 992, 953.	6.0-6.4, 5.6-5.65, 3.3, 2.2, 1.2-1.6.

[1]reported value from reference (63); [2]reported value from reference (64); [3]reported value from reference (64); [4]reported value from reference (66).

filtrate was washed with 0.1N HCl, brine, and saturated $H_2O/NaHCO_3/NaCl$ and dried with $MgSO_4$. After evaporing the solvent, the product was allow to recrystallize from petroleum ether at 5 °C. The overall recovery was greater than 40%. The characterization results are list in Table 3.2.

3.5.3 Synthesis of N,N'-Bis-Acryloyl-Cystamine (BAC) Crosslinker

N,N'-bis(acryloyl)-cystamine (BAC) can be syntheiszed from the reaction of acryloyl chloride (1 mol) with cystamine (2 mol) by either the same procedure in Section 3.5.2 or a heterogeneous phase reaction. A general procedure for the heterogeneous phase reaction is:

Cystamine dihydrocholoride (10 mmol) was dissolved in 15 ml of 3.5 M NaOH and 10 ml chloroform mixture. This solution was heated to 50 °C and 5 ml of chloroform containing 20 mmol of acryloyl chloride was added dropwise with constant stirring over 15 min while the reaction temperature was maintained near 50°C. After separating the phases while still warm, the aqueous phase was discarded. The remaining organic phase was cooled to room temperature and the product was precipitated in the solution. The white crystall product was recovered by filtration and recrystallized from chloroform to give a yield above 60%. The mp of the product was 120-121°C. Its infrared spectrum (KBr pellet) shows major peaks at 3253, 3067, 1653, 1622, 1555, 1312, 1254, 123, 1075, 992, 961, and 806 cm^{-1}. Its NMR spectrum ($CDCl_3$) gave δ = 2.9 (2H) triplet, 3.7 (2H) quartet, 5,6 (1H) multiplet, and 6.1 (2H) multiplet.

3.5.4 Synthesis of Terpolymer Poly(NiPAAm-co-SA-n-N-Alkylacrylamide) Networks

NiPAAm-co-SA-co-n-N-alkylacrylamide networks were synthesized by micellar copolymerization using either MBAAm or BAC as a crosslinker. For aqueous redox polymerization, ammonium persulfate (AP) and TEMED wre used as initialtors. At first, various amounts of hydrophobic monomers, n-N-butyl-, n-N-octyl-, n-N-decyl-, n-N-dodecyl-, n-N-tetradecyl-, and n-N-octdecyl-acrylamide, were stabilized by either SDS or Brij 30 (1-5%) in aqueous solution with proper stirring and temperature control. Then aqueous solutions of various amounts of mixed comonomer (NiPAAM and SA), crosslinker (MBAAm or BAC), and TEMED was carefully added into the micelle solution with stirring and N_2 bubbling for 15 min. The total monomer content in water was 10 wt% unless specified. After the addition of AP, the complete mixture were injected between precooled clean glass plates separated by 2 mm thick gaskets (2 mm OD crosslinked silicone rubber O-ring material) with extreme care taken to avoid the introduction of air bubbles into the solution. The plates wre clamped securely and suspended in an ice/water bath at temperatures less than 5 °C for 24 h. The resulting gel films were then separated from the plates and allowed to swell in deionized water/methanol (60/40) for a week, followed by swelling in pure deionized water at room temperature until no release of surfactant was detected. Swollen terpolymer gel membranes were subsequently cut into disks of 1 cm diameter using a cork borer, dried ambiently for 1 day, and under vacuum for 3 days at room temperature.

3.5.5 Swelling Measurement

The same procedures described in section 2.2.3 of Chapter 2 was used except only the gel equilibrium swelling ratio at different temperatures was measured. Temperature modulation was controlled from low to high.

3.5.6 Model Amphiphile SDS Loading and Release Measurement

The model amphiphile SDS was loaded by the *in situ* gel polymerization method. Release measurements of SDS from gels began immediately after gel membranes were separated from the glass plates molds, cut, and equilibrated in water for 24 hr. Release of SDS was measured by both HPLC assay and gel swelling ratio monitoring. The HPLC analytical conditions were: μ-Bondapak C_{18} column as a stationary phase, water as a mobile phase, UV (λ=225 nm) as a detection wavelength, 0.8 ml/min flow rate, 10 μl injection volume, internal standard method as quantitation calculation. The swelling ratio monitoring method sterms from the gel swelling ratio changing as ionic SDS releases due to the Donnan equilibra approximation at constant temperature,

$$\frac{M_t}{M_\infty} = \frac{SW_0 - SW_t}{SW_0 - SW_\infty} \tag{3-9}$$

where M_t is the amount of SDS measured at each time interval, M_∞ equilibrium value, SW_0 the initial swelling ratio measured, SW_t the swelling ratio at each time interval, SW_∞ the equilibrium swelling ratio. Overall release mesurement was under either "normal" conditions (no changes of aqueous media) or "sink" conditions (equal volumes of fresh aqueous media replaced after each sampling).

4.1 Results and Discussion

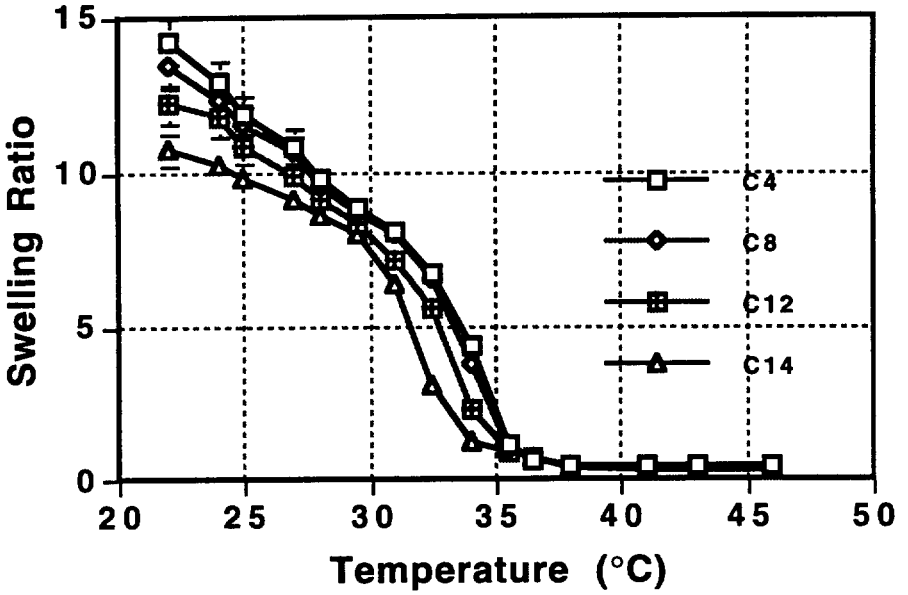

Fig. 3-2 Thermo-sensitive swelling behavior of terpolymer (NiPAAm/SA/Cn, 95/3/2, 0.8 mol% MBAAm) gels in 0.05M PBS buffer (pH 7.3).

Fig. 3-2 and 3-3 show differences in temperature-dependent swelling equilibra for four network systems-poly(NiPAAm-co-SA-co-n-N-butyl-, n-N-octyl-, n-N-dodecyl-, n-N-tetradecylacrylamide)-with the same copolymer ratio, 95/3/2, and crosslinker MBAAm (Fig. 3-2) or BAC (Fig. 3-3), respectively. All four networks with either MBAAm or BAC show their critical temperature between 30 and 35 °C.

The networks demonstrate higher swelling capability at temperatures below their critical points and shrink dramatically (swelling ratio near unity) as temperatures increase above their respective critical points. After introducing a hydrophobic comonomer, n-N-alkylacrylamide, with varying alkyl side chain length, the networks decrease their swelling ratios at temperatures below their critical points, and their critical temperatures decrease with increasing length of the alkyl side chain.

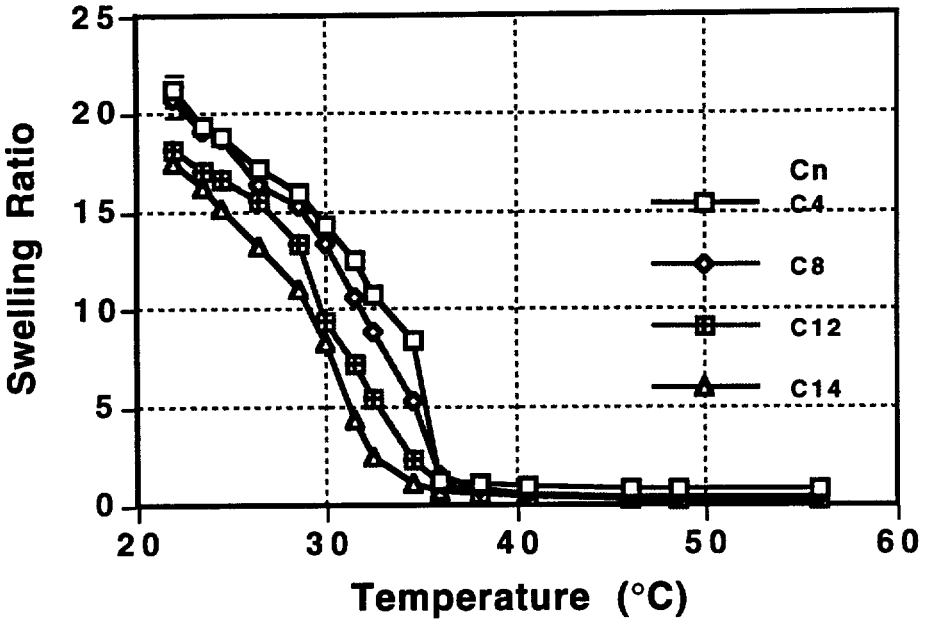

Fig. 3-3 Thermo-sensitive swelling behavior of terpolymer (NiPAAm/SA/Cn, 95/3/2, 1.5 mol% BAC) gels in 0.05M PBS buffer (pH 7.3).

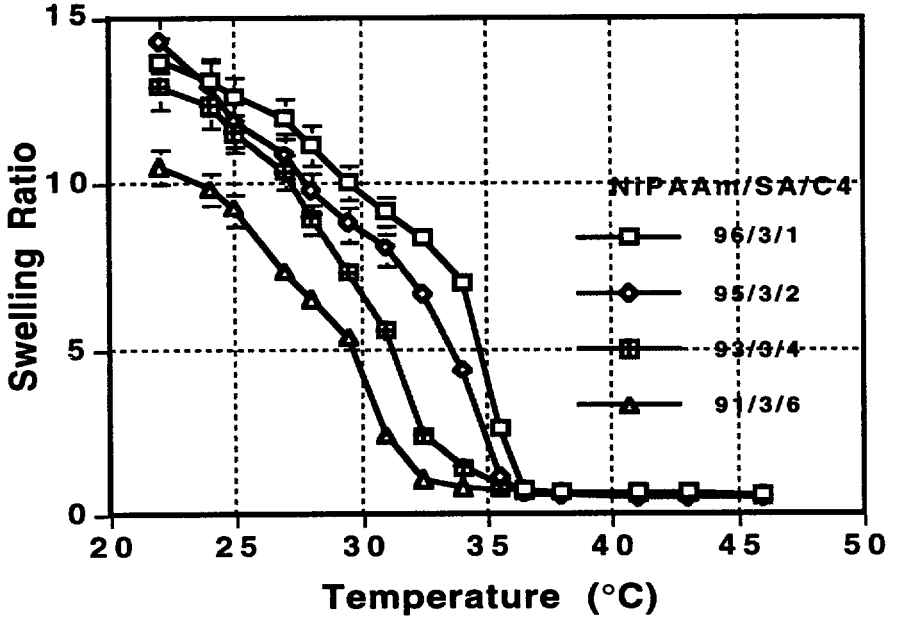

Fig. 3-4 Thermo-sensitive swelling behavior of terpolymer (PNiPAAm/SA/C4, 0.8 mol% MBAAm) gels in 0.05M PBS buffer (pH 7.3).

Fig. 3-4 shows the temperature-dependent swelling equilibra for poly(NiPAAm-co-SA-co-n-N-butylacrylamide) networks with fixed amounts of hydrophilic comonomer (SA)

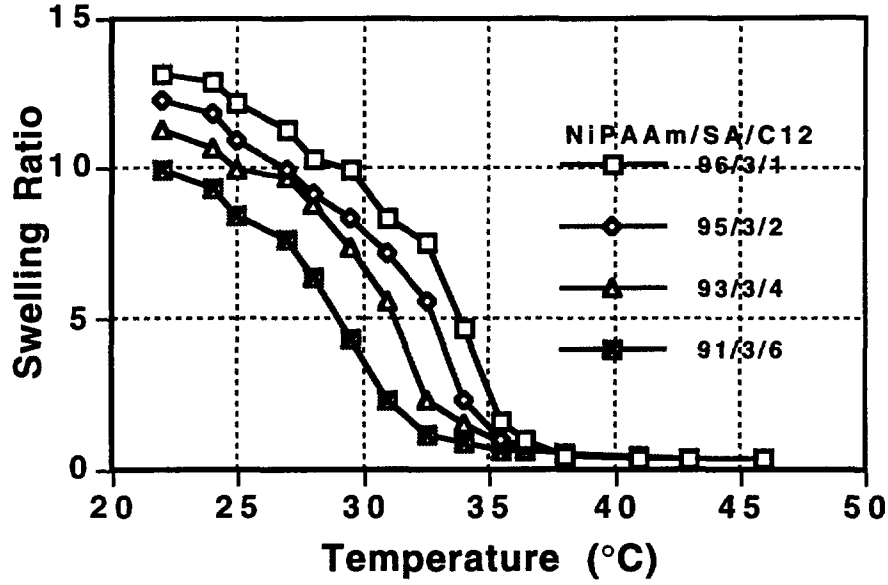

Fig. 3-5 Thermo-sensitive swelling behavior of terpolymer (NiPAAm/SA/C12, 0.8 mol% MBAAm) gels in 0.05M PBS buffer (pH 7.3).

incorporation (3 mol%) and four different amounts of hydrophobic comonomer (n-N-butylacrylamide) incorporation (1, 2, 4, 6 mol%). All of the four networks demonstrate their thermo-sensitive sweling behavior with critical points between 28-35 °C. Fig. 3-5 shows the temperature-dependent swelling equilibra for poly(NiPAAm-co-SA-co-n-N-dodecylacrylamide) networks with fixed amounts of (SA) incorporation (3 mol%) and four different amounts of n-N-dodecylacrylamide incorporation (1, 2, 4, 6 mol%). All four network demostrate their thermo-sensitive swelling behavior with the critical temperatures between 27 to 35 °C. Fig, 3-4 and 3-5 show nearly identical results in response to the amount of hydrophobic comonomer, either n-N-butyl- or n-N-dodecyl-acrylamide, incorporated. Swelling ratios decrease and critical points shift to lower temperature as the amount of network hydrophobic comonomer incorporation increases.

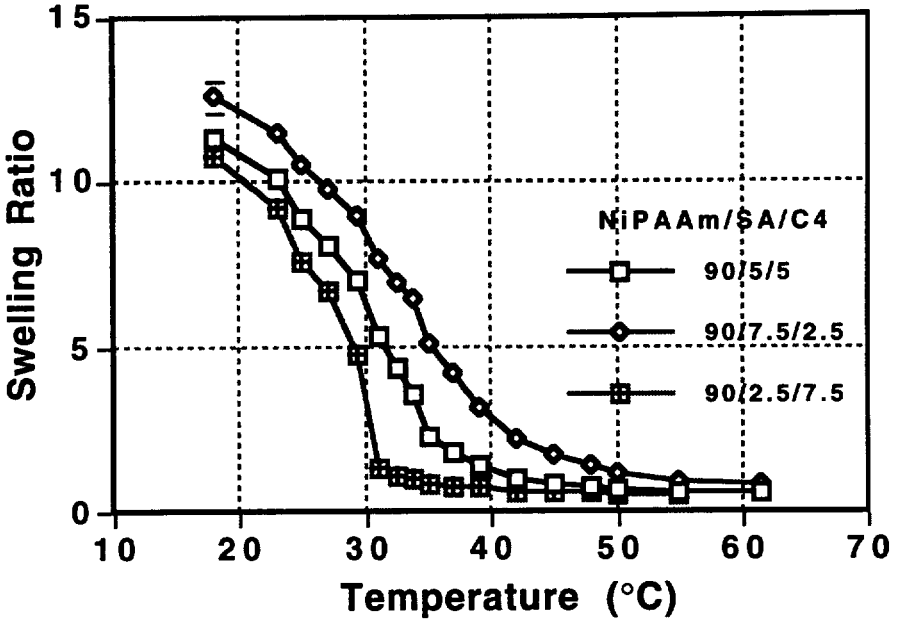

Fig. 3-6 Thermo-sensitive swelling behavior of terpolymer (PNiPAAM/SA/C4, 0.8 mol% MBAAm) gels in 0.05M PBS buffer (pH 7.3).

Fig. 3-6 shows the temperature-dependent swelling equilibria for three networks, poly(NiPAAm-co-SA-co-n-N-butylacrylamide) with three different copolymer ratios, 90/7.5/2.5, 90/5/5, 90/2.5/7.5. Fig. 3-7 shows the temperature-dependent swelling equilibria for three networks, poly(NiPAAm-co-SA-co-n-N-tetradecylacrylamide) with three different copolymer ratios, 95/4/1, 95/2.5/2.5, 95/1/4. Generally, both two figures show the same results for netwok swelling in response to hydrophilic/hydrophobic comonomer ratio changes. When the amount of hydrophilic comonomer (SA) incorporation increases, networ temperature-dependent swelling profiles shift to the right and up (higher swelling ratio, higher critical temperature points). On the other hand, network swelling profiles shift down to the left (lower swelling ratio, lower critical temperature points) as the amount of hydrophobic comonomer, either n-N-butyl- or n-N-tetradecyl-acrylamide, incorporation increases. Network swelling is delicately balanced

bythe function of each individual hydrophilic or hydrophobic comonomer species incorporated in the network.

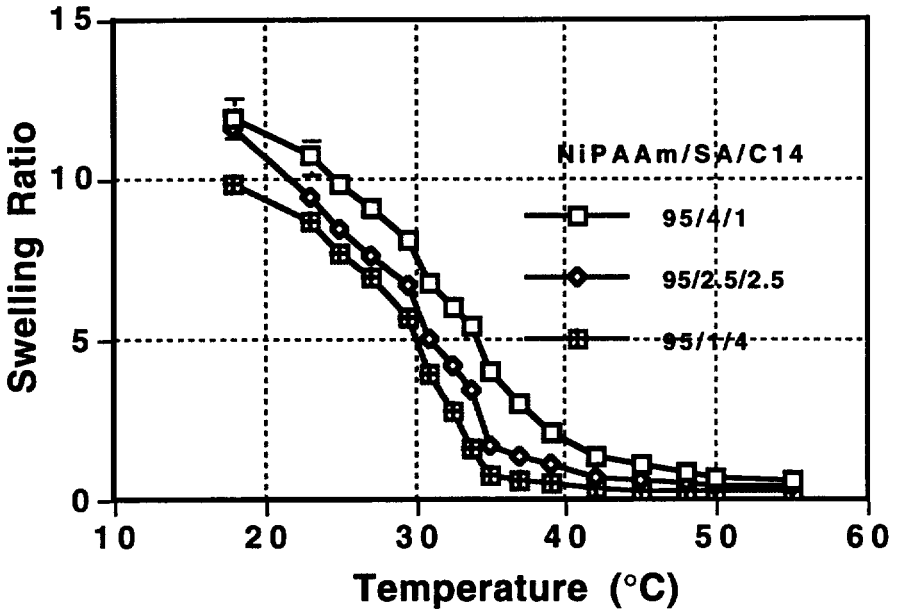

Fig. 3-7 Thermo-sensitive Swelling behavior of terpolymer gels (NiPAAm/SA/C14, 0.8 mol% MBAAm) in 0.05M PBS buffer (pH 7.3).

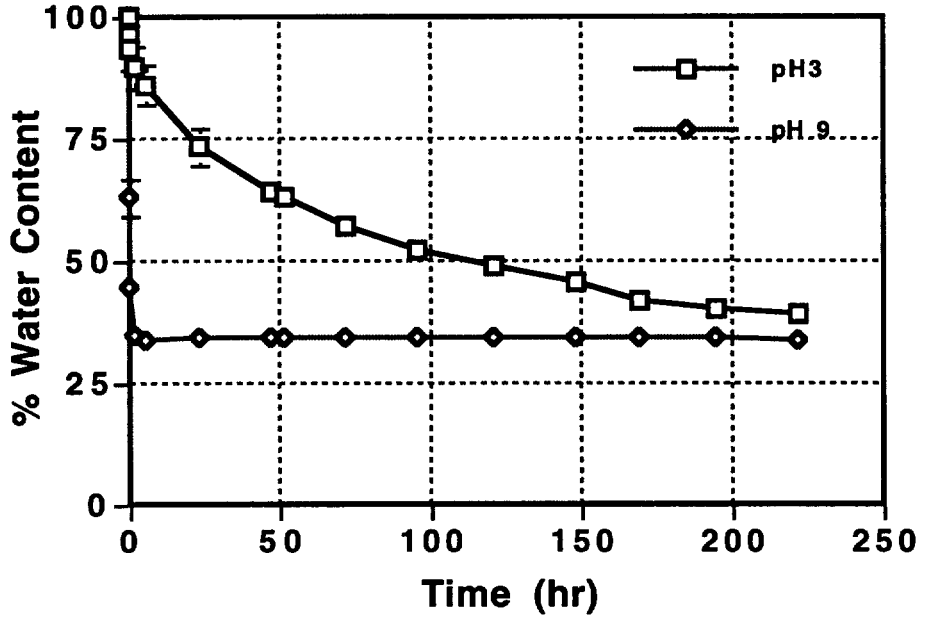

Fig. 3-8 Swelling kinetics of terpolymer (NiPAAm/SA/C4, 95/3/2) gels undergoing thermo-transition from 25 to 40 °C in different pH media.

Fig. 3-8 shows the swelling kinetics for terpolymer (NiPAAm-co-SA-co-n-N-butylacrylamide, 95/3/2) gels undergoing thermo-transition from 25 to 40 °C in different pH media. When media temperature jumps from below the gel critical temperature ($T<T_c$) to above the critical temperature ($T>T_c$), terpolymer gels deswell very quickly in basic media and extremely slowly in acidic media. Similar results have been discussed in detail in Chapter 2 with regard to the effect of ionized vs. neutralized SA in the copolymer gels is a bit higher than corresponding NiPAAm/SA gels after 200 hrs (Figure 2-2). Fig. 3-9 shows the temperature-dependent swelling equilibra for poly (NiPAAm-co-SA-co-n-N-butylacrylamide) (95/3/2) networks with three different amounts of the crosslinker, BAC (1, 1.5, and 2.5%). Network thermo-sensitive swelling behavior as well as critical points do not change, except the swelling ratio decreases as the network crosslinking density increases. Like the common crosslinker MBAAm, bis(acryloyl)-cystamine crosslinker behaves as a normal crosslinking agent during the network synthesis.

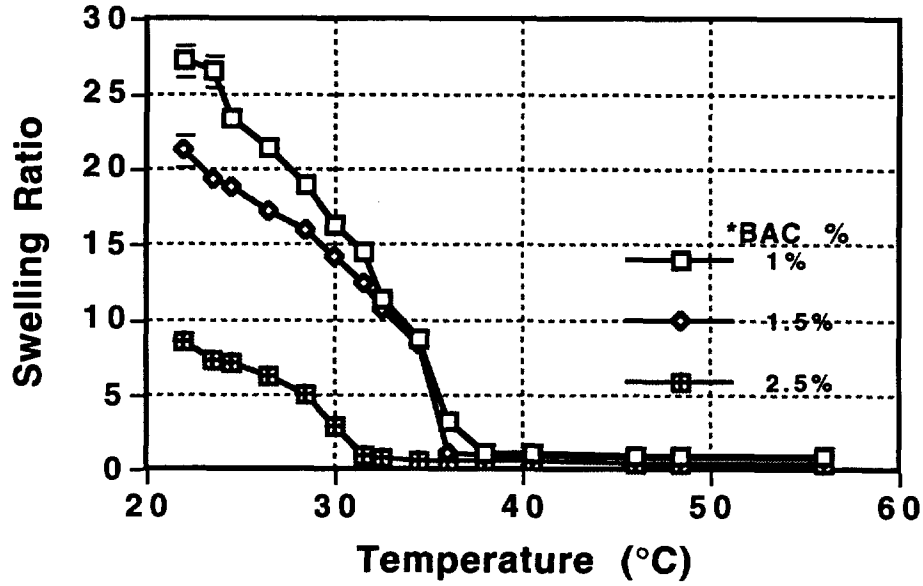

Fig. 3-9 Effect of crosslinker concentration on thermo-sensitive swelling behavior of terpolymer (NiPAAm/SA/C4, 95/3/2) gels in 0.05M PBS buffer. (*mol% to monomers)

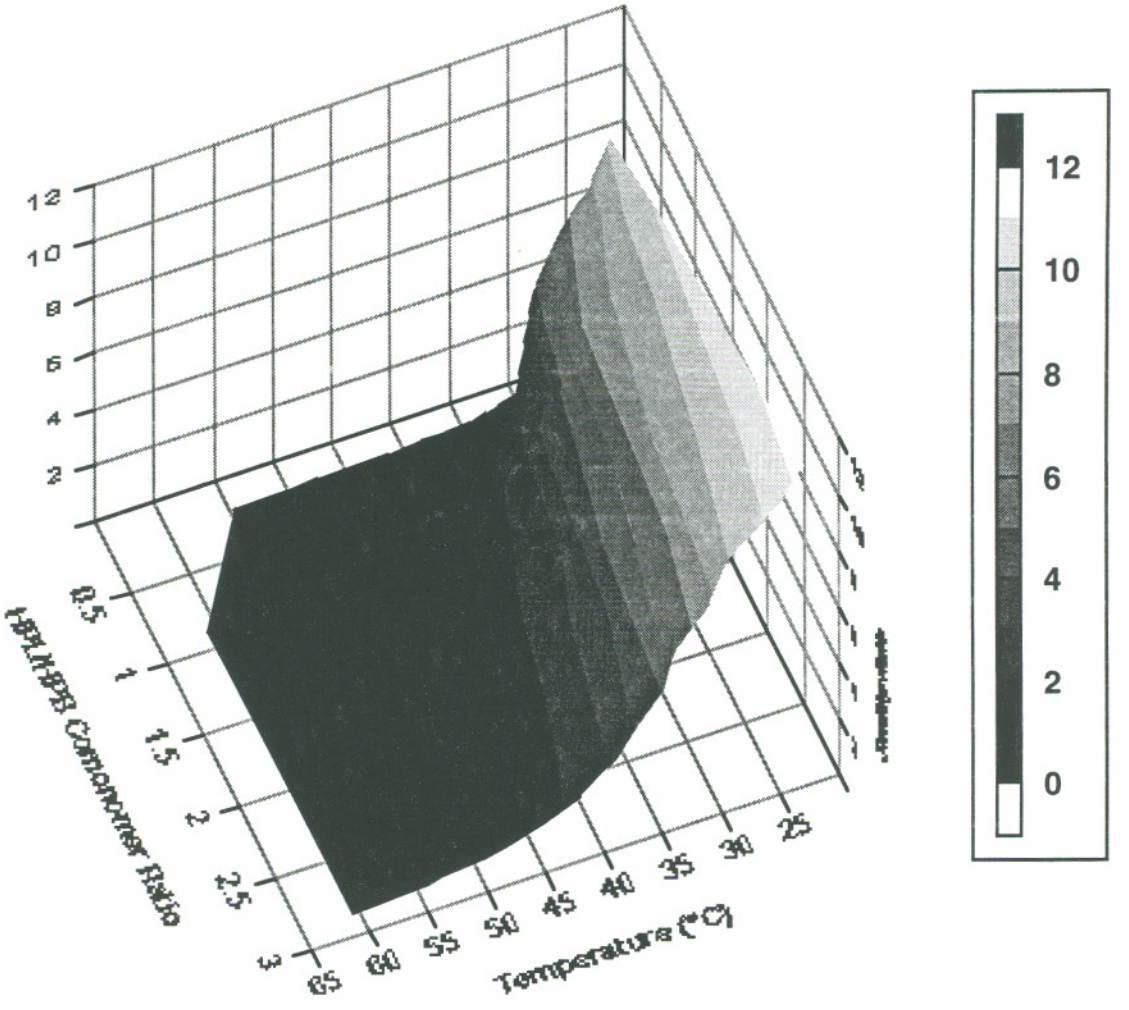

Fig. 3-10 Temperature-dependent swelling equilibra of amphiphilic networks, crosslinked poly(NiPAAm-co-SA-n-N-butylacrylamide), vs. hydrophilic SA and hydrophobic RMAAm comonomer ratio in 0.05M PBS buffer (pH 7.3).

Fig. 3-10 summarizes the effects of network hydrophilic and hydrophobic comonomer ratio on the temperature-dependent swelling equilibra for PNiAAm amphiphilic networks. Although none of the currently existing theoretical models can describe the temperature critical swelling behavior of PNiAAm gels quantitively, esp. in the mixing part of the gel free energy expression discussed in section 3.4.1 of this chapter, the fuction of ionized hydrophilic comonomer SA can be estimated properly by an ideal Donnan equilibria

approach (eq 3-8) as the networks have very high swelling ratio, very low incorporation of ionized SA (less than 10 mol%), and remain in equilbrium.

The hydrophobic contribution to the mixing term of gel free energy has been expressed as (36)

$$\Delta G^{hydrophobic} = C_a + C_b T + C_c T^2 \qquad (3\text{-}10)$$

where C_a, C_b, and C_c are system-dependent parameters that can be related to the characters (amount and length of the alkyl side chain) of the hydrophobic species in the networks. (67) It would be interesting to see how to fit these empirical parameters using experimental approaches.

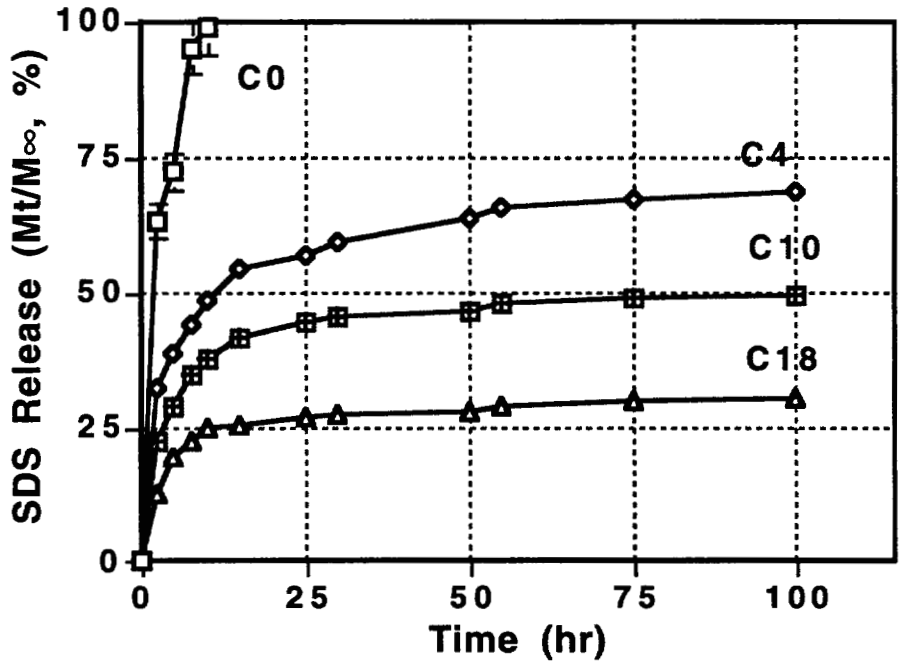

Fig. 3-11 SDS release from terpolymer (PNiPAAm/SA/Cn, 95/2.5/2.5, 0.8 mol% MBAAm) in water under "normal" conditions (no release media changing) at 25 °C mesaured by HPLC.

Fig. 3-11 shows the sodium dodecyl sulfate (SDS) release profiles from four different networks, crosslinker poly(NiPAAm-co-SA)(95/5), poly(NiPAAm-co-SA-n-N-butyl-, n-N-decyl-, n-N-octadecylacrylamide) (95/2.5/2.5), in water at 25 °C by HPLC measurement. Except for the poly(NiPAAm-co-SA) gels, all three other samples's release profiles demonstrate first-order (first 25 hr) to pseudo-zero-order (after 25 hr) kinetics (detailed discussion of hydrogel diffusion kinetics is found in Chapter 4). Release rates decrease dramatically as network alkyl chain length increases. This is proposed to result from increasing hydrophobic interactions (binding) between SDS hydrocarbon chains and the network alkyl side chains. Release profiles from poly(NiPAAm-co-SA) gels (no pendent alkyl side chain introduced) show very rapid release kinetics (within 10 hrs).

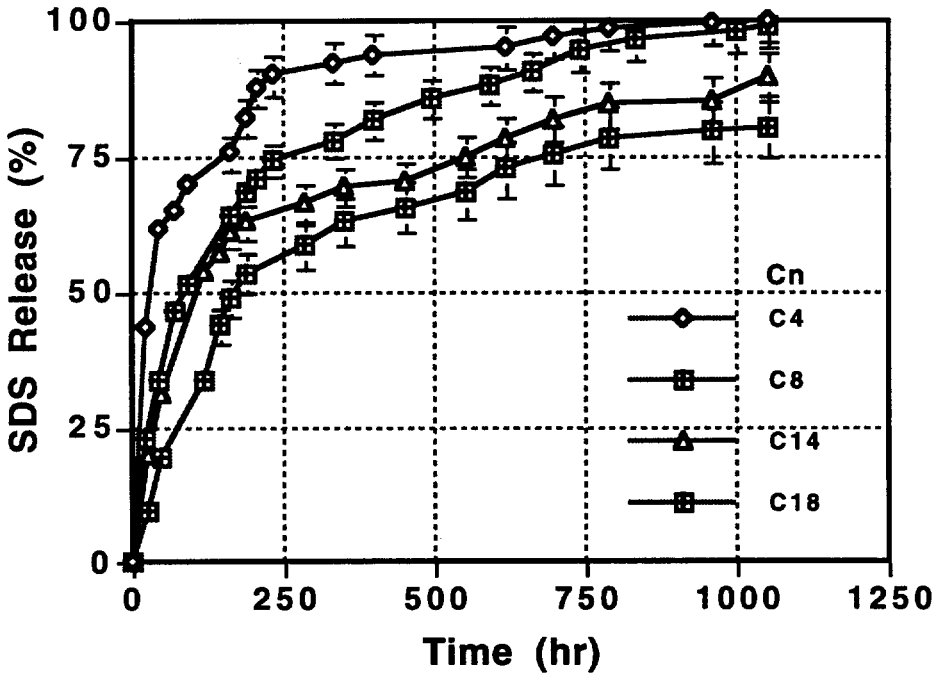

Fig. 3-12 SDS Release from terpolymer (PNiPAAm/SA/Cn, 95/2.5/2.5, 0.8 mol% MBAAm) gels in water under "sink" condition at 25°C measured by swelling ratio monitoring.

Fig. 3-12 shows SDS release profiles from four different networks, poly(NiPAAm-co-SA-co-n-N-butyl, n-N-decyl-, n-N-tetradecyl-, n-N-octadecylacrylamide) (95/2.5/2.5)

in water by swelling ratio monitoring measurement under fixted temperature 25°C. All release profiles exhibit interesting long-term pseudo zero-order release kinetics over the initial 200 hour period, particularly in networks containing long alkyl side chains. Release rates decrease as network alkyl chain lengths increase duo to the hydrophobic chain-chain interactions.

Fig, 3-13 shows SDS release profiles from three different networks, poly(NiPAAm-co-SA-n-N-decylacrylamide), with fixed SA amount (2.5 mol%) and different amounts of n-N-decylacrylamide comonomer incorporation (1, 2, 3 mol%) measured by swelling ratio changes monitored at 25 °C. All the release curves show the same kinetic pattern. However, release rates decreae as the amount of hydrophobic components increase due to enhancement of hydrophobic interactions between SDS and network alkyl chains.

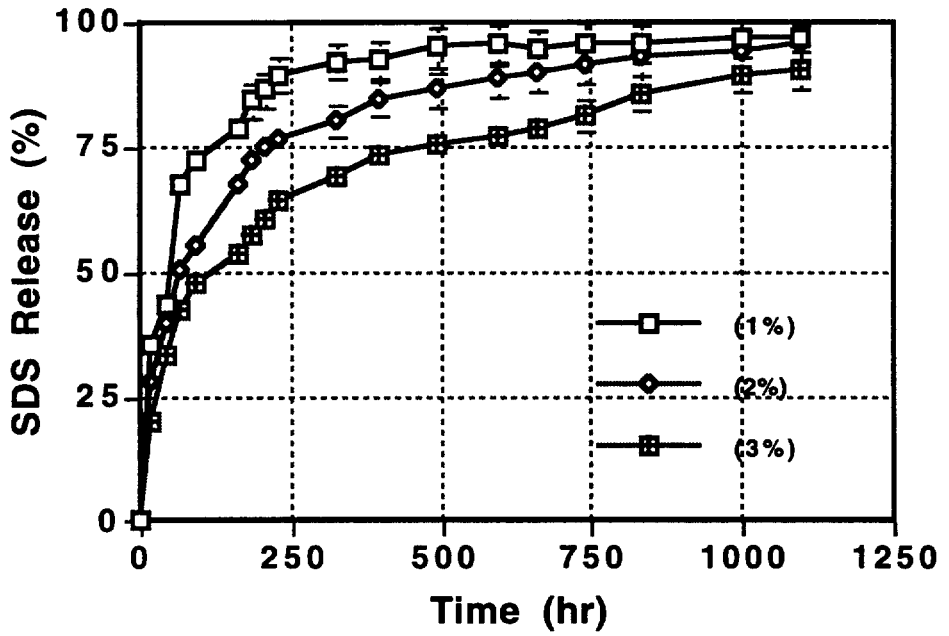

Fig. 3-13 SDS release from terpolymer (PNiPAAm/SA/ C10, 0.8 mol% MBAAm) gels in water under "sink" condition at 25 °C measured by swelling ratio monitoring.

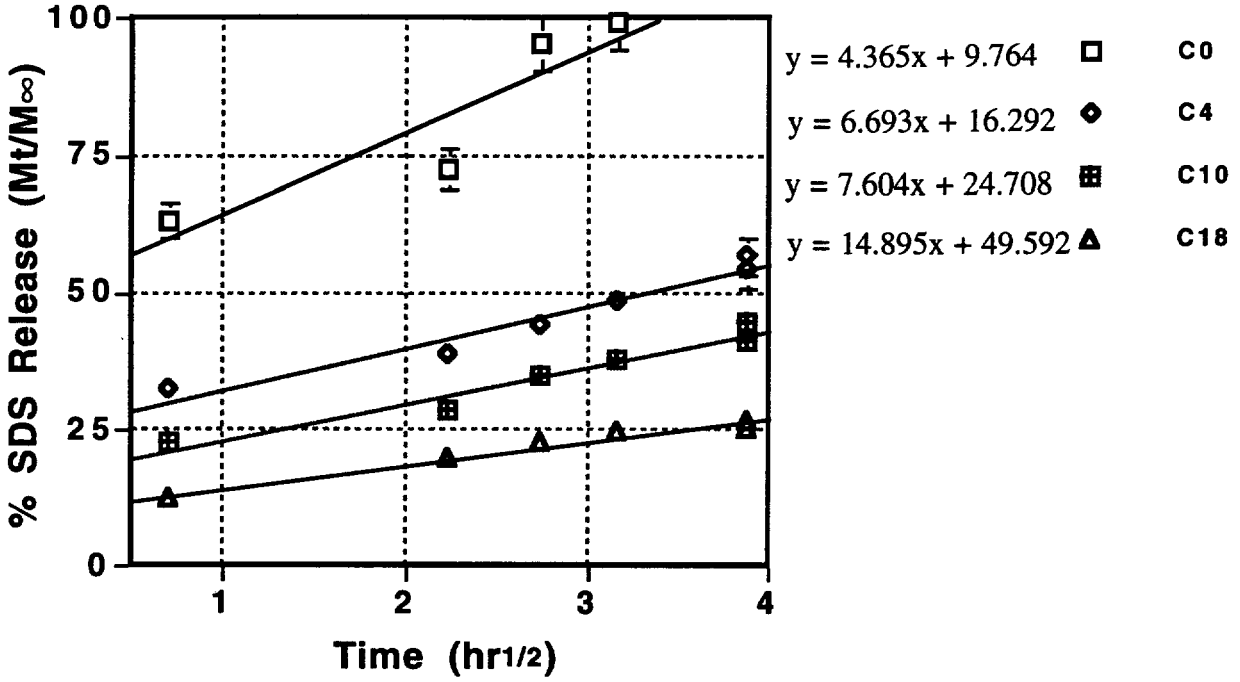

Fig. 3-14 SDS release vs square root of time from terpolymer (NiPAAm/SA/Cn, 95/2.5/2.5, 0.8 mol% MBAAm) networks during the first 16 hrs in water under "normal" conditions at 25 °C measured by HPLC.

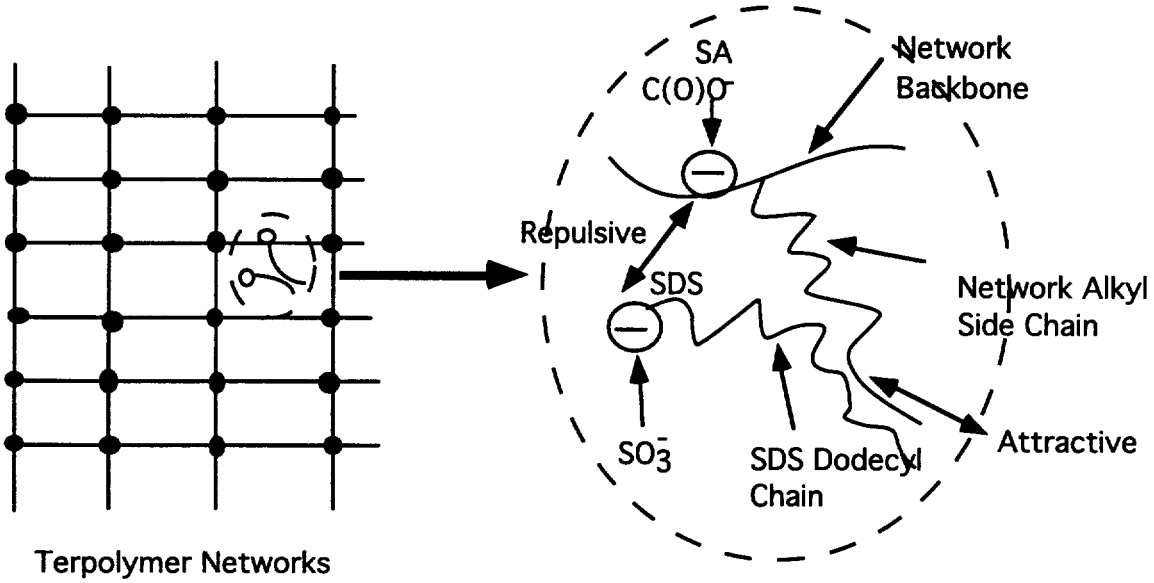

Fig. 3-15 Schematic diagram of the hydrophobic chain-chain interaction between terpolymer networks and SDS.

Fig. 3-14 shows SDS release vs. square root of time from terpolymer (PNiPAAm/SA/Cn, 95/2.5/2.5, 0.8 mol% MBAAm) during the first 16-hr release period in water at 25 °C measured by the HPLC method. All curves display a linear pattern with fits indicated from linear regression. During the first 16-hr release period from the four different gels, SDS release shows classic first-order diffusion kinetics and obeys Fickian laws. "Free" diffusion of SDS (unhindered chain-chain interactions in the networks) is predominant during the early period as indicated by these kinetics. Beyond this release period, release kinetics changes to zero-order as discussed above in Fig. 3-10 to Fig. 3-13.

Fig. 3-15 shows the schematic diagram of molecular associations due to hydrophobic chain-chain interactions (labile binding) between amphiphilic networks of crosslinked poly(NiPAAm-co-SA-co-RAAm), and sodium dodecyl sulfate (SDS). Their partial structural similarity is also illustrated in this figure. Correlation with thermodynamic data reported (67-68) for hydrophobic binding between alkyl chains in two different polymers show the standard free energy changes for interaction which is a linear function of the alkyl chain length from n=1 to n=16. This indicates that each methylene group of the alkyl chain makes equivalent contributions to interaction to SDS. This helps provide semiquantitive explainations about the results of SDS release vs. network hydrophobicity, such as the length and amount of alkyl side chain incorporated. Detailed kinetic studies of transport phenomena in hydrogels are discussed in Chapter 4.

Reference

1. Yu, H. and Grainger, D. W., ACS Polymer Preprints (Am. Chem. Soc., Div. Polym. Chem.), 34, 820 (1993).

2. Ivan, B., Kennedy, J. P., and Mackey, P. W., ACS Symposium Series 469, 194 (1991).

3. Winnik, F. M., Rinsdorf, H, and Venzmer, J., Macromolecules, 24, 1678 (1991).

4. Kungwatchakun, D. and Irie, M., Makromol., Chem., Rapid Commun., 9, 243 (1988).

5. Snyder, W. D. and Kotz, I. M., J. Am. Chem. Soc., 97, 4999 (1967).

6. Elaissaf, J., J. Appl. Polym. Sci., 22, 873 (1978).

7. Nguyen, A. L. and Luong, J. H. T., Enzyme Microb. Technol., 12, 663 (1990).

8. Fujishige, S., Polym. J., 19, 297 (1987)

9. Schild, H. G. and Tirrell, D. A., Langmuir, 7, 665 (1991).

10. Wooten, W. C., Blanton, R. B., and Coover, H. W., J. Polym. Sci. XXV, 403 (1957).

11. Otake, K., Inomata, H., Konno, M., and Saito, S., Macromolecules, 23, 283 (1990).

12. Chiklis, C. K. and Grasshoff, J. M., J. Polym. Sci., Part A-2, 8, 1617 (1970).

13. Heskin, M. and Guillet, J. E., J. Macromolec. Sci. Chem. 2, 1441 (1969).

14. Schild, H. G. and Tirrell, D. A., Macromolecules, 24, 948 (1991).

15. Priest, J. H., Murray, S. L., Nelson, J. R., and Hoffman, A. S., ACS Symposium Series 350, 255 (1987).

16. Shields, D. J. and Cover, H. W., J. Polym. Sci., XXXIX, 532 (1959).

17. Kennedy, J. P. and Otsu, T., J. Macromolec. Sci. Rev. Macromol. Chem., C6(2), 237 (1972).

18. Mortimer, G. A., J. Appl. Polym. Sci., 18, 2847 (1974).

19. Zurakowaska-Orszagh, J. Polym. Sci., 19, 720 (1978).

20. Yamada, N., Okano, T., Sakai, H., Karikusa, F., Sawasai, Y., and Sakurai, Y., Makromolek. Chem., Rapid Commun, 11, 571 (1990).

21. Schild, H. and Tirrell, D. A., J. Phys. Chem., 94, 4352 (1990).

22. Hoffman, A. S., Afrassiabi, A., and Dong, L. C., J. Control. Rel., 11, 255 (1986).

23. Hirose, Y., Amiya, T., Hirokawa, Y., and Tanaka, T., Macromolecules, 20, 1342 (1987).

24. Matsuo, E. S. and Tanaka, T., J. Chem. Phys., 88, 1695 (1988).

25. Tanaka, T., Sato, E., Hirokawa, Y., Hirotsu, S., and Peetermans, J., Phys. Rev. Lett., 55, 2455 (1985).

26. Abel, E. P. and Bowman, W. A., U.S. Pat. 4,504,569 (1985).

27. Bowman, W. A., Eur. Pat. Appl., 121,141 (1984).

28. Anon., Res. Discl., 277, 336 (1987).

29. Pelton, R. H. and Chibante, P., Colloids Surf., 20, 247 (1988).

30. Pelton, R. H., Langmuir, 5, 816 (1989).

31. Turner, S. R. and Siano, D. B., U. S. Pat., 4,520,182 (1985).

32. Yamamoto, I., Iwasaki, K., Hirotsu, S., J. Phys. Sco., Jpn., 58 (1), 210 (1989).

33. Hirotsu, S., Hirokawa, Y., and Tanaka, T., J. Chem. Phys., 87, 1392 (1987).

34. Marcheti, M., Prager, S., and Cussler, E. L., Macromolecules, 23, 3445 (1990).

35. Lee, K. K., Cussler, E. L., Marcheti, M., and McHugh, M. A., Chem. Eng. Sci., 45, 766 (1990).

36. Otake, K., Inomata, H., Konno, M., and Saito, S., J. Chem. Phys. 91, 1345 (1990).

37. Prange, M. M., Hooper, H. H., and Prausnitz, J. M., ALCHE J., 35, 803 (1989).

38. Lundberg, R. D., *Encyclopdia of Polymer Science and Engineering*, Vol. 8, p393, Wiley-Interscience, New York (1987).

39. Marchetti, M., Prager, S., and Cussler, E. L., Macromolecules, 23, 1760 (1990).

40. Eichinger, B. E., Macromolecules, 21, 3060 (1988).

41. Flory, P. J., *Principle of Polymer Chemistry*, Cornell University Press, Ithaca, New York (1963).

42. Taylor, L. D. and Cerankowski, L. D., J. Polym. Sci., Part A: Polym. Chem. 13, 2551 (1975).

43. Odian, G., *Principles of Polymerization*, Wiley-Interscience, New York (1981).

44. Weil, E. D., *Encyclopedia of Chemical Technology*, Vol. 22, p.152, John & Wiley, New York (1973).

45. Webster, O. W., Hertler, W. R., Sogah, D. Y., Farnham, W. B., and RajanBabu, J. Am. Chem. Soc., 105, 5706 (1983).

46. Walker, J. A. and Vause, C. A., Sci. Am. 253, 98 (1987).

47. Fujishige, S., Kubota, K., and Ando, I., J. Phys. Chem., 93, 3311 (1989).

48. Kubota, K., Fujishige, S., and Ando, I., J. Phys. Chem., 84, 5154 (1990).

49. Inamata, H., Goto, S., and Saito, S., Macromolecules, 23, 4887 (1990).

50. Williams, C., Brochard, F., Frisch, H. L., Annu. Rev. Phys. Chem., 32, 433 (1981).

51. James, H. M. and Guth, E., J. Chem. Phys., 15, 669 (1947).

52. Mark, J. E. and Erman, B., *Rubberlike Elasticity A Molecular Primer*, Wiley & Sons, New York (1988).

53. Flory, P. J. and Erman, B., Macromolecules, 12, 2782 (1982).

54. Flory, P. J., J. Chem. Phys., 66, 5720 (1977).

55. Brandup, J. and Immergut, E. H., Eds. *Polymer Handbook*, 2nd ed., Wiley-Interscience, New York (1975).

56. Ricka, J. and Tanaka, T., Macromolecules, 17, 2916 (1984).

57. Rice, S. A. and Harris, F. E., Z. Phys. Chem. Neue Folge, 8, 207 (1956).

58. Gehrke, S. H., Andrews, G. P., and Cussler, E. L., Chem. Eng. Sci., 41, 2153 (1986).

59. Tsuchida, G. and Abe, K., Adv. Polym. Sci., 45, 1 (1982).

60. Butler, K., Thomas, P. R., and Tyler, G. J., J. Polym. Sci., 48, 357 (1960).

61. Erickson, J. G., U.S. Pat. 2,451,436 (1948)

62. Erickson, J. G., J. Am. Chem. Soc., 74, 6281 (1952).

63. Jordan, E. F., Jr., Riser, G. R., Parker, W. E., Wrigley, A. N., J. Polym. Sci., 4, A2, 975 (1966).

64. Specht, E. H., Neuman, A., Neher, H. T., U.S. Pat. 2,773,063 (1956)

65. Ringsdorf, H., Venzmer, J., and Winnik, F. M., Macromolecules, 24, 1678 (1991).

66. Kranzlein, G. and Corell, M., Ger. Pat. 752,481 (1952).

67. Nemethy, G and Sheraga, H. A., J. Chem. Phys., 66, 1773 (1962).

68. Molyneux, P. and Cornarakis-lentzos, M., Colloid Polym. Sci., 257, 855 (1979).

Chapter 4 Controlled Release Studies of Model Bioactive Compounds from Novel PNiPAAm Hydrogels

4.1 Introduction

Medical and pharmaceutical applications of synthetic polymers have contributed significantly to the quality and effectiveness of the present health care system. These applications range from contact lenes to implantable prostheses, from artificial skin to vascular grafts, from the artificial heart to controlled delivery systems. Current biomaterials research relies heavily on synthetic polymers in most applications requiring compliance with soft or connective tissue, cardiovascular implantation, or being non-irritating to the skin for transdermal applications. Polymers also can be synthesized to meet the strict regulatory and safety requirements as biomaterials. For example, they must be biocompatible, interacting with assorted tissues and organs in non-toxic manners, and not destroy the cellular constituents of the body with which they interface.

In recent years, numbers of new drugs have fallen tremendously . This can be attributed partially to wide acceptance of current treatments for common diseases or "accepted" dogma. Moreover, stringent regulatory rules governing introduction of new drugs together with the limited life span of patent protection and cost make development of new drugs extremely difficult. In addition to the numerous advantages of controlled drug delivery, another attractive feature is that controlled delivery technology may be used to improve existing drug formulations and permit renewed patent protection.

Drug delivery challenges have grown enormously with the advent of a multitude of new protein and peptide drugs. Particular difficulties are encountered protecting these agents from a harsh degradative gastric environment as well as in optimizing delivery of therapeutic and non-toxic doses. Also even for controlled delivery dosages, very few systems are available which administer these drugs according to long-term first or zero-order sustained release kinetics and/or complex dosage regimens (i.e. intermittent and pulsatile therapies). These unconventional delivery strategies are proposed to maximize

drug efficacy and minimize side effects and tolerance development (1,2). Furthermore, the significance of pulsatile drug delivery, particularly for regulatory peptides and proteins, is not well understood. Pharmacodynamic data is scant due to the difficulty in achieving these system kinetics. Clearly, successful development of such delivery systems remain a significant challenge.

Among the wide array of synthetic biomaterials applied to biomedical and pharmaceutical fields, hydrogels have achieved significant attention on account of their good biocompatibility and controllable permeability (3,4). For controlled delivery applications, these materials are particularly suitable to deliver entrapped drug in an aqueous medium and regulate drug release by controlling gel swelling and crosslinking density. Moreover, some hydrogels have shown abilities to undergo phase transitions and demonstrate reversible, large swelling-deswelling kinetics in response to environmental changes including solvent composition (5,6), ionic strength (7), pH (8), temperature (6, 8-10), electric field (11), and light (12,13). These hydrogels are interesting candidates to achieve sustained and pulsatile release strategies for drugs under control from external stimuli (14-19).

In this chapter, theroretical modeling studies of diffusion in hydrogels are reviewed. Treatments of mass transfer in heterogenous structures by multi-component controlled diffusion approaches are also discussed. Several bioactive agents, including hydrophilic co-enzyme vitamin B12, the hydrophobic steroid progesterone, and amphiphilic peptides insulin and interferon have been chosen as model drugs. Their release kinetics from both thermo- and pH- sensitive ionizable and amphiphilic PNiPAAm networks have been investigated and discussed in detail throughout this chapter.

4.2 Theoretical Framework for Mass Transfer in Hydrogels

4.2.1 Fickian First and Second Laws

4.2.1.1 Description of Diffusion

In general, the partial molar energy of a solute (uncharged) in solution is given by

$$\mu = \mu^0 + RT \ln a \tag{4-1}$$

where μ is the partial molar free energy, μ^0 is the partial free energy in the standard state, R is the universal gas constant, T is the absolute temperature, and a is the activity of the solute. If the solution is dilute, it can treated as ideal and Eq. (1) may then be written as

$$\mu = \mu^0 + RT \ln C \tag{4-2}$$

where C is the molar concentration of the solute. The change in molar free energy $d\mu$ due to a concentration gradient dC is then

$$d\mu / dC = d (\mu^0 + RT \ln C) / dC \tag{4-3}$$

or

$$d\mu = RT (dC / C)$$

so the force

$$F = - d\mu / dx = - RT / C (dC / dx) \tag{4-4}$$

where negative sign arises because C and x increase in opposite directions. The friction force, F_f, is proportional to the velocity of the molecule, v, and with the proportionality constant, f.

$$Ff = Nvf \tag{4-5}$$

where N is Avogadro's constant. Therefore

$$Nvf = - (RT / C) (dC / dx) \tag{4-6}$$

or

$$J = Cv = - (RT / Nf) (dC / dx) = - (kT / f) (dC / dx) = - D (dC / dx) \tag{4-7}$$

where J is the solute flux and k is Boltzman's constant, and D is the diffusion constant. This is the one dimensional form of the Fickian first law (20-23). Under non-steady state condition, Eq. 7 becomes

$$J = - D (x) (\partial C / \partial x)_t \tag{4-8}$$

here the diffusion coefficient is assumed to be independent of time but position.

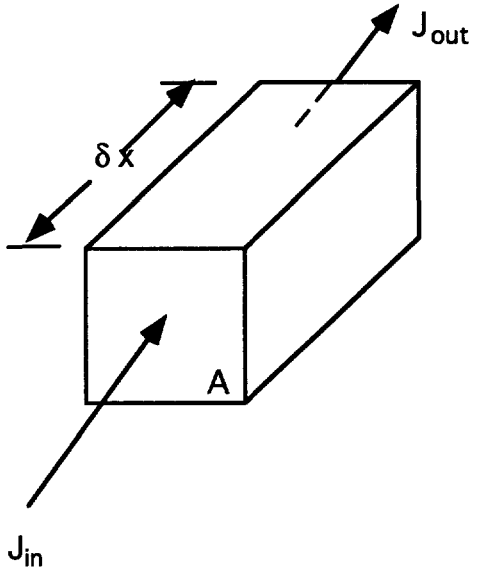

Fig. 4-1 Mass flow through a rectangular box (d x is a length and A is a cross sectional area), J_{in} is the influx and J_{out} is outflux.

Figure 4-1 depicts the flow of molecules through a rectangular box of length δx and surface area A.

$$J_{in} = J(x)$$

$$= - D(x)[\partial C(x\,,\, t)/\partial x]_t \tag{4-9}$$

$$J_{out} = J(x + \delta x)$$

$$= -D(x)[\partial C(x,t)/\partial x]_t - \delta\,[D(x)\,\partial C\,(x\,,\, t)\,/\,\partial x\,]_t \tag{4-10}$$

Therefore,

$$\delta C\,/\,\delta t$$

$$= (\,J_{in}\,A - J_{out}\;A)\,/\,V$$

$$= (\,J_{in}\,A - J_{out}\;A)\,/\,(\,A\;\delta x\,)$$

$$= \{-\,D\,(\,\partial C\,/\,\partial x\,)_t\,A + [\,D(\,\partial C\,/\,\partial x\,)_t\; + \delta\,D(\,\partial C\;/\,\partial x\,)_t\,]\,A\,\}\,/\,(A\;\delta x\,) \tag{4-11}$$

or

$$\delta C\,/\,\delta t\; = \delta\,[\,D\,(\,\partial C\,/\,\partial x\,)_t\,]\,/\,\delta x$$

By taking limits

$$\lim_{\delta_t \to 0} = (\delta C\,/\,\delta_t) = \lim_{\delta=0} = \delta[D(\delta C\,/\,\delta x)]_t$$

gives

$$\partial C\,/\,\partial t = \partial[\,D\,(\,\partial C\,/\,\partial x\,)]_t\,/\,\partial t \tag{4-12}$$

which is the Fickian second law. If D is independent of position, then Eq. 4-12 becomes

$$\partial C\,/\,\partial t = D\,(\,\partial^2 C\,/\,\partial X^2\,) \tag{4-13}$$

4.2.1.2 Molecule Size and Diffusivity

It is intuitive that as the molecular size of a solute increases, its diffusivity decreases because the larger the molecule, the more frictional resistance to its motion would be experienced. Diffusion-size relationships are expressed by the famous Stokes-Einstein equation

Table 4.1 Diffusion Coefficient of Some Molecules (20-21,24)

Molecule	MW	R [a]	D_{obs} (cm^2 / sec)	D_{cal} (cm^2 / sec)	% error
H_2O	18	-	2.54×10^{-5}	-	-
CH_3OH	32	0.824 [b]	1.37×10^{-5}	2.10×10^{-5}	53
Myoglobin	16,000	-	1.13×10^{-6}	-	-
Insulin	41,000	0.731 [c]	8.20×10^{-7}	8.30×10^{-7}	1.2
Hemoglobin	68,000	0.617 [c]	6.90×10^{-7}	7.00×10^{-7}	1.4
DNA	135,000	0.491 [c]	2.50×10^{-7}	5.60×10^{-7}	-
Urease	470,000	0.324 [c]	5.30×10^{-7}	3.70×10^{-7}	-

[a] $R = MW_1 / MW_2$;

[b] MW_1 = MW of H_2O and MW2 = MW of CH_3OH.

[c] MW_1 = MW of myoglobin and $MW2 = MW$ of insulin, hemoglobin, DNA and urease. (Myoglobin was chosen as the reference molecule in this series.)

$$D = (kT) / (6\pi r\eta) \qquad (4\text{-}14)$$

where r is molecular radius, η is the viscosity of the diffusing medium. For a molecule considered to be a sphere, its molecular weight (MW) is

$$MW = N \rho V = N \rho (4\pi r^3 / 3) \tag{4-15}$$

wher r is van der Waals radius of the molecule and ρ is the molecular density. So,

$$D \propto 1/(MW)^{1/3} \tag{4-16}$$

Table 4.1 lists several molecules with their diffusion coefficients, both experimentally determined and calculated from Eq. 16. Obviously, in some cases, the calculated diffusion coefficients differ markedly from their observed values where the assumptions on which Stoke's law was derived are not valid. (1)

4.2.1.3 Solute Binding and Its Diffusivity

When a molecule diffuses through a matrix, there may be interactions between drug and matrix not described in Fickian laws. The effect of such binding can be introduced as follows:

Let

$$C = C_f + C_b \tag{4-17}$$

where C_f equals the concentration of the freely diffusible solute and C_b is the concentration of the bound solute. If one assumes that the concentration of the bound solute is directly proportional to the free solute concentration, then

$$C_b = K' C_f \tag{4-18}$$

where K' is the proportionality constant. So, in one dimension

$$J = - D\, dC_f / dx = - [\, D / (\, 1 + K' \,)\, dC / dx \,] \qquad (4\text{-}19)$$

Thus, reversible adsorption occurring within the matrix can decrease the overall flux by a factor of $1 / (1 + K')$.

4.2.2 Modeling Studies of Drug Release and Diffusion from Polymers

4.2.2.1 Reservoir Systems

A molecule diffusing from a reservoir will experience the following steps:

(1) Dissolution into the dispersion medium of the reservoir.

(2) Diffusion within the dispersion medium

(3) Partitioning into the membrane.

(4) Diffusion across the membrane.

(5) Partitioning into the receptor medium.

(6) Diffusion across the stagnant diffusion layer.

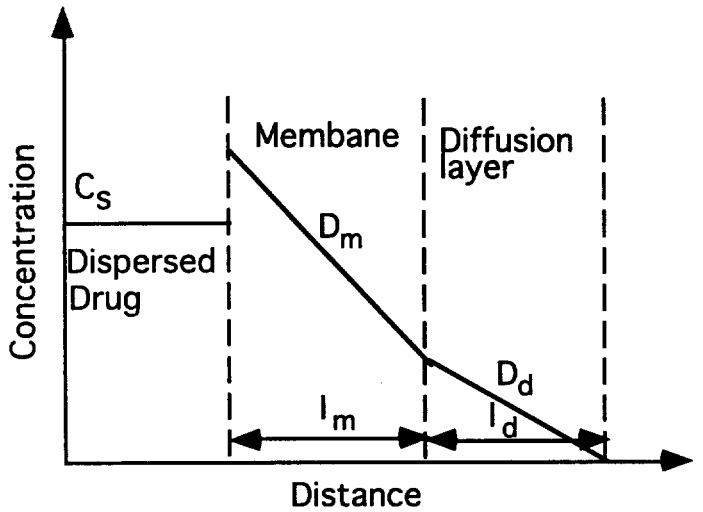

Fig. 4-2 Schematic diagram of the concentration profile in reservoir system.

Diffusion across the membrane is the most important transfer process and the one which ultimatly controls the effectiveness of the device (Fig. 4-2).

Under these conditions the cumulative amount of the drug released per unit area, Q_t, at a given time can be calculated by solving Eq. 7.

$$Q_t = (C_S K D_m D dt) / (K D_m l_m + D_d l_d) \quad (4\text{-}20)$$

where C_S is the solubility of the drug in the dispersion medium; K is the partition coefficient of the drug between the membrane and the reservoir medium; D_m is the diffusion coefficient of the drug in a membrane of thickness l_m; and D_d is the diffusion coefficient of the drug in the boundary layer of the thickness l_d. (25) Drug release could be zero order (linear function of time) if the diffusion coefficient is constant. Normally, after short periods of release time the release rate is faster than the predicted by Eq. 20, which is appropriate for steady-state conditions. This is the so-called "burst effect" which is generally considered the result of release of initially saturated drug in the surface layer. The release of drug over the complete time course can also be described mathematically by solving the Fickian second law of diffusion, Eq. 4-12, 4-13.

4.2.2.2 Monolithic Systems

4.2.2.2.1 Drug Dissolved in the Device

If drug is dissolved homogeneously within the solid polymer matrix and it is assumed, for simplicity, that one planar surface is available for release, the amount of drug released obtained by solving Fickian second law, Eq. 4-13 (26) is:

$$M_t = M_\infty [1 - \frac{8}{\pi^2} \sum_{n=1}^{\infty} \frac{1}{(2n-1)^2} \exp(-\frac{(2n-1)^2 \pi^2 D_m t}{4 l_m^2})] \quad (4\text{-}21)$$

where M_∞ is the amount of drug released in an infinite time period. Drug release is first-order and a linear relationship is found between the amount of released and the square root of time. It is possible to construct a monolithic device having a specific character to provide approximate zero-order kinetics. (27)

4.2.2.2.2 Drug Dispersed in the Device

If drug cannot dissolve into the polymer, dispersions can be formulated. Drug release has been modeled using a layer depletion mechanism (Fig. 4-3). (28)

$$M_t=A[D_m t C_s(2C_0-C_s)]^{1/2} \qquad (4\text{-}22)$$

Release is proportional to the square root of time.

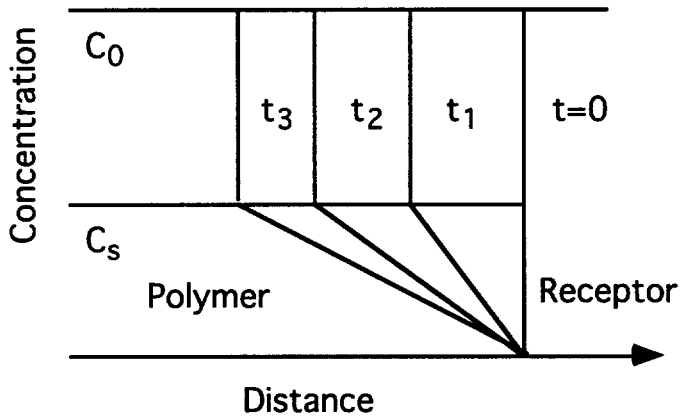

Fig. 4-3 Schematic diagram of concentration profile of drug loading C_0 and solubility C_s within a monolithic device.

At high loading, a drug can form a continuous capillary network throughout the polymer and release is governed by drug leaching through this region, described as:

$$Q_t = [\frac{\varepsilon}{\tau} D_m(2C_0 - \varepsilon C_s)C_s t]^{1/2} \qquad (4\text{-}23)$$

where ε is the porosity and τ the tortuosity of the polymer matrix. (28)

4.2.3 Diffusion in Heterogeneous Systems

It is incorrect to treat diffusion associated with heterogeneous structures by Fickian laws. Instead, non-Fickian approaches, moving boundary approaches, as well as irreversible thermodynamic approaches are widely used. (23, 29-31)

Heterogeneous structures occur when dealing with layered structures (laminates); each layer can be composed of a different material. Alternatively, heterogeneous structures occur when considering systems in which particulates of one phase are dispersed throughout another continuous phase. Both of these heterogeneous structures can be found in some polymer systems. One result of this heterogeneity is that the diffusion coefficient can no longer be assumed constant throughout the system.

Diffusion of ions, in general, cannot be treated by the simple passive Fickian relationships because ions interact electrostatistically with themselves, the solvent, and the polymers. Treatments of irreversible thermodynamics are used to deal with these cases. Essentially irreversible thermodynamics provides a theoretical framework for handling coupling between different transport phenomena, such as simultaneous osmotic gradients, pressrue differences, and electrical potential differences.

Moving boundary and non-Fickian diffusion occurs in swellable polymer systems when the boundries of a polymer change and polymer chain relaxation occurs with time upon exposure to a solvent system.

Also, the release kinetics of macromolecules such as proteins and polypeptides from polymers are complex. The difficulties include the introduction of concentration-dependent diffusion coefficients and the problems involved when a long chain has to "random walk" along narrow connecting channels in the porous network of the polymer matrix reptation (27,32).

4.2.4 Modeling Studies for Hydrogel Swelling-Controlled Release Systems

The available models for hydrogel swelling-controlled release systems can be divided into two categories: one-phase and two-phase models. A one-phase model simply treats the hydrogel as a single phase with two species being transported with in it, while two-phase model treats the hydrogel as consisting of distinct gel and glassy phases with the diffusivities of the two species being different in each phase. The transport of both penetrant (solvent) and drug are considered as Fickian diffusion processes (Eq. 4-8, 4-12) in most of these treatments.

4.2.4.1 One-Phase Models

One simple model was proposed by assuming that diffusion of the penetrant obeys the Fickian law in one dimension, and that a linear relationship exists between changes in gel network demensions and the extent of penetrant uptake. (33) The position of the gel-water interface upon swelling is then defined by

$$X(t) = \delta/2 + A\, t^{1/2} \qquad (4\text{-}24)$$

where δ is gel thickness and A is a proportionality constant. The equation is obtained from the solvent penetrating into the gel network by Fickian diffusion (proportional to $t^{1/2}$), The rest of the treatment is similar to that for a monolithic dispersed drug system ($C_0 > C_S$). Solutions to these governing equations (Eq. 4-8, 4-12) gives the fraction of drug released as a function of the square-root of time.

Another type of model simply considers simultaneous two-component diffusion (non-ideal Fickian) of drug and penetrant in a continuous medium governed by Eq. 4-8, 4-

12, where the diffusion coefficients are structure- and concentration-dependent arising from free-volume treatment,

$$D \approx D^0 \exp [-\beta(C - C_S)] \quad (4\text{-}25)$$

where D^0 is the standard diffusion coefficient of the species, C_S is the equilibrium solubility of the species in the hydrogel and β is a system constant.(34-35) These models can be fit to experimental data through adjustment of the parameters. However, the drug release and swelling ratio cannot be simultaneously fitted by a single set of parameters for any particular experiment. (36)

4.2.4.2 Two-Phase Models

Diffusivities of moving species in hydrogels may be substantially different in gel glassy and swollen phases. Anomalous diffusion may also be observed due to stress effects that accompany the relaxation phenomena in swelling. The mathematical treatment of such a system must involve moving boundary(ies), which comprise a swollen-glassy polymer interface if relaxation is not accompanied by volume expansion and gel-medium and swollen-glassy polymer interface if volume expansion is significant. A governing differential equation must be chosen for each species in each phase under isothermal conditions.

If the gel volume is assumed to be unaffected by polymer relaxation, diffusion of drug and water are simply described by Eq. 4-12 in each individual phase with moving boundary X(t). (37) X(t) is defined by a water mass balance under the assumption that water does not diffuse in the glassy region.

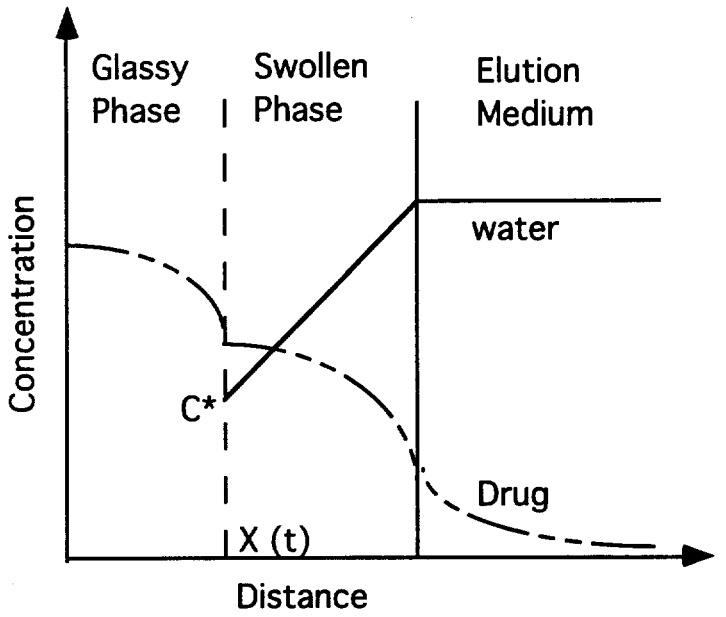

Fig. 4-4 Schematic diagram of the simulation results of two-phase models for a semi-infinitegel slab without considering volume change.

Concentration profiles of this model for certain special cases are shown in Fig. 4-4. The solution to these equations shows that the amount of drug accumulated in the medium at any time is propotional to the square-root of time.

A two-phase Fickian diffusion model with significant volume expansion has been proposed by Peppas et al, (38). The equations and boundary settings are the same as the Rudolph model (37) but with different X(t) definition,

$$(\partial C_C / \partial x)_{x=X(t)} = 0 \qquad (4\text{-}26)$$

where C_C is the penetrant (water) concentration inside the gel. The gel-medium interface is defined by a volume balance on the penetrant absorbed; the volume expansion of gel is proportional to the volume of the penetrant absorbed. By assuming that the diffusivity of the drug in the glassy polymer is negligibly small compared to that in the gel, thus modifying the situation to one of pseudo steady-state, the release rate is again found to be proportional to $t^{1/2}$.

Also, several modeling approaches deal with two-phase Case II diffusion with or without volume changes. (34, 38). Case II transport is a consequence of the fact that polymer chain relaxation is the rate determining step to release (much slower than diffusion of the penetrant within the gels. In this case the swollen-glassy interface, X(t), is defined as the innermost limit of dispersal of the penetrant. Zero-order release is achievable by this approach. Detailed treatments and results can be found in the original literature. (34, 36)

In general, release of drug from hydrogels can be expressed in the simple form of

$$(\frac{M_t}{M_\infty}) = kt^n \tag{4-27}$$

where k, n are system parameters that depend on the nature of polymer, penetrant and drug. Different values of n indicate the type of drug transport occuring in the gels and some examples are shown in Table 4.2 (39)

Table 4.2 Values of n and the Corresponding Release Mechanisms

n = 0.5	Fickian diffusion
n = 1.0	Pseudo-Case II transport
n > 1.0	Pseudo-super-Case II
0.5 < n < 1.0	Anomalous transport

Diffusivity in hydrogels has been succefully described by a free-volume approach (40)

$$\frac{D}{D_0} = \Psi(q)\exp[-B(\frac{q}{v_0})(\frac{1}{H} - 1)] \tag{4-28}$$

where D is the diffusion coefficient of drug in the gel, D_0 is the diffusion coefficient in pure penetrant (water), V_0 is the free volume of pure penetrant, H is the degree of swelling

(hydration), q is the characteristic volume of the hole required for movement of drug, B is a proportionality factor reflecting the cross-section, $\psi(q)$ represents the "sieve mechanism" by which small molecules are permitted to diffuse and large molecules are not owing to the absence of holes of appropriate size in the networks. Their extended models include the effect of crosslinks and number-average molecule weight between crosslinks in determining the size of the mesh or sieve opening, (41)

$$\frac{D}{D_0} = k_1 \frac{M_x - M^*_x}{M - M^*_x} \exp\left(\frac{-r^2 k_2}{Q-1}\right) \tag{4-29}$$

where M_X is the number-average molecule weight between crosslinks, M is the number-average molecular weight for the original polymer without crosslinking, M^*_X is the value of M_X below which drug cannot diffuse, r is the characteristic radius of drug, Q is the swelling ratio, and k is a system constant. A slightly modified expression has been provided (42)

$$\frac{D}{D_0} = k_1 \xi \exp\left[-\frac{k_2 r^2 \xi}{M^2 (Q-1)}\right] \tag{4-30}$$

where ξ is the mesh size representing the space between four tetrafunctional crosslinks or entanglements in the gels.

4.3 Experimental

4.3.1 Materials

All solvents used were reagent grade. N-isopropylacrylamide (NiPAAm, Eastman Kodak) was recrystallized twice from benzene/hexane (4:6). Sodium acrylate (SA, Pfaltz & Bauer) was used as recieved. Methylene-bis-acrylamide (MBAAm, Aldrich) was recrystallized from ethanol. The hydrophobic monomer, n-N-alkylacrylamide (RAAm)

was synthesized and purified from its respective n-alkylamine (Aldrich) by the same method described in Section 3.4.2. N,N'-bis(acryloyl)-cystamine (BAC) was synthesized and purified from acryloyl chloride (Aldrich) and cystamine (Aldrich) by the same method described in Section 3.4.3. Tetramethylethylenediamine (TEMED, Aldrich), ammonium persulfate (AP, Aldrich), sodium dodecyl sulfate (SDS, Sigma), 4 lauryl ether (Brij 30, Sigma) were used as recived without further purification. Vitamin B_{12} (VB_{12}, Sigma), progesterone (Sigma), human insulin (Eli Lilly), bovine insulin (Sigma), and human γ-interferon (Genetech) were used as recieved. Fluorescein isothiocyanate (FITC) / Zeolite (10%, Molecular Probes) was used as recieved. All buffer salts and solutes were reagent grade compounds. Water for buffers, gel swelling and release measurement was first reverse-osmosis filtered (deionized) and then Millipore filtered to yield purified water having 18 MΩ / cm resistivity.

4.3.2 Copolymer (PNiPAAm-co-SA) Gels Synthesis

Crosslinked poly N-isopropylacrylamide-co-sodium acrylate (PNiPAAm-co-SA) networks was synthesized and purified by the same method described in Section 2.2.2.

4.3.3 Terpolymer (PNiPAAm-co-SA-co-RAAm) Gels Synthesis

Crosslinked poly (N-isopropylacrylamide-co-sodium acrylate-co-n-N-alkylacrylamide) (PNiPAAm-co-SA-co-RAAm) networks with crosslinker methylene-bis-acrylamide (MBAAm) or N, N'-bis(acryloyl)-cistamine (BAC) were synthesized and purified by the same method described in Section 3.4.4.

4.3.4 FITC Fluorescent Modification of Peptides (43)

Peptide (insulin or interferon) was mixed with 10% fluorecein isothiocyanate (FITC)/zeolite (peptide/FITC = 1:1, molar ratio) in 0.05M Tris buffer (pH 8.2) and shaken for 15 min. The reaction was quenched by cysteine (10 times excess to peptide). Liquid phase FITC-peptide, free FITC and cysteine were then separated from solid phase zeolite by centrifugation. Finally pure FITC-peptide was separated and collected from free FITC, and cysteine by size exclusion chromatography (SEC) (Sephadex G-100 gel in buffer).

4.3.5 Drug Loading

4.3.5.1 Solvent Sorption Methods

Drug (vitamin B_{12}, FTIC-insulin and interferon, 0.2~10%) was dissolved in 0.05M PBS buffer (pH 7.4) solution. Progesterone (0.5~10%) was dissolved in methanol/water (65/35) solution. Pre-dried gel disks were put into drug solutions and equilibrated at 20 °C for three days. The swollen gels disks were dried at 5 °C for 48 hrs and and under vacuum at room temperature for one day prior to release measurements.

4.3.5.2 *In situ* Polymerization Methods

Various amounts of FITC-insulin or interferon were dissolved in aqueous solutions of stabilized monomer, crosslinker, initiator, and surfactant homogeneously at 5 °C for polymerization (procedures are similar to the amphiphilic gel synthesis discussed in Section 3.4.4). Upon polymerization gels were separated from glass molds, the gel membrane was carefully placed in water/methanol (80/20) solutions at 25 °C for one day. Before immersion into release medium for release measurement, the gel disks were gently rinsed

with PBS solution (25°C) and tapped with a dampened Kim™-wipe towel to remove excess adherent solution from the surface.

4.3.6 Drug Release Measurement

Drug-gel disks loaded by either solvent sorption or *in situ* polymerization were immersed into sampling vials with prefilled release medium (PBS buffer at pH 7.3, 20 ml) at predetermined testing temperatures. These vails were immersed in a shaking water bath (Americal Scientific) oscillating at Hz.

Vitamin B_{12} release was measured by a reverse phase HPLC method (Waters) at room temperature with μBondpak C_{18} as the stationary phase, methanol/water (35/65) as mobile phase, 0.8 ml/min as flow rate, VIS 560nm as a detection wavelength, 1μl as injection volume.

Progesterone release was measured by a reverse phase HPLC method (Waters) at room temperature with μBondpak C_{18} as the stationary phase, methanol/water (80/20) as mobile phase, 0.6 ml/min as flow rate, UV 240 nm as the detection wavelength, 1 μl as injection volume.

FITC-insulin or interferon release was measured by fluorescence spectroscopy (Perkin-Elmer) with a 500nm excitation wavelength and 520nm emission wavelength.

M_∞ is the amount of released drug measured at infinite time. In these experiments, M_∞ was an equilibrium value measured under each testing condition (less than 2% deviation after three days consecutive sampling).

4.4 Results and Discussion

4.4.1 Controlled Release of Hydrophilic Vitamin B_{12}

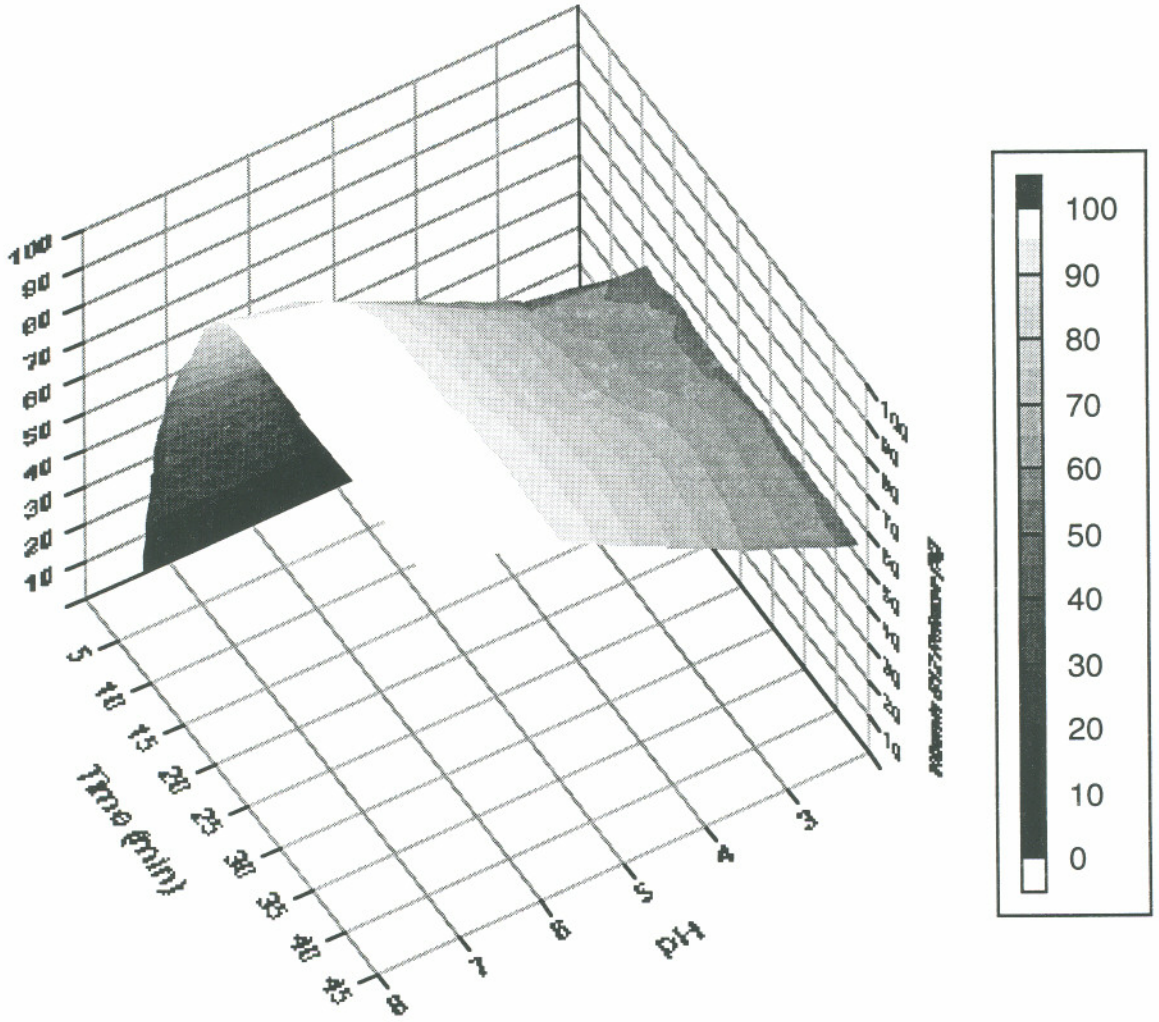

Fig. 4-5 Vitamin B12 release from PNiPAAm-co-SA (97/3, 4 mol% of MBAAm), gels in different pH media (0.05M ionic strength) at 37 °C. Loading: solvent sorption (2.5% solution).

Vitamin B_{12} is a water soluble coenzyme involved in amino acid, fatty acid, and nucleic acid metabolism. (44) A deficiency of vitamin B_{12} causes macrocytic anemi which leads ultimately to irreversible neural damage and death. Recent experiments with mice suggests that methyl-vitamin B_{12} may be a tumor suppressor, especially for gastric cancer. (45) A gastric protein, intrinsic factor, is responsible for absorption of the vitamin. In

fact, very limited vitamin B12 absorption occurs in an oral dosage form due to the degradation in the harsh low pH stomach media. (46) Thermo- and pH-sensitive hydrogels which shrink in acidic media and swell in neutral or weak basic media are attractive candidates to protect the drug, ensuring passage through acidic gastric media follow by adsorption in the weakly basic GI track.

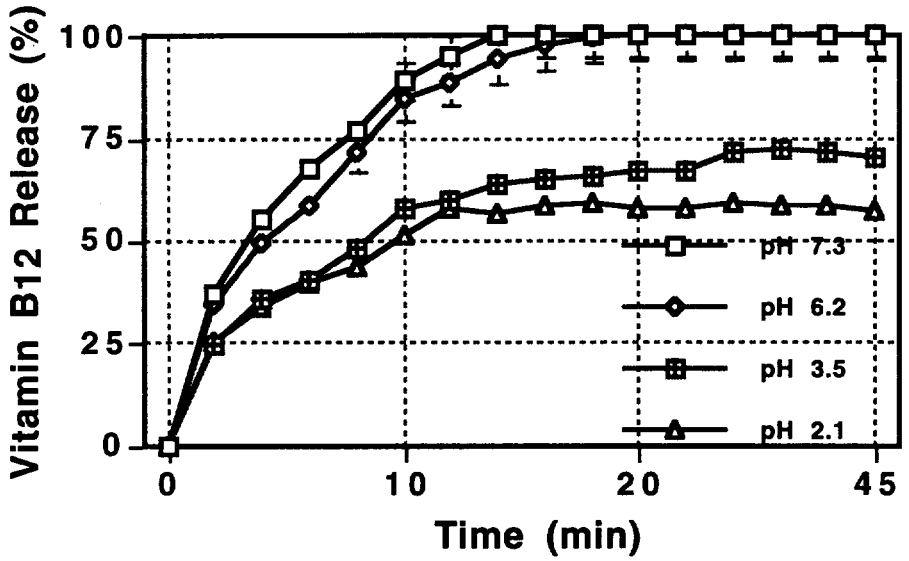

Fig. 4-6 Vitamin B12 release from PNiPAAm-co-SA (97/3, 4 mol% MBA) gels in different pH media (0.05M buffer concentration) at 37°C. Loading: solvent sorption (2.5% solution).

Fig. 4-5, 4-6 show vitamin B_{12} release profiles from PNiPAAm-co-SA, 97/3, with 4 mol% MBAAm in different pH media at 37 °C. Only about 60 to 70% of vitamin loads are released in acidic media at pH 2.1 and 3.5, respectively, through the entire period of measurement. Amounts of vitamin B_{12} release increase substantially when gels are immersed in neutal or basic release media. Release rates also increase with increasing media pH.

These results can be simply explained by the pH-sensitive swelling properties of PNiPAAm/SA gels discussed in Chapter 2, where the gels have high swelling ratios in neutral or basic media, and lower swelling ratios in acidic media. In neutral or basic media,

release kinetics are basically first-order, close to the kinetics expected for ideal Fickian diffusion in monolithic systems (see Eq. 27 and Fig. 4-7).

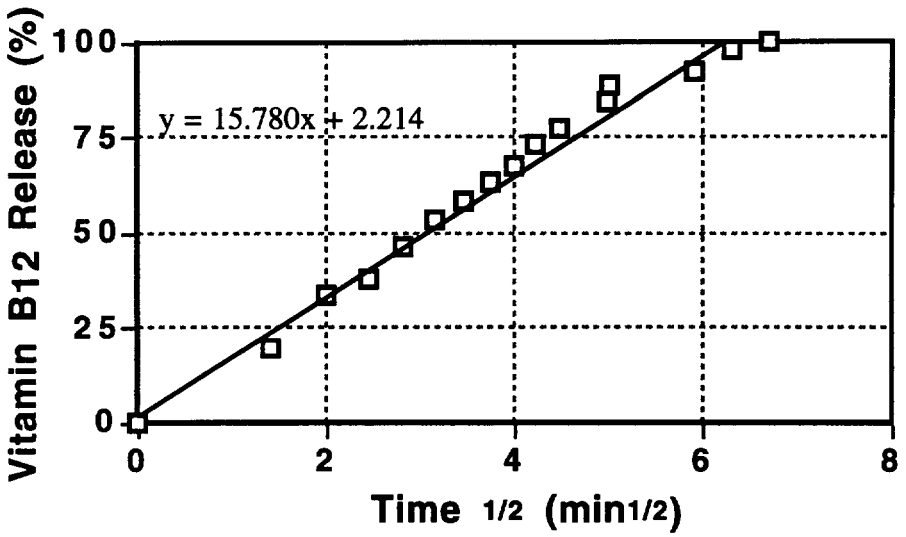

Fig. 4-7 Vitamin B12 release from PNiPAAm/SA, 97/3, with 4 mol% MBA, in 0.05M PBS (pH 7.3, 37°C). Loading: solvent sorption (5% solution).

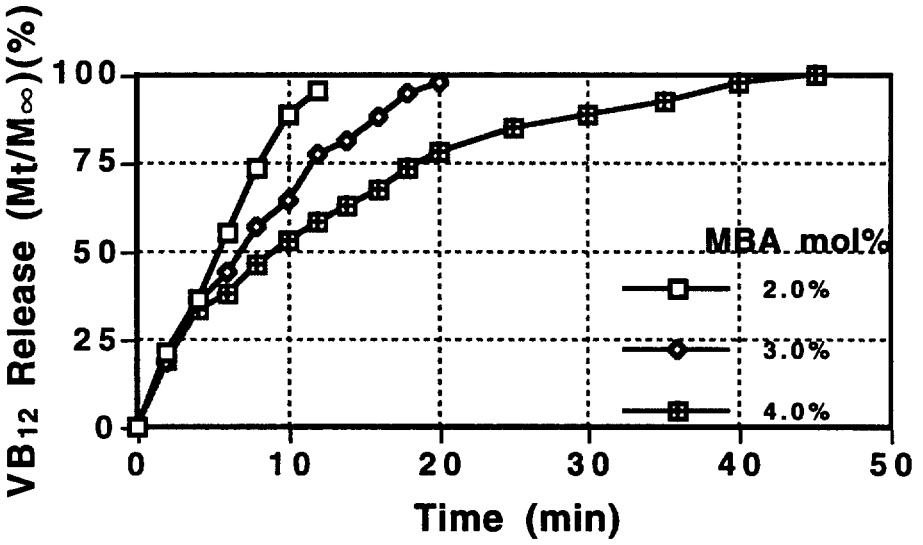

Fig. 4-8 Vitamin B12 release profile from PNiPAAm/SA (97/3) gels at 37°C in 0.05M PBS (pH 7.3). Loading: solvent sorption (1.5% solution).

Fig. 4-8 shows the effect of crosslinking density on release of vitamin B12 from PNiPAAm-co-SA (97:3) in 0.05M PBS buffer (pH 7.3) at 37 °C. Release rate decreases

as gel network crosslink density increases. This can be interpreted by examining Eq. 28 and 29, where increasing of crosslinking density decreases the network mesh size, ξ, thus decreasing drug diffusivity in the gel.

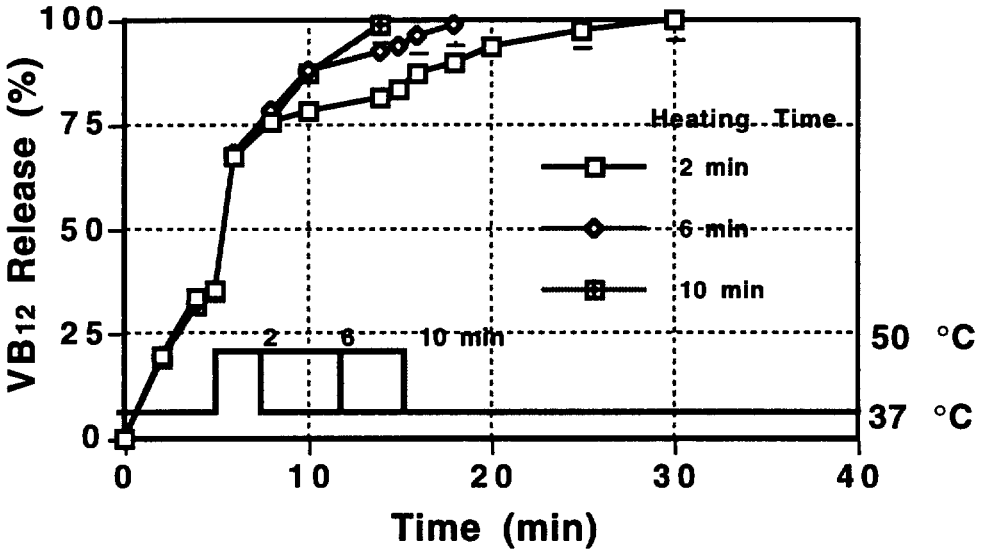

Fig. 4-9 VB_{12} thermo-stimulated release profiles from PNiPAAm/SA (97/3, 2 mol% MBA) gels in PBS (pH 7.3). Loading: solvent sorption (4% solution).

Fig. 4-9 shows vitamin B_{12} release profiles from PNiPAAm/SA (97/3, with 2 mol% MBA) gels in 0.05M PBS buffer solution with temperature jumping from 37°C to 45°C with various heating pulse durations. All release profiles show pulatile release patterns induced by thermo-stimuli. The amount (pulse height) and kinetics of agent release are controlled through the duration and magnitude of the applied thermal pulse.

Fig. 4-10 shows vitamin B_{12} release from PNiAAm/SA (97/3, 2 mol% MBA) gels in 0.05M PBS buffer under different heating temperatures but fixed heating time. Again, all release profiles exhibit pulsatile release patterns. The amount of the agent released (pulse height) and the release kinetics are controllable by the applied heating temperature.

The thermo-sensitive sweling behavior of PNiPAAm/SA gels has been discussed in detail in Chapter 2.

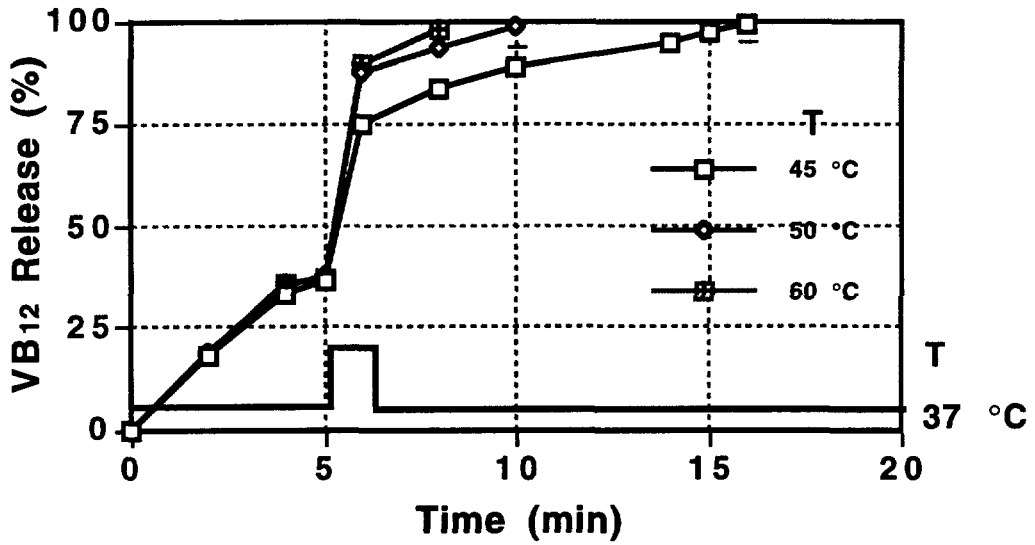

Fig. 4-10 Vitamin B12 pulsatile release profile from PNiPAAm/SA (97/3, 2 mol% MBA) gels at various stimuli temperatures (2 min heating) in PBS (pH 7.3). Loading: solvent sorption (4% solution).

Thermo-stimulated drug release mechanisms from these gels can be simply interpreted from Fig. 4-11. When medium temperature is increased above the gel critical temperature, gels begin to shrink and mechanically squeeze the entrapped drug out of the gel matrix. Deswelling processes are more efficient when little or no collapsed polymer "skin" layer forms on the gel surface during collapse (see Chapter 2). The collapsed PNiPAAm skin layer on the gel surface above the critical temperature acts to block flow of entrapped solute and solvent out of the gels. This property has been adopted recently to achieve so-called switched "on-off" drug delivery in PNiPAAm gel systems. (47, 48) The dense collapsed gel skin layer can be "broken" through the incorporation of ionic species into the framework of NiPAAm gels (Chapter 2). From the results of Fig. 4-9 and 4-10, vitamin B_{12} release induced by this mechanical effect is observed, supporting the results in

Chapter 2. Thus, it is possible to achieve highly efficient pulsatile delivery utilizing reversible mechanically existed diffusion via thermo-stimulation of ionized PNiPAAm gels.

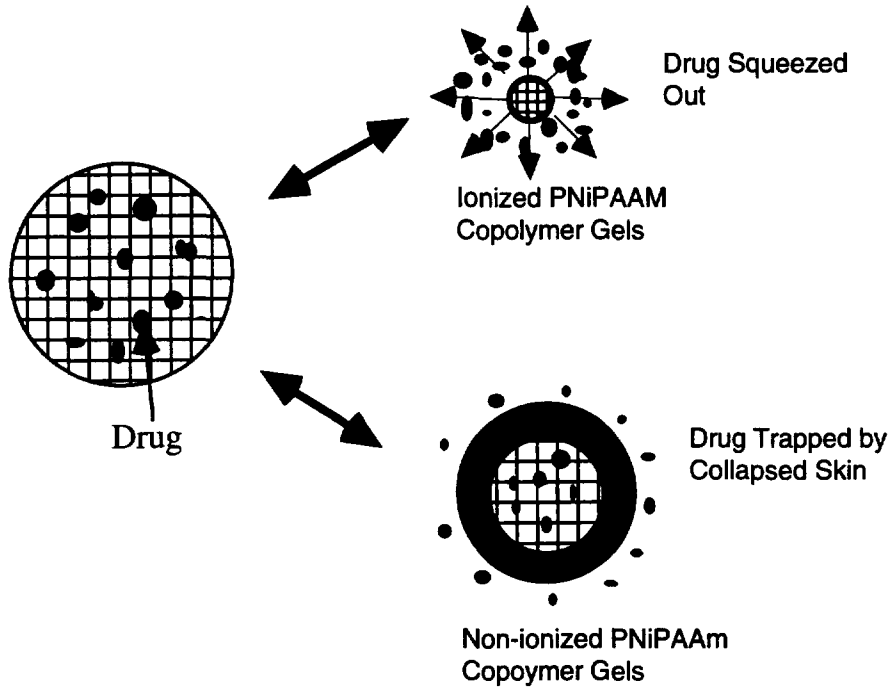

Fig. 4-11 Schematic diagram of thermo-stimulated release of drug from ionized and non-ionized PNiPAAm gels.

The effect of loading level on the release of vitamin B12 from NiPAAm/SA hydrogels in PBS buffer at 25 °C is shown in Fig. 4-12. In general, the initial rate of release increases as the sample loading increases. Loading of vitamin B12 below 2% produces an initial burst relatively slower then that at higher loading, and release kinetics are more first-order dominated. This can be interpreted as a more significant drug pore diffusion mechanism contribution at higher drug loading due to the concomitant increase in the gel pore fractional volume, increasing the release rate and fraction of drug within the pores.

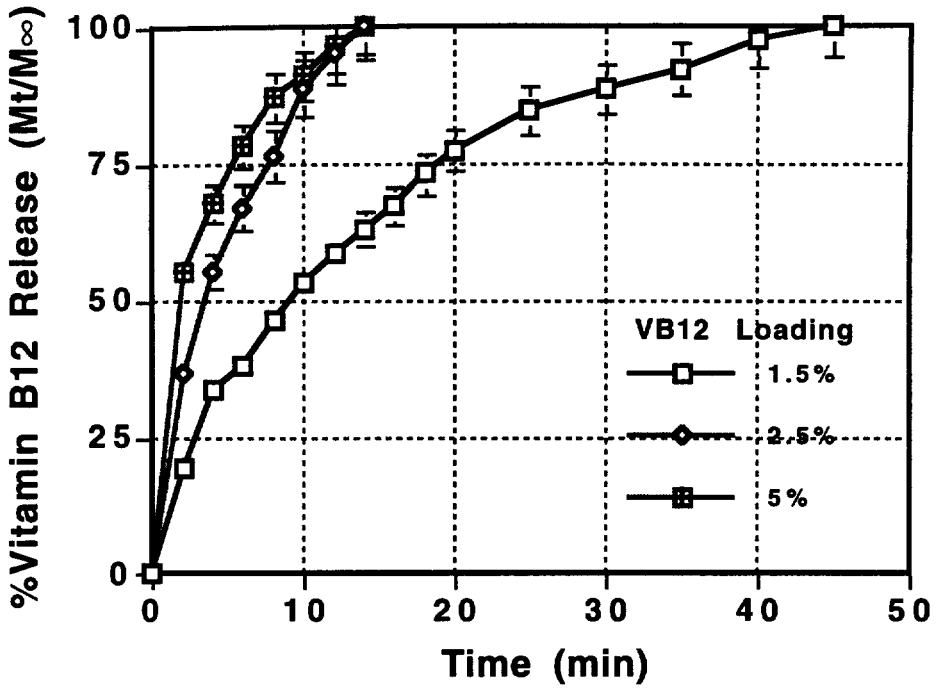

Fig. 4-12 Effect of Vitamin B12 loading on its release profiles from NiPAAm/SA (97/3) hydrogels at 25 °C in 0.05M PBS buffer (pH 7.3).

4.4.2 Controlled Release of the Amphiphilic Polypeptides, Insulin and Interferon

A polypeptide is a linear macromolecule formed as the result of condensation of various hydrophilic and hydrophobic amino acids. Besides covalent disulfide bonds which crosslink several major peptide domains, other associations including hydrogen bonding, ionic interactions, and hydrophobic interactions, are responsible for stabilizing protein three-dimensional structure. Usually polypeptides manifest distinctly amphiphile character imparted by multiple domains, amino acid diversity, and structure. The issues of sustained and pulsatile controlled delivery of regulatory peptides have been addressed in Chapter 1 and Section 4.1 of this chapter. A new development is their delivery by thermo- and pH-

sensitive amphiphilic networks discussed in Chapter 3. Regulatory peptides such as insulin and interferon are chosen as model agents here, and their sustained and pulsatile release characters from PNiPAAm-co-SA-co-RAAm gels have been investigated.

Insulin is an essential polypeptide hormone that controls blood glucose concentration and stimulates glycogen, fat, and protein synthesis within many cells. It has two linear peptide chains crosslinked by two disulfide bonds. In the normal healthy human body, release of insulin from the pancreas is regulated in some ways (constant or pulsatile fashion) by the amount of glucose in the blood. Usually diabetic patients have low circulating insulin concentrations because their pancreas cannot produce sufficient amounts of the hormone. Almost all are treated by daily insulin injections. Long-term sustained and/or pulsatile delivery of insulin will provide significant benefits for treating diabetics with convenient, more reliable therapy, avoiding complications with patient compliance.

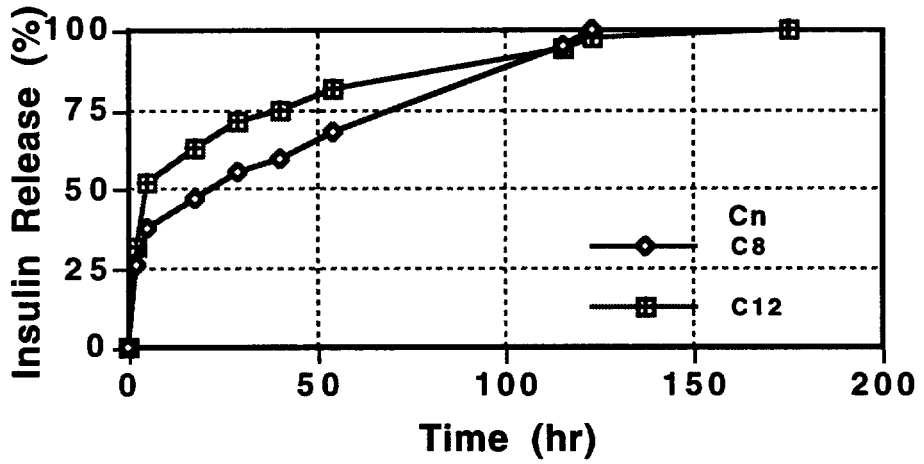

Fig. 4-13 Insulin release from terpolymer (PNiPAAm /SA/Cn, 95/3/2, 1.0 mol% BAC) gels in 0.05M PBS (pH 7.3) at 25 °C, loading: solvent sorption (0.7% solution).

Fig. 4-13 shows FITC-insulin release from terpolymer gels (PNiPAAm-co-SA-RMAAm, 95:3:2, with 1% BAC as crosslinker) containing different pendent alkyl chain lengths in 0.05M PBS buffer (pH 7.3) at 25 °C. Insulin was loaded by the solvent sorption method. Basically, a two-stage release pattern is observed in Figure 4-13.

Initially, insulin releases very quickly (to about 50% loading) due to a surface burst effect followed by slow pseudo-zero-order release. Surface burst release of insulin increases as the pendent alkyl chain length of the gels increases. Surface burst effects can be induced by the initial gel swelling and/or the extent of the surface layer incorporation of the agent in the gels. Hence, with solvent sorption loading, the more that hydrogel hydrophobicity or heterogeneity increases, the more surface layer incorporation of the insulin increases. In the second release stage of zero-order kinetics, release rate decreases as the network alkyl chain length increases. The hydrophobic interaction between the polypeptide chain and gel networks are proposed to play a significant role giving rise to such a release pattern.

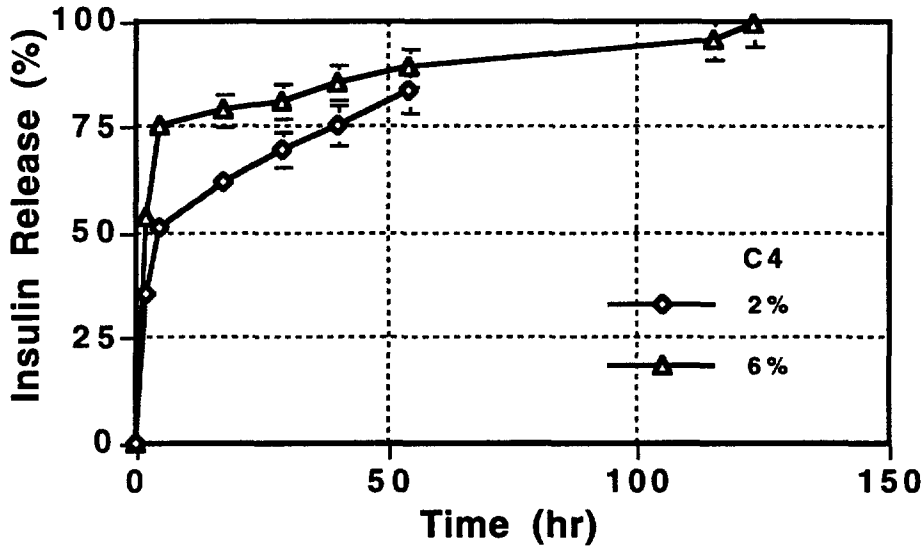

Fig. 4-14 Insulin release from terpolymer gels (PNiAAm /SA/C4, 3% SA fixed, with BAC) in 0.05M PBS (pH 7.3, 25 °C). Loading: solvent sorption (0.7% solution).

Fig. 4-14 shows insulin release from terpolymer PNiPAAm-co-SA-co-butylacrylamide (95/3/2, 91/3/6, with 1% BAC as crosslinker) gels in 0.05M PBS (pH 7.3) at 25°C by solvent sorption loading. A two-stage release pattern consistis of a first three-hour surface burst release followed by a slow pseudo-zero-order release. Again, the surface layer incorporation of the peptides increases and release rate decreases as the

amount of hydrophobic comonomer incorporation on the network increases (increase in system hydrophobicity or heterogeneity). A grapic summary of these trends and results can be seen in Fig. 4-15.

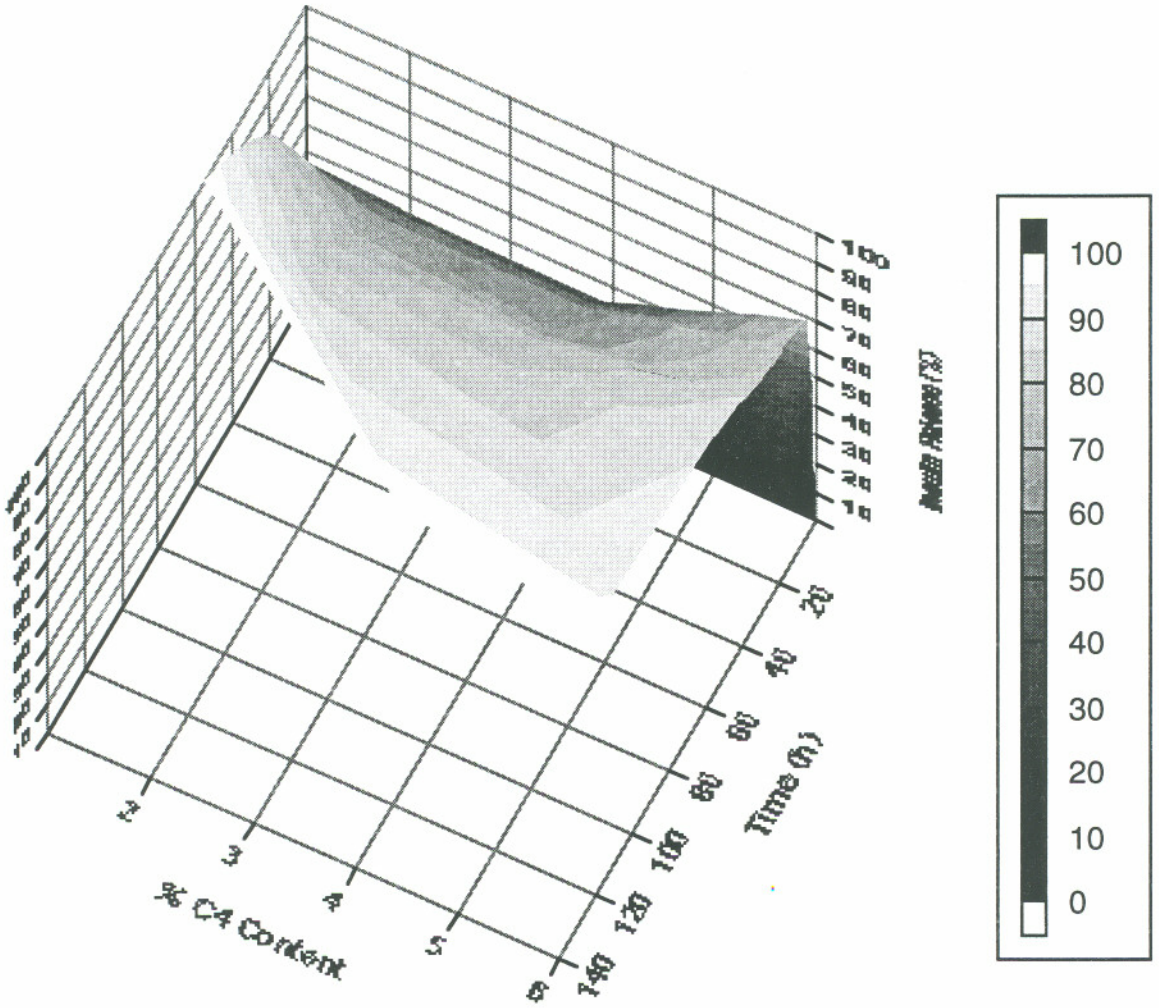

Fig. 4-15 The effect of the amount of hydropobic comonomer incororation on insulin release from terpolymer PNiPAAm-co-SA-co-Butylacrylamide (3 mol% SA fixed, 1 mol% BAC as croslinker) gels in 0.05M PBS buffer (pH 7.3) at 25 °C.

Fig. 4-16 shows insulin release from terpolymer gels (PNiPAAm-co-SA-co-RMAAm, 95/3/2, with 1.5 mol% BAC as crosslinker) in 0.05M PBS (pH 7.3) at 25 °C

with *in situ* loading. A remarkable extended zero-order release profile of insulin is observed. Release rate decreases as the pendent alkyl chain length of the gels increases due to proposed hydrophobic interactions. When gel pendent alkyl chain lengths exceed C_{12}, their effect on the release of insulin remains constant. Almost none of the initial burst release seen with the sorption method has been observed in this experiment due to reduced agent surface incorporation from the loading method and gel pre-equilibrium (gels loaded

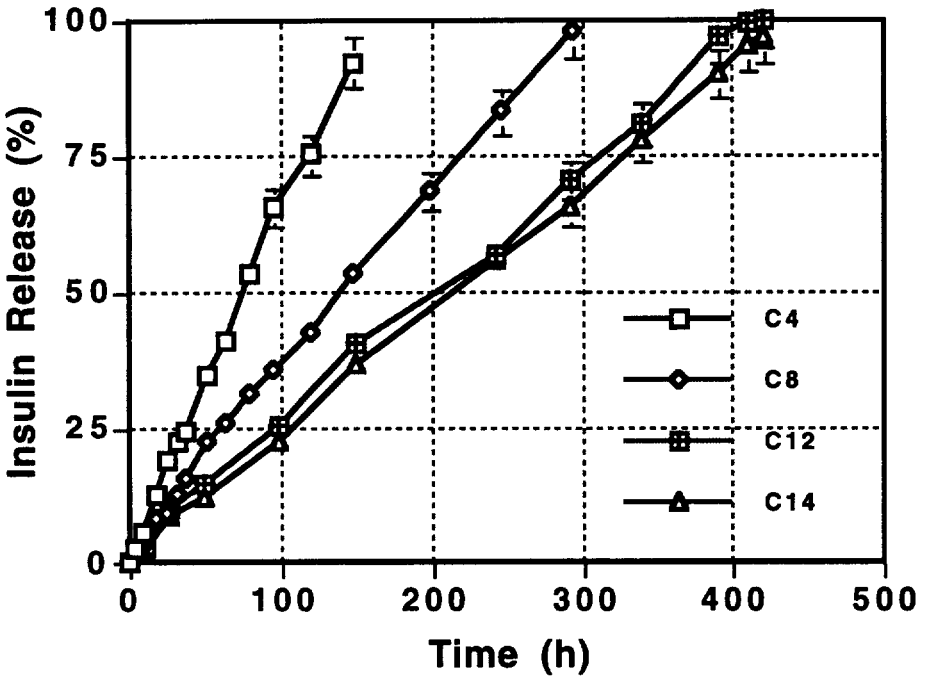

Fig. 4-16 Insulin release from terpolymer gels (PNiPAAm /SA/Cn, 95/3/2, with 1.5 mol% BAC) in 0.05M PBS (pH 7.3, 25 °C). Loading: *in situ* polymerization (0.5% solution).

with insulin have been pre-equilibrated in solution for 24 hours before their release measurement begins). The same results for the entire series of gels are shown in Fig. 4-17.

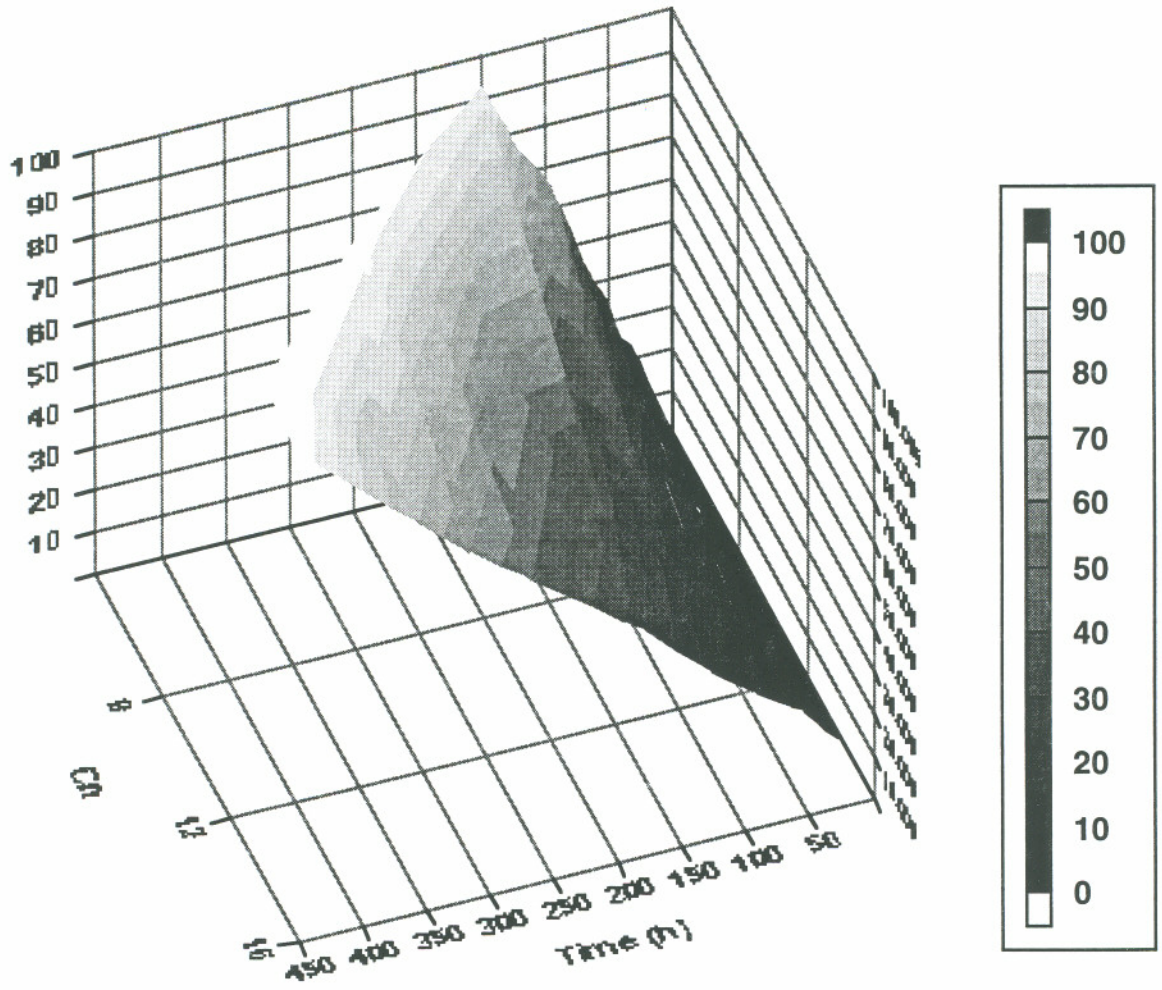

Fig. 4-17 The effect on pendent alkyl chain length of the gels on the release of insulin from terpolymer gels, PNiPAAm-co-SA-co-RMAAm (95/3/2, with1.5 mol% BAC as crosslinker) in 0.05M PBS (pH 7.3, 25°C). Loading: *in situ* polymerization.

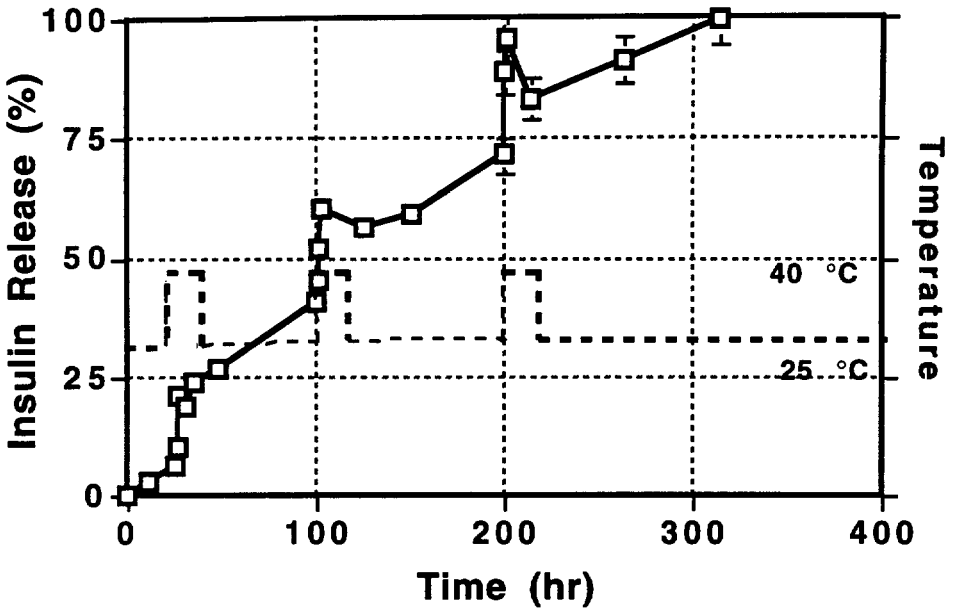

Fig. 4-18 Insulin pulsatile release from terpolymer gels (PNiAAm/SA/C12, 95/3/2, 1.5 mol% BAC) by temperature stimuli in 0.05M PBS (pH 7.3). Loading: *in situ* polymerization (0.5% solution).

Fig. 4-18 shows pulsatile release profiles of insulin from terpolymer PNiPAAm-co-SA-co-dodecylacrylamide gels (95/3/2 with 1.5 mol% BAC) in 0.05M PBS with pulsatile temperature stimuli (temperature cycling between 25 °C and 40 °C). Release curves show a pulsatile kinetic pattern corresponding to the thermo-pulse onset. The release peak height is controllable by the duration of the elevated applied temperature pulse. The thermosensitive swelling behavior of PNiPAAM-co-SA-co-RMAAm) gels has been discussed in Chapter 3, and the mechanism of thermo-pulsatile release by thermo-sensitive gels has been discussed in Section 4.4.1 of this chapter and Fig. 4-11.

Interferons comprise a group of immune system proteins which act physiologically by triggering the synthesis of "antiviral" proteins. These proteins can find their way to other cells and prevent the replication of viruses. No controlled release studies of genetically engineered interferon have been reported over the past two decades since their discovery. Fig. 4-19 shows FITC-interferon release from terpolymer gels (PNiPAAm-co-

SA-co-dodecylacrylamide, 95/3/2) gels with different amount of crosslinker BAC (0.3 mol% and 2.1mol%) in 0.05M PBS at 25 °C with *in situ* polymerization loading. The same zero-order release pattern as shown for insulin is observed in the figure. Release rate decreases as gel network crosslinking density increases. Furthermore, the feed concentration of crosslinker BAC with the range of 1 to 2 mol% has a minor effect on the peptide release kinetics from the gels. Thus, proposed hydrophobic interactions between the peptides and networks appear to be one of the major factors governing the overall peptide release kinetics in the gel system.

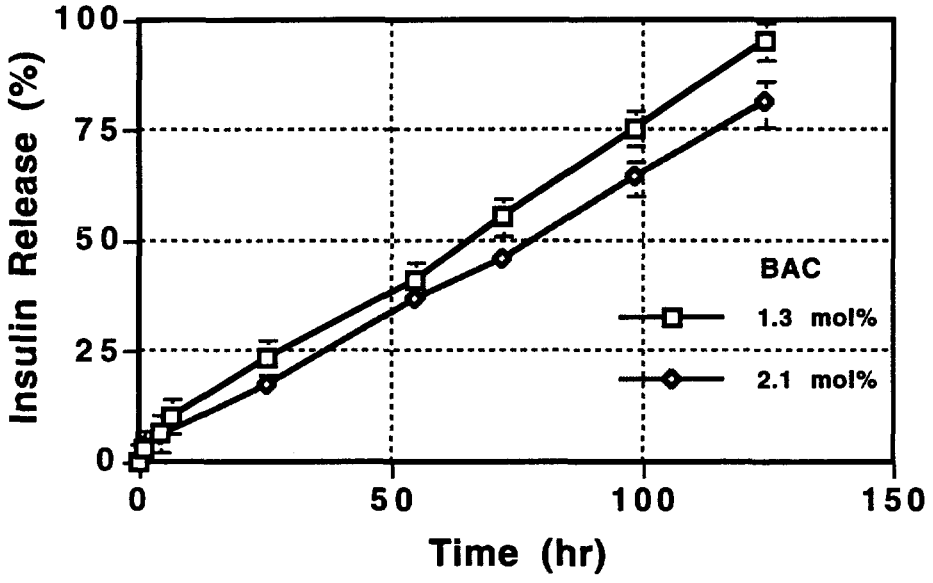

Fig. 4-19 Effect of crosslinking density on interferon release from terpolymer gels (PNiPAAm/SA/C12, 95/3/2) in 0.05M PBS (pH 7.3, 25 °C). Loading: *in situ* polymerization (0.24% solution).

4.4.3 Controlled Release of Hydrophobic Steroid, Progesterone

Progesterone is the female sex steroid hormone which is synthesized from cholesterol by the corpus luteum in the ovary. The main pharmaceutical use of progesterone is its contraceptive application to prevent ovulation. Because it is taken up by

the liver and rapidly inactivated, progesterone cannot be administered orally. Progesterone is a hydrophobic compound which is insoluble in water.

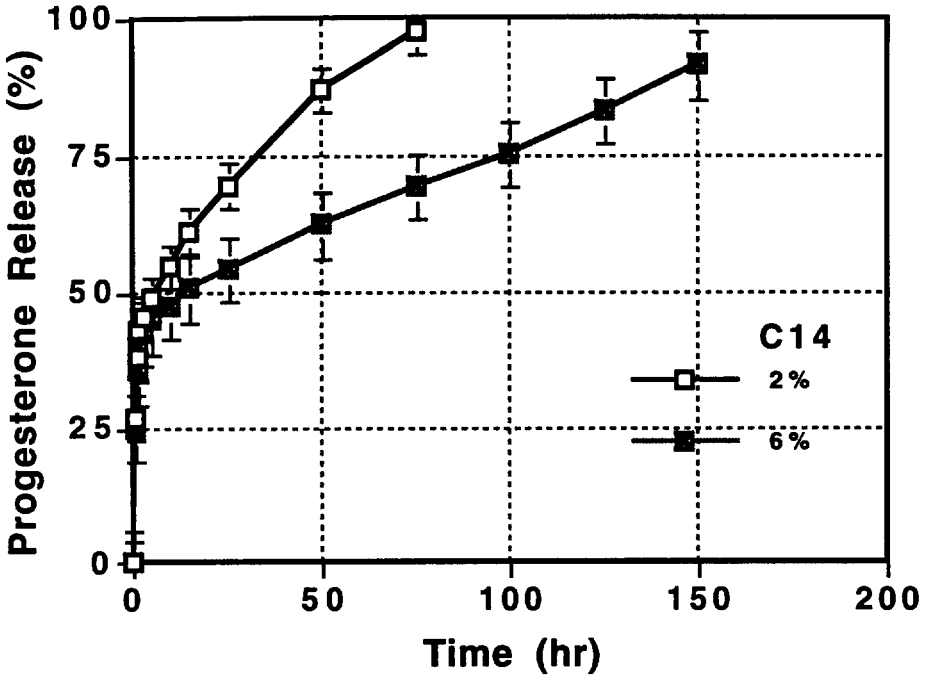

Fig. 4-20 Progesterone release from terpoly gels (PNiPAAm/SA/C14, 3% SA fixed, with 1 mol% MBA) in 0.05M PBS (pH 7.3, 25°C). Loading: solvent sorption (3% solution).

Fig. 4-20 shows progesterone release profiles from two terpolymer gels (PNiPAAm/SA/C14, 95/3/2, 91/3/6, with the same 1 mol% MBA as crosslinker) by solvent sorption loading. Similarly, both two-stage release patterns are observed in Figure 4-18. Initially, progesterone releases very quickly (to about 40% loading) due to a surface burst effect followed by slow pseudo-zero-order release. In the second stage of pseudo zero-order release, release rate decreases as the network alkyl chain length increases. The hydrophobic interaction between the progesterone hydrocarbon cyclic group and gel networks are proposed to play a significant role giving rise to such release patterns.

Fig 4-21 shows progesterone release profiles from two terpolymer gels (PNiPAAm/SA/C14, 95/3/2) with different amounts of crosslinker MBA (1 mol% and 4.5

mol%) by solvent sorption loading. Again, both two-stage release patterns are observed in Figure 4-21. However, in the second stage of pseudo zero-order kinetics, release rate decreases drastically as the network crosslinking density increases. Poor dispersion of progesterone in release media (PBS) is responsible for these relatively large deviations of the quantitative detections in both Fig 4-21 and Fig. 4-21.

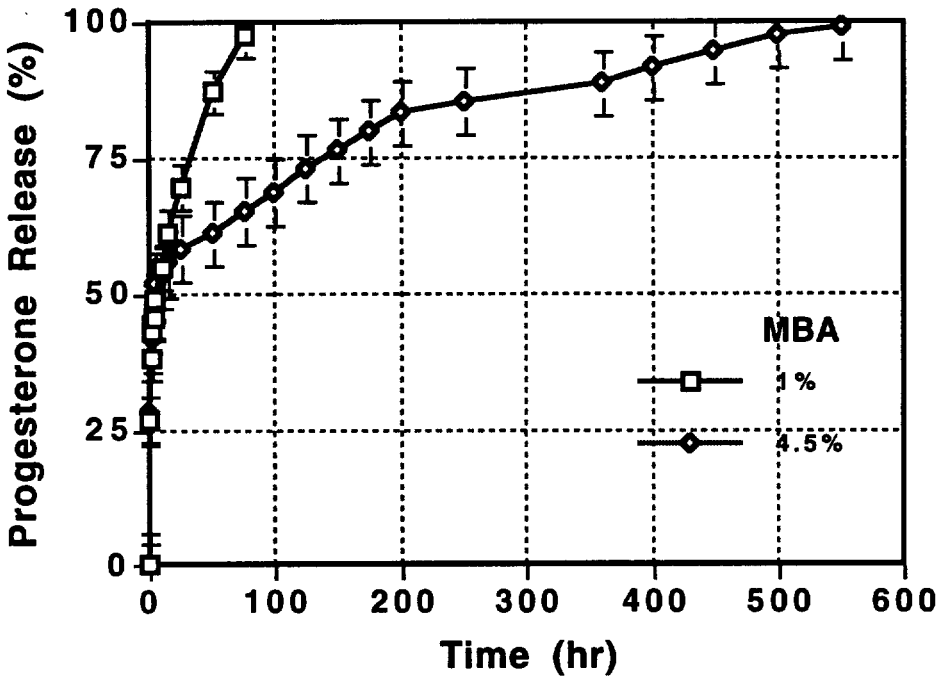

Fig. 4-21 Effect of crosslinking density on progesterone release from terpolymer gels (PNiPAAm/SA/C14, 95/3/2) in 0.05M PBS (pH 7.3, 25 °C). Loading: solvent sorption (3% solution).

4.4.4 Further Discussions

Fickian laws (Eq. 4-8, 4-13) comprise the simplest theory widely used to describe diffusion phenomena. A general explanation of the laws is that solute travels down its concentration gradient with a flux J, and the factor is the diffusivity D which is proportional to the 'jump length' of the average molecule multiplied by its 'velocity'. Unfortunately,

Fickian laws tell nothing about the interaction between components in co- and counter diffusion, nothing about intereacton between solute and polymer systems and nothing about osmotic effects. Fickian laws are adequate to describe simple diffusion in a binary mixture. However, modifications of Fickian Laws regarding solute binding within polymer networks have been discussed in Section 4.2.1.3 of this chapter. Ultimately, more comprehensive theories for diffusion must be developed to account for more complex phenomena associated with solute diffusion through heterogeneous media.

4.4.4.1 Multicomponent Controlled Diffusion --- A Different View

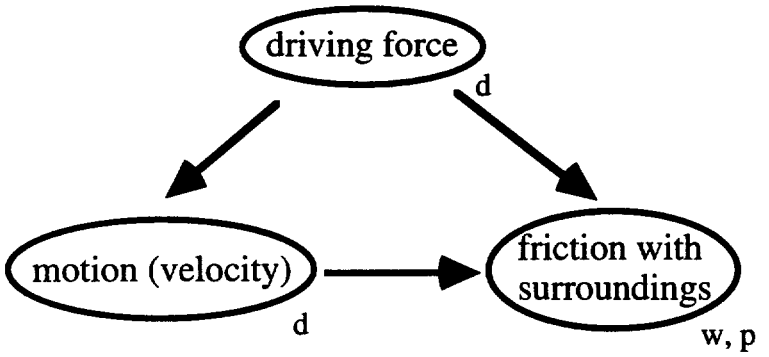

Fig. 4-22 Scheme of the friction equation for diffusion (sunscripts, d, refers to drug; w, to water; p, to polymer).

For consideration of drug diffusion from a polymer matrix (i.e., gels) in water, modern theories take a very different approach. (47-50) The main scheme in these theories is depicted in Fig. 4-22 where a driving force is exerted on each species (drug) that moves the drug through its medium (water and polymer matrix), counter balanced by friction with the other species.

The driving force consists of several contributions. The first one is the gradient of the chemical potential. For dilute solutions, the gradient is of the form:

$$-\frac{d\mu_d}{dx} = -RT\frac{d\ln c_d}{dx} \propto -\frac{1}{c_d}\frac{dc_d}{dx} \tag{4-31}$$

Its releationship with Fickian Laws is discussed in section 4.2.1.1 of this Chapter. In non-ideal systems, the gradient should be

$$-\frac{d\mu_d}{dx} = -RT\frac{d\ln a_d c_d}{dx} \tag{4-32}$$

where a_d is the activity coefficient of the drug.

The complete driving force might include many other forces, such as electrical, pressure, etc.

$$(Forces)_d = -\frac{d\mu_d}{dx} - Fz_d\frac{d\Phi}{dx} - V_d\frac{dp}{dx} - \cdots \tag{4-33}$$

where Z_d is charge number, and V_d is molar volume.

The driving force gives each species an average velocity, v, which induces friction with the other components. The friction is proportional to the velocity difference between the species

$$f_{1,2} = \zeta_{1,2}x_{1or2}(v_1 - v_2) \tag{4-34}$$

where $\zeta_{1,2}$ is the friction coefficient between the two species, and x is the mole fraction. So, transport equations for the two moving components, drug and water, are (polymer matrix is assumed to be stagnant, v_p=0):

$$\begin{aligned}\sum(forces)_d &= \zeta_{dw}x_w(v_d - v_w) + \zeta_{dp}x_p v_d \\ \sum(forces)_w &= \zeta_{dw}x_d(v_w - v_d) + \zeta_{wp}x_p v_w\end{aligned} \tag{4-35}$$

where the first terms on the right side of the equations denote the friction between the mobile components. The last terms denote friction with the polymer matrix. If the forces and friction coefficients or diffusivity are known, these equations can be solved to yield the

velocities and fluxes. These equations are called the Maxwell-Stefen equations for diffusion (51). Friction coefficients may be regarded as inverted diffusion coefficients,

$$\zeta_{dw} = \frac{RT}{D_{dw}} \tag{4-36}$$

For drug diffusion in swollen hydrogel systems assuming that water is stagnant and that the only driving force is a chemical potential, Eq. 4-35 can be writtern as

$$-\frac{1}{c_d}\frac{dc_d}{dx} = a\frac{1}{D_{dw}}x_w v_d + b\frac{1}{D_{dp}}x_p v_d = \left(\frac{a}{D_{dw}} + \frac{b}{D_{dp}}\right)v_d \tag{4-37}$$

where x_W and x_P can both be considered to be 1 and a, b are system parameters. The mathematics for solving this equation can be very complicated. But, for a general approximation and estimation, two key factors should be carefully examined: thermodynamic properties of the mixture and the diffusivities. Diffusivity in hydrogels has been briefly discussed in section 4.2.4 of this chapter. If no other strong intermolecular interactions involved, the diffusivity of the drug can be approximately evaluated from "free volume" approaches. (40-42, 52,53) The logarithm of the diffusivity, D_{dp}, vs. the inverse of the swelling ratio should have a linear relatonship. However, D_{dw} is unknown and certainly has a dynamic value not equal to $D_{(dw)0}$ in pure water. When strong intermolecular interactions between the drug and polymer are involved, D_{dp} will be far more complicated to quantitively describe by considering network structure, diffusion mechanisms such as "free volume" theory, strong intermolecular interactions, as well as drug physicochemical propeties . Thus, it is not surprising that some drugs such as insulin can release from amphiphilic networks by zero-order rather than first-order kinetics.

Review of many of the zero-order controlled delivery systems reported include: (a) geometric device modification (54), (b) rate controlling barrier types (55,56), (c) establishing a nonuniform concentration distribution profile of the drug across the polymer matrix (d) polymer undergoing controlled rupture during release (57), (e) swelling-

controlled delivery systems based on glassy hydrogels (58), and (f) chemical reaction types (59). All of these approaches can be interpreted by considering time/position-dependent diffusivities of the species through multicomponent controlled diffusion theory approaches.

References

1. Mazer, N. A., J. Contr. Rel., 11, 343 (1990).

2. Kost, J. Ed., *Pulsed and Self-Regulated Drug Delivery*, CRC Press, Boca Raton (1990).

3. Ratner, B. D. and Hoffman, A. S., in *Hydrogels*, ACS Synposium Series, Andrade, J. Ed., 31 (1976).

4. Peppas, N. A., Ed., *Hydrogels in Medicine and Pharmacy*, Vol 1 and 2, CRC Press, Boca Raton (1986).

5. Katayama, S., Hirokawa, Y., and Tanaka, T., Macromolecules, 17, 2461 (1984).

6. Hirokawa, Y. and Tanaka, T., J. Chem. Phys., 81, 6379 (1984).

7. Ohmine, I., and Tanaka, T., J. Chem. Phys., 77, 5725 (1982).

8. Tanaka, T. Fillmore, D., Sun, S. T., Nishio, I., Swislow, G., and Shah, Phys. Rev. Lett., 45, 1636 (1980).

9. Tanaka, T., Phys. Rev. Lett., 40, 820 (1978).

10. Tanaka, T., Sci. Am., 244, 124 (1981).

11. Tanaka, T., Nishio, I., Sun, S. T. and Ueno-Nishio, S., Science, 218, 467 (1971).

12. Irie, M. and Knrgwatchakun, D., Macromolecules, 19, 246 (1986).

13. Ishihara, K., Hamada, N., Kato, S. and Shinohara, I., J. Polym. Sci., Polym. Chem. Ed., 22, 121 (1984).

14. Hoffman, A. S., Afrassiabi, A., and Dong, L. C., J. Contr. Rel., 4, 213 (1986).

15. Bae, Y. H., Okano, T., Hsu, R., and Kim, S. W., Makromol. Chem., Rapid Commun., 8, 481 (1987).

16. Siegel, R. A. and Firestone, B. A., Macromolecules, 21, 3254 (1988).

17. Peppas, N. A. and Klier, J., J. Contr. Rel., 16, 203 (1991).

18. Sawahata, K., Hara, M., Yasunaga, H., and Osada, Y., J. Contr. Rel., 14, 253 (1990).

19. Kwon, I. C., Bae, Y. H., Okano, T., Berner, B., Kim, S. W., Makromol. Chem., Macromol. Symp., 33, 265 (1990).

20. Eisenberg, D. and Crothers, D., *Physical Chemistry with Applications to the Life Sciences,* Benjanin/Cummings, Menlo Park, CA (1979).

21. Laider, K. J. and Meiser, J. H., *Physical Chemistry*, Benjamin/Cummings, Menlo Park, CA (1982).

22. Tanford, C., *Physical Chemistry of Macromolecules*, John Wilry & Sons, New York (1961).

23. Crank, J., *The Mathematics of Diffusion*, 2nd. Ed., Clarendon Press, Oxford (1975).

24. Chang, R., *Physical Chemistry with Applications to Biological Systems,* 2nd Ed., MacMillan Press, New Tork (1981).

25. Baker, R. W. and Lonsdale, H. K., in *Controlled Release of Biologically Active Agents*, Tanrquary, A. C. and Lacey, R. E., Ed., Plenum, New Tork, 15 (1974).

26. Hadgraft, J., Int. J. Pharm., 2, 279 (1979)

27. Siegal, R. A. and Langer, R., Pharm. Res., 1, 1 (1983)

28. Higuchi, W. I., J. Pharm. Sci., 56, 315 (1967)

29. Kedem, O. and Katehalsky, A., J. Gen. Physiol., 45, 153 (1961-62).

30. Katchalsky, A. and Carran, P. F., in *Non-equilibrium Thermodynamics in Biophysics,* Harvard University Press, Cambridge, MA (1965).

31. Fischer, K. A. and Stoeckenius, W., in *Biophysics*, Hoppe, W., Lohmann, W., Mark, H., and Ziegler, H., Eds, Springer-Verlog, Berlin (1983)

32. Seigel, R. A., in *Controlled Release of Drugs: Polymers and Aggregate Systems*, Rosof, M. Ed., VCH Press (1989)

33. Lee, P. I., in *Controlled Release of Pesticides and Pharmaceuticals*, Lewis, D. H., Ed., Plenum Press, New York, 39 (1981)

34. Frisch, H. L., J. Polym, Sci. Polym. Phys. Ed., 16, 1651 (1978).

35. Korsmeyer, R. W., Lustig, S. R., and Peppas, N. A., J. Polym. Sci. Polym. Phys. Ed., 24, 395 (1986)

36. Korsmeyer, R. W., Meerwall, E. V., and Peppas, N. A., J. Polym. Sci. Polym. Phys. Ed., 24, 409 (1986).

37. Rudolph, F. B., J. Polym. Sci. Polym. Phys. Ed., 17, 1709 (1979).

38. Singh, S. K. and Fan, L. T., Biotechn. Prog., 2, 145 (1986).

39. Peppas, N. A., in *Recent Advances in Drug Delivery Systems*, Anderson, J. M. and Kim, S. W. Eds, Plenum Press, New York, 279 (1984).

40. Yosuda, H., Lamaze, C. E., J. Macromol. Sci. Phys., 85, 111 (1971).

41. Reinhart, C. T. and Peppas, N. A., J. Membr. Sci., 18, 227 (1984).

42. Peppas, N. A. and Moynihan, H. J., J. Appl. Polym. Sci., 30, 2589 (1985).

43. Tietze, F., Mortimore, G. E., and Lomax, N. R., Biochim. Biophys. Acta, 59, 336 (1962).

44. Gaby, S. K., Bendich, A., Singh, V. N., and Machlin, L. J., *Vitamin Intake and Health: a Scientific Review,* Marcel Dekker (1991).

45. Mclutyre, P. A., Hahn, R., Couley, C. L., and Glass, B., Bull. Johns Hopkins Hosp., 104, 309 (1959).

46. Shimizu, N., Hamazoe, R., Kanayama, H., Maeta, M., and Koga, S., Oncology, 44, 169 (1987).

47. Lightfoot, E.N., *Transport Phenomena and Living Systems*, Wiley, New York, (1974).

48. Spiegler, K. S., *Principles of Energetics*, Springer-Verlag, Berlin (1982).

49. Wesselingh, J. A. and Krishna, R., *Mass Transfer*, Ellis Horwood, Chichester (1990).

50. Wesselingh, J. A., J. Contr. Rel., 24, 47 (1993).

51. Mark, H., in *Encyclopaedia of Polymer Science and Engineering*, 5, John Wiley & Sons, (1986).

52 Muhr, A. H. and Blanshard, J. M. V., Polymer, 23, 1012 (1982).

53. Lodge, T. P., J. Polymer Sci., B28, 2607, 2629 (1990).

54. Rhine, W. D., Sukhatme, V., Heieh, D. S. T., and Langer, R. S., in *Controlled Release of Bioactive Materials*, Baker, R. W. Ed., Academic Press, New York (1980).

55. Olanoff, L., Koinis, T., and Anderson, J. M., J. Pharm. Sci., 68, 1147 (1979).

56. Obermeyer, A. S. and Nicholas, L. D., in *Controlled Release Polymeric Formulations*, Paul, D. R. and Harris, F. W., Eds., ACS Symp. Ser. 33, American Chemical Society, Washington, D. C. (1976).

57. Roorda, W. E., deVries, M. A., de Leede, L. G. J., de Boer, A. G., Breimer, D. D., and Junginger, H. E., J. Contr. Rel., 7, 45 (1988).

58. Peppas, N. A. and Franson, N. M., J. Polym. Sci. Polym. Phys. ed., 21, 983 (1983).

59. Shah, S. S., Kulkarni, M. G., and Mashelkar, R. A., J. Membr. Sci., 51, 83 (1990).

Chapter 5 Summary

5.1 Summary

The field of controlled delivery of drugs has drawn on expertise from a number of scientific disciplines including chemistry, polymer science, bioengineering, pharmacology, biology, and medicine. As the name implies, the objectives of controlled drug delivery are to disseminate a drug when and where it is needed and at the optimun dose. However, the development of controlled drug delivery has relied heavily on the design and use of polymers. More needs have arisen for polymeric materials with more specific drug-delivery properties. In this research, several groups of new polymeric networks based on crosslinked poly (N-isopropylacrylamide) (PNiPAAm) hydrogels have been developed. Their physicochemical properties as well as potential applications for controlled drug delivery are summarized:

(1) Introduction of small quantities of an ionic, hydrophilic co-monomers (sodium acrylate and methacrylamidopropyl trimethylammonium chloride) into crosslinked NiPAAm hydrogel networks substantially alter the thermo-sensitive swelling and collapse behavior of these gel systems during discontinuous volume transitions occurring at their critical points. Swelling ratios in swollen gel states below the critical point are significantly greater than those of pure NiPAAm gels, and collapsed states are much more condensed, approaching swelling ratios near unity for all copolymer gels studied. This behavior is interpreted in terms of a gel structural model which considers the effect of hydrophilic co-constituents on water transport in transition state networks undergoing critical phenomena. That crosslinked NiPAAm homopolymer gels cannot collapse completely due to a dehydrated, dense polymeric skin overlying the gel exterior above the critical transition produces a nonequilibrium entrapment of water within the gel that supports this model. Complete network collapse after substantially enhanced swelling in the copolymer gel systems provides evidence that water entrapped by gel collapse can diffuse both in and out

of the gel, even after polymer skin formation on the gel surface. These phenomena are, to some extent, both composition and pH dependent, although minute amounts of ionic co-monomers (0.5 mol%) produce the typical behavior. The ability of ionized co-monomers to remain charged and interact electrostatically with aqueous media and itself within the copolymer network over a wide range of ionic strengths and pH values is proposed to explain significantly increased swelling and collapse behavior in the crosslinked copolymer gel systems over that for pure NiPAAm.

(2) Amphiphilic networks based on crosslinked poly (N-isopropylacrylamide-co-sodium acrylate-co-n-N-alkylacrylamide) demonstrate some unique and interesting thermo-sensitive swelling behavior in water as well as amphiphile diffusivity. Networks swelling and thermo-sensitive critical points are readily adjusted by controlling levels of hydrophilic and hydrophobic comonomer. Network amphiphile (surfactant) release kinetics can be easily controlled using this tunable network swelling: fine tuning by type and amount of alkyl side chain incorporated, broad control by network crosslinking density. Submacroscropic hydrophobic domains in the networks are proposed to play a significant role in achieving long-term zero-order release for amphiphiles.

(3) Model drugs, such as hydrophilic coenzyme (vitamin B_{12}), amphiphilic peptides (insulin and interferon), and hydrophobic steroid (progesterone), can be successfully delivered in various controlled manners by ionized and amphiphilic PNiPAAm gels. Vitamin B_{12} release profiles from PNiPAAm-co-SA copolymer gels exhibit a first-order kinetic pattern under constant temperature. Thermo- and pH- responsive pulsatile release characters from ionized PNiPAAm gels are extensively improved in terms of release pulse control and various temperature stimuli means applied due to the efficient thermo-sensitive swelling and deswelling nature of ionized PNiPAAm gels. Peptide (insulin and interferon) release from amphiphilic terpolymer PNiPAAm gels produces two different kinetic profiles dependent on two different sample loading methods. By solvent sorption loading, a two-

stage release pattern consisting of a distinct surface burst release follow by a slow pseudo-zero-order release is observed, while by *in situ* polymerization loading, a remarkable extended zero-order release profile is observed. Release rate decreases as the length and amount of the pendent hydrophobic alkyl chains incorporated increase due to propsed hydrophobic interactions between the peptide and gel networks. Pulsatile release profiles of peptide are achievable using amphipilic PNiPAAm gels. The release profiles of progesterone from amphiphilic PNiPAAm gels loaded by solvent sorption is close to that for the peptides: a two-stage release pattern with shorter release duration. Similarly, release rates decrease as the amount of the pendent alkyl chains incorporated increases. In general, release rates for all the model drugs investigated decrease as the network crosslinking density increases. While the simplest Fickian laws of diffusion have been extensively applied to describe the drug diffusivity in hydrogels, resulting in frequent models for first-order release kinetics, drug diffusivity (especially for amphiphilic or hydrophobic drugs) in amphiphilic terpolymer gels may be better interpreted by considering both time- and position-dependent diffusivities of permeating species through a multicomponent controlled diffusion theory approach.

Appendix

Chemical Structures for Compounds Used in This Research

I. Monomers:

NiPAAm

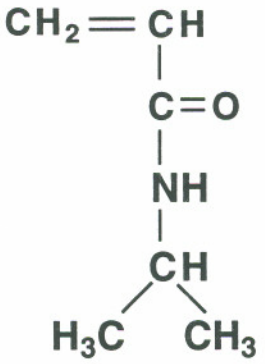

NaAc or SA

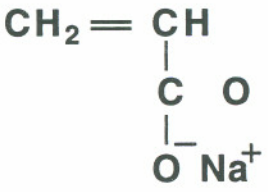

n-N-Alkylacrylamide

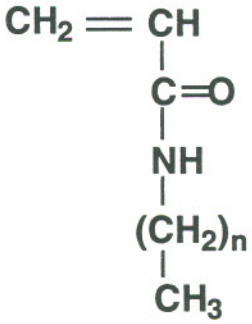

n=3,7,9,11,13,17

II Crosslinkers:

MBAAm

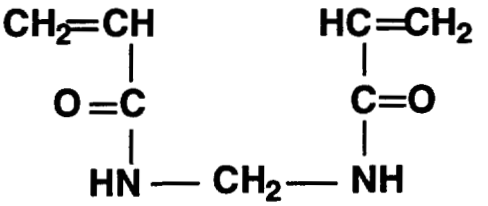

N,N'-bis(acryloyl)-cystamine (BAC)

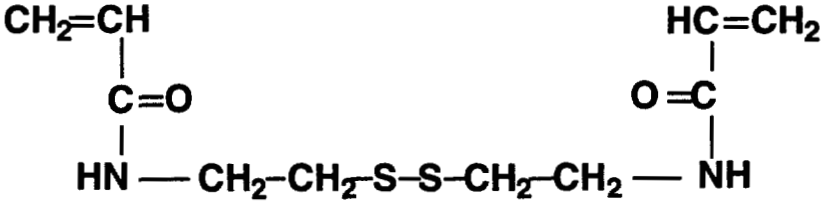

III Initiators:

Ammonium persulfate (AP) $(NH_4)_2S_2O_8$

Tetramethylenediamine (TEMED) $[CH_2CH_2N(CH_3)_2]_2$

IV Stabilzers:

Sodium dodecyl sulfate (SDS) $CH_3(CH_2)_{11}OSO_3Na$

4 lauryl ether (Brij 30) $CH_3(CH_2)_{11}(OCH_2CH_2)_4OH$

Biographical Sketch

PERSONAL Born 9/7/62, Shanghai, China

EXPERIENCE

9/80-7/84 B.Sc. study, China Textile University, Shanghai, China,
(Major: Textile Chemistry)

9/84-1/87 M.Sc., study, China Textile University, Shanghai, China
(Major: Textile Chemistry and Applied Polymer Sciences)

1/87-8/90 Research associate and project coordinator, China Textile University, Shanghai, China
(Topics: Functional finish of textiles; speciaty polymers)

9/90-6/94 Ph.D. study, Department of Chemistry, Biochemistry, and Molecular Biology, Oregon Graduate Institute of Science and Technology, Portland, Oregon
(Major: Chemistry)

PUBLICATIONS

1. H. Yu and D. W. Grainger, "Novel Thermosensitive Amphiphilic Networks Synthesis and Charcterization", Polym. Prepr. (Am. Chem. Soc. Div. Polym. Chem.), Vol. 34, p820, 1993.

2. H. Yu and D. W. Grainger, "Thermosensitive Swelling Behavior of Ionized NiPAAm Gels", Polym. Prepr. (Am. Chem. Soc. Div. Polym. Chem.), Vol. 34, p829, 1993.

3. H. Yu and D. W. Grainger, "Novel Thermo-responsive Amphiphilic Networks Synthesis and Protein Drug Delivery Application", Proceedings of the 20th International Symposium on Controlled Release of Bioactive Materials, July 25-30, 1993, Washington, D.C., U.S.A, p28.

4. H. Yu and D. W. Grainger, "Thermo-sensitive Swelling Behavior in Crosslinked N-isopropylacrylamide Networks: Cationic, Anionic, and Ampholytic Hydrogels", J. Appl. Polym. Sci., Vol. 49, p1553-1563, (1993).

5. H. Yu and D.W. Grainger, "Amphiphilic Thermosensitive N-isopropylacrylamide Terpolymer Hydrogels Prepeared by Micellar Polymerization in Aqueous Media", Macromolecules, 1993, in press.

6. H. Yu and D. W. Grainger, "Modified Release of Hydrophilic, Hydrophobic and Peptide Agents from Ionized Amphiphilic Gel Networks", J. Contr. Rel., 1993, submitted.

PRESENTATIONS

1. Poster, "Model Amphiphile SDS Release from Thermo-, pH-Sensitive Amphiphilic Networks", the Sixth International Symposium on Recent Advance in Drug Delivery Systems, Feb. 22-25, 1993, Salt Lake City, Utah, U. S. A.

2. Speaker, "Novel Thermosensitive Amphiphilic Networks Synthesis and Physicochemical Characterization", the 205th American Chemical Society National Meeting, Mar. 28- Apr. 2, Denver, Colorado, U. S. A.

3. Speaker, "Thermo-sensitive Swelling Behavior in Cationic, Anionic, and Ampholytic NiPAAm Gels", the 205th American Chemical Society National Meeting, Mar. 28- Apr. 2, Denver, Colorado, U. S. A.

4. Invited Speaker, "Novel Thermo- and pH- Sensitive Amphiphilic Networks and Peptide Delivery", the 20th International Symposium on Controlled Release of Bioactive Materials, July 25-30, 1993, Washington, D. C., U. S. A.